

**A Comparative Study of the *In vitro* Antiproliferative  
Activity of the Extracts from the Different Developmental  
Stages of *Pleurotus tuber-regium***

WONG Sze Man

A Thesis Submitted in Partial Fulfillment  
of the Requirements for the Degree of  
Master of Philosophy  
in  
Biology

©The Chinese University of Hong Kong  
September 2006

The Chinese University of Hong Kong holds the copyright of the thesis. Any person(s) intending to use a part or whole of the materials in the thesis in a proposed publication must seek copyright release from the Dean of the Graduate School.



Thesis/Assessment Committee

Professor Peter Chi-Keung Cheung (Chair)

Professor Ming-Chiu Fung (Thesis Supervisor)

Professor Yum-Shing Wong (Committee Member)

Professor Jennifer Man-Fan Wan (External Examiner)

<b>Thesis Committee</b>	<b>-----i</b>
<b>Acknowledgement</b>	<b>-----ii</b>
<b>Abstract (English Version)</b>	<b>----- iii</b>
<b>Abstract (Chinese Version)</b>	<b>-----v</b>
<b>Content Page</b>	<b>-----vi</b>
<b>List of Tables</b>	<b>----- x</b>
<b>List of Figures</b>	<b>----- xii</b>
<b>Abbreviations</b>	<b>----- xvii</b>



## Thesis Committee

Prof. Peter Chi-Keung Cheung

Prof. Ming-Chiu Fung

Prof. Yum-Shing Wong

Prof. Jennifer Man-Fan Wan (External Examiner)

## Acknowledgement

I would like to express overwhelming gratitude to my supervisor, Prof. Peter Chi-Keung Cheung, for his guidance and valuable advice to this project. It is my honor to have Prof. Ming-Chiu Fung and Prof. Yum-Shing Wong to be my thesis committee. I would like to give special thanks to Prof Fung for his advice in data analysis and Prof. Wong for kindly providing the Hs68 cell line.

I am deeply appreciative of Mr. Ka-kei Wong for sharing his data to make this project successful.

I am grateful to Dr. Mei Zhang and Miss Connie Kin-Ming Lai for sharing their experience and providing me much information in doing the *in vitro* antiproliferation assays.

I would also like to offer my heartfelt thanks to Miss Elaine Wong and Miss Lim for assisting me in the flow cytometric analysis. Besides, my project could not be finished smoothly without the technical support of our lab technician, Mr C.C. Li.

Last but not least, I am obliged for the support and encouragement from my labmates and friends, as well as my family, during these two years of postgraduate study.

## Abstract

The chemical compositions and *in vitro* antiproliferative activities of the water extracts from the fruiting body (coded as HWE1, HWE2 and HWE3 for three consecutive hot-water extraction, respectively), mycelium (EDP) and culture medium (CEP) of a novel edible mushroom *Pleurotus tuber-regium* (PTR) were analyzed and compared. CEP and EDP were high in carbohydrate content (83.4% and 87.2%, respectively) and low in protein content (15.9% and 3.24%, respectively). Meanwhile, the three HWEs had comparatively higher protein content (>30.4%). HWEs having molecular weight above  $156 \times 10^4$  were rich in glucose (49.2-60.5%) and had substantial amount of mannose (20.4-26.9%) and galactose (14.8-16.3%), speculating that they were heteropolysaccharide-protein complexes. As previously reported, EDP was rich in glucose (87.3%) with a moderate MW of  $50.9 \times 10^4$  while CEP was mannan-rich (76.0%) with a low MW of  $4.4 \times 10^4$ , suggesting they were probably glucan and mannan, respectively.

The inhibitions on *in vitro* growth and proliferation of human acute promyelocytic (HL-60) and chronic myelogenous leukemia cells (K562) retarded by PTR extracts (concentration ranging from 12.5  $\mu\text{g/ml}$  to 400  $\mu\text{g/ml}$ ) were more significant ( $p < 0.05$ ) than those of human breast cancer (MCF-7) and hepatocellular carcinoma (HepG2). No significant inhibition on normal monkey kidney (Vero) and human foreskin (Hs68) cells was found, suggesting that the antiproliferative activity of the PTR extracts was tumor-selective. HWE2 (approximate  $\text{LC}_{50}$  value: 25  $\mu\text{g/ml}$ ) possessed the strongest growth inhibition on HL-60 cells whereas CEP (approximate  $\text{IC}_{50}$  value: 150  $\mu\text{g/ml}$ ) had the most potent antiproliferative effect on HL-60 cells. Strong cytotoxicity against K562 cells was demonstrated by HWE2 and CEP (both having an approximate  $\text{LC}_{50}$  value of 25  $\mu\text{g/ml}$ ) while HWE3 (approximate  $\text{IC}_{50}$  value: 100  $\mu\text{g/ml}$ ) reduced the % of proliferating K562 cells most significantly ( $p < 0.05$ ).

All PTR extracts induced apoptosis in HL-60 cells with an increase of Bax/Bcl-2 ratio. However, apoptosis was not readily induced by CEP and HWE3 in K562 cells and resistance to apoptosis might have occurred after HWE2 and EDP treatments. Analysis from flow cytometry and western blot demonstrated that EDP caused G<sub>2</sub>/M arrest at 24 hours by lowering the Cdk1 expression of HL-60 cells and

HWE2 caused S arrest which might be correlated with a depletion of Cdk2 and the increase of cyclin E expression in HL-60 cells. Therefore, PTR extracts isolated from different developmental stages of the mushroom have different chemical compositions which may influence their *in vitro* antiproliferative efficacies and corresponding mode of actions.



## 摘要

本文就可食用的虎奶菇 (*Pleurotus tuber-regium*) 的子實體 (代號為 HWE1, HWE2 及 HWE3)、其菌絲體及培養基 (代號為 EDP 及 CEP) 的水提溶液的化學成份及抗增生作用進行分析和比較。CEP 及 EDP 的碳水化合物含量較高 (83.4% 和 87.2%)，但其蛋白質含量低 (15.9% 和 3.24%)。三個 HWE 樣本則含有較多蛋白質 (>30.4%)。它們的分子量大於  $156 \times 10^4$  及含大量葡萄糖 (49.2-60.5%)、甘露糖 (20.4-26.9%) 及半乳糖 (14.8-16.3%)，估計它們是異多醣-蛋白複合物。根據以往結果，EDP 含大量葡萄糖 (87.3%) 及其分子量為  $50.9 \times 10^4$ ，CEP 則含大量甘露糖 (76.0%) 及其分子量為  $4.4 \times 10^4$ ，估計它們分別是葡聚糖和甘露聚糖。

劑量由 12.5 至 400  $\mu\text{g/ml}$  的虎奶菇提取物對急性骨髓性白血病細胞 (HL-60) 及慢性骨髓性白血病細胞 (K562) 的體外生長及增殖的抑制作用比對人類胸腺癌細胞 (MCF-7) 及人肝癌細胞 (HepG2) 明顯的大 ( $p < 0.05$ )。而對正常猴腎細胞 (Vero) 及人類上皮層纖維母細胞 (Hs68) 則沒有明顯影響。這證明了虎奶菇提取物具有腫瘤選擇性。對於 HL-60 細胞，HWE2 ( $\text{LC}_{50}$  值約為 25  $\mu\text{g/ml}$ ) 具有最大的生長抑制作用，而 CEP (其  $\text{IC}_{50}$  值均約為 150  $\mu\text{g/ml}$ ) 則對 HL-60 細胞具有最大抗增生作用。HWE2 和 CEP 對 K562 細胞具有很強的細胞毒性 ( $\text{LC}_{50}$  值約為 25  $\mu\text{g/ml}$ )。HWE3 則明顯能減少增生中的 K562 細胞百分比 ( $\text{IC}_{50}$  值 100  $\mu\text{g/ml}$ )。

所有虎奶菇提取物均能引起 HL-60 細胞的細胞程式死亡 (apoptosis) 及增加 Bax/Bcl-2 比率。但是，CEP 及 HWE3 並不能引起 K562 細胞的細胞程式死亡，而且經 HWE2 及 EDP 處理後，K562 細胞可能對細胞程式死亡產生了抵抗性。流式細胞技術 (flow cytometry) 及西方墨點法 (western blot) 證明了 HL-60 細胞在經過 EDP 24 小時處理後其 Cdk1 的水平有明顯降低，而細胞亦停留在 G<sub>2</sub>/M 期。HWE2 減低 Cdk2 及增加 cyclin E 蛋白表達水平，使 HL-60 細胞停留在 S 期。所以，不同發展階段虎奶菇的提取物具有不同的化學成份，從而產生不同的抗增生效用及相對的作用機理。

## Content Page

<b>Chapter 1 Introduction</b>	<b>1</b>
1.1 Cancer treatment and potential novel antitumor agents	1
1.2 History of mushroom polysaccharides in medical uses	1
1.3 Life cycle of mushroom	3
1.4 Classification of antitumor mushroom polysaccharides	5
1.4.1 $\beta$ -glucans	5
1.4.2 Heteropolysaccharides	7
1.4.3 Polysaccharide-protein complexes	7
1.5 Structure-activity relationship of mushroom polysaccharides	8
1.5.1 Lentinan as typical example	9
1.5.2 Molecular weight	10
1.5.3 Conformation	10
1.5.4 Chemical modification	11
1.5.5 Degree of branching	13
1.6 Antitumor mushroom polysaccharides obtained from different developmental stages	17
1.7 Mechanisms of <i>in vitro</i> antitumor activity of mushroom polysaccharides: cell cycle arrest and apoptotic induction	20
1.7.1 Cell cycle regulation	21
1.7.2 Induction of apoptosis	24
1.8 The novel strategies for cancer treatment	27
1.9 Literature Review on <i>Pleurotus tuber-regium</i>	30
1.10 Objectives	33
<b>Chapter 2 Materials and Methods</b>	<b>35</b>
2.1 Materials	35
2.1.1 Assay kits	35
2.1.2 Mushroom samples	35
2.1.3 Cell lines and their subculture	36
2.1.4 Antibodies	37
2.2 Extraction of mushroom polysaccharides	38
2.2.1 Hot-water extracts from mushroom fruiting body	38



2.2.2 Hot-water extracts from mushroom mycelia -----	38
2.2.3 Exo-polysaccharides from submerged fermentation	
medium -----	39
2.3 Chemical and physio-chemical composition of PTR extracts -----	41
2.3.1 Neutral monosaccharides -----	41
2.3.1.1 Acid Depolymerization -----	41
2.3.1.2 Neutral sugar derivatization -----	42
2.3.1.3 Determination of neutral sugar composition by GC-	43
2.3.2 Uronic acid (acidic monosaccharides) content -----	45
2.3.3 Total carbohydrate content -----	46
2.3.4 Protein content -----	46
2.3.5 Molecular weight and the homogeneity -----	47
2.4 <i>In vitro</i> growth inhibitory effects-----	48
2.4.1 Trypan blue dye exclusion method -----	48
2.4.2 Colorimetric 3-(4,5-dimethylthiazol-2-yl)-2,5-diphenyl	
tetrazolium bromide (MTT) assay -----	49
2.5 <i>In vitro</i> cell proliferation assay -----	50
2.6 Cell-cycle analysis -----	51
2.7 Apoptotic determination -----	52
2.8 Expression of proteins involved in apoptosis and cell-cycle -----	52
2.8.1 Preparation of cell lysates -----	53
2.8.2 Determination of protein concentrations -----	53
2.8.3 Western blot -----	54
2.9 Statistics -----	57
<b>Chapter 3 Results and Discussion -----</b>	<b>58</b>
3.1 Yield of extract samples isolated from different developmental	
stages of PTR-----	58
3.2 Chemical characteristics of hot-water extracts isolated from	
different stages of PTR -----	60
3.2.1 The total carbohydrate and protein content of PTR extracts-	60
3.2.2 The monosaccharide composition of PTR extracts -----	62
3.3 Molecular weight distribution of PTR extracts -----	64
3.4 Chemical characterization of PTR extracts -----	69

3.5 Cytotoxic effect of PTR extracts on various cell line <i>in vitro</i> -----	71
3.5.1 Effect of PTR extracts on HL-60 cell viability-----	71
3.5.2 Effect of PTR extracts on K562 cell viability-----	74
3.5.3 Effect of PTR extracts on MCF-7 cell proliferation-----	76
3.5.4 Effect of PTR extracts on HepG2 cell proliferation-----	76
3.5.5 Effect of PTR extracts on normal cell proliferation-----	78
3.6 Effect of PTR extracts on the proliferation rate of various cell lines <i>in vitro</i> -----	78
3.6.1 Effect of PTR extracts on HL-60 cell proliferation -----	79
3.6.2 Effect of PTR extracts on K562 cell proliferation -----	79
3.6.3 Effect of PTR extracts on MCF-7 cell proliferation -----	80
3.6.4 Effect of PTR extracts on HepG2 cell proliferation -----	80
3.6.5 Effect of PTR extracts on normal cell proliferation -----	84
3.7 Summary of the cytotoxic and antiproliferative activities exhibited by PTR extracts -----	84
3.8 Analysis of the effect of PTR extracts on the cell-cycle phases of HL-60 and K562 cells -----	87
3.8.1 Effect of CEP on cell-cycle phases of HL-60 and K562 cells -----	87
3.8.2 Effect of EDP on cell-cycle phases of HL-60 and K562 cells -----	92
3.8.3 Effect of HWE1 on cell-cycle phases of HL-60 and K562 cells-----	95
3.8.4 Effect of HWE2 on cell-cycle phases of HL-60 and K562 cells-----	98
3.8.5 Effect of HWE3 on cell-cycle phases of HL-60 and K562 cells-----	102
3.8.6 Summary -----	105
3.9 The effect of PTR extracts on expression of cellular proteins involved in cell-cycle control and apoptotic pathway in HL-60 cells -----	106
3.9.1 Expression of Bcl-2 and Bax proteins in HL-60 cells treated with PTR extracts -----	106
3.9.2 Expression of cyclins and Cdks in HL-60 cells by PTR	



extracts----- 115

3.9.3 The plausible antiproliferative mechanism(s) involved in  
PTR extracts on HL-60 cells ----- 117

**Chapter 4 Conclusions and Future works ----- 120**

4.1 Conclusions ----- 120

4.2 Future works ----- 122

**References ----- 124**

**Related Publications ----- 144**

## List of Tables

Table 1.1	The conformation, molecular weight and <i>in vivo</i> and <i>in vitro</i> antitumor activities of the polysaccharide fractions derived from Lentinan -----	15
Table 1.2	Examples of antitumor mushroom polysaccharides isolated from different developmental stages -----	16
Table 2.1	The antibodies used in determination of expression of proteins --	37
Table 3.1	The yield, total carbohydrate and protein content of the PTR extracts-----	60
Table 3.2	The monosaccharide composition of the PTR extracts -----	64
Table 3.3	The molecular weight ( $M_w$ ) of the PTR HWE1, HWE2 and HWE3 -----	69
Table 3.4	The effect of concentration of PTR extracts on the proliferation of MCF-7 cells determined by MTT method was expressed as relative % of proliferating cells (mean $\pm$ S.D., n=5)-----	77
Table 3.5	The effect of concentration of PTR extracts on the proliferation of HepG2 cells determined by MTT method was expressed as relative % of surviving cells (mean $\pm$ S.D., n=5) -----	77
Table 3.6	The effect of concentration of PTR extracts on the proliferation of MCF-7 cells determined by BrdU incorporation method was expressed as relative % of proliferating cells (mean $\pm$ S.D., n=5) -	83

Table 3.7	The effect of concentration of PTR extracts on the proliferation of HepG2 cells determined by BrdU incorporation method was expressed as relative % of proliferating cells (mean±S.D., n=5) -	83
Table 3.8	Numeric expression of the relative cell number on the cell-cycle phases and apoptosis of HL-60 cells by CEP at 300 µg/ml -----	90
Table 3.9	Numeric expression of the relative cell number on the cell-cycle phases and apoptosis of K562 cells by CEP at 300 µg/ml -----	91
Table 3.10	Numeric expression of the relative cell number on the cell-cycle phases and apoptosis of HL-60 cells by EDP at 400 µg/ml -----	93
Table 3.11	Numeric expression of the relative cell number on the cell-cycle phases and apoptosis of K562 cells by EDP at 400 µg/ml -----	94
Table 3.12	Numeric expression of the relative cell number on the cell-cycle phases and apoptosis of HL-60 cells by HWE1 at 400 µg/ml ----	96
Table 3.13	Numeric expression of the relative cell number on the cell-cycle phases and apoptosis of K562 cells by HWE1 at 300 µg/ml -----	97
Table 3.14	Numeric expression of the relative cell number on the cell-cycle phases and apoptosis of HL-60 cells by HWE2 at 200 µg/ml ----	100
Table 3.15	Numeric expression of the relative cell number on the cell-cycle phases and apoptosis of K562 cells by HWE2 at 200 µg/ml -----	101
Table 3.16	Numeric expression of the relative cell number on the cell-cycle phases and apoptosis of HL-60 cells by HWE3 at 200 µg/ml ----	103
Table 3.17	Numeric expression of the relative cell number on the cell-cycle phases and apoptosis of K562 cells by HWE3 at 100 µg/ml -----	104



## List of Figures

Figure 1.1	The typical life cycle of mushroom including the stages of mycelial hypha, sclerotium and fruiting body -----	4
Figure 1.2	A fruiting body on the top of a sclerotium of <i>Pleurotus tuber-regium</i> (PTR) -----	4
Figure 1.3	The key regulators in the cell cycle -----	22
Figure 1.4	Simplified main apoptotic pathways: the extrinsic death receptors-dependent pathway (left) and the intrinsic mitochondria-dependent pathway (right) -----	27
Figure 1.5	Sclerotia of <i>Pleurotus tuber-regium</i> (PTR)-----	32
Figure 2.1	Fruiting body (left) and mycelia (right) of <i>Pleurotus tuber-regium</i> (PTR) -----	35
Figure 2.2	Hot water extraction scheme of fruiting bodies of PTR -----	40
Figure 2.3	The freeze-dried powder of PTR extracts from (a) mycelium and (b) culture medium.-----	41
Figure 3.1	The SEC profile of pullulan standards by a TSK3000PW column at 30°C with sodium chloride (0.2M) at a flow rate of 3.0 ml/min and RI detection -----	67
Figure 3.2	The SEC profile of pullulan standards by a TSK5000PW column at 30°C with sodium chloride (0.2M) at a flow rate of 3.0 ml/min and RI detection -----	67

- Figure 3.3      The HPLC chromatogram of HWE1 obtained by a TSK5000 column with detection by refractive index (black line) alone and together with UV absorbance(blue line). The eluent was 0.2M sodium chloride at a flow rate of 3.0 ml/min and the column was kept at 30°C ----- 68
- Figure 3.4      The HPLC chromatogram of HWE2 obtained by a TSK5000 column with detection by refractive index (black line) alone and together with UV absorbance(blue line). The eluent was 0.2M sodium chloride at a flow rate of 3.0 ml/min and the column was kept at 30°C ----- 68
- Figure 3.5      The HPLC chromatogram of HWE3 obtained by a TSK5000 column with detection by refractive index (black line) alone and together with UV absorbance (blue line). The eluent was 0.2M sodium chloride at a flow rate of 3.0 ml/min and the column was kept at 30°C ----- 68
- Figure 3.6      The effect of concentrations of PTR extracts on the viability of HL-60 cells determined by trypan blue exclusion method was expressed as the relative % surviving cells, mean  $\pm$ S.D. (n=5), against the log concentration of extracts. Different letters represent the significant difference between the means of the number of cells in control group and treatment group by Student's t-test (\*  $p < 0.05$ , #  $p < 0.01$ )----- 73
- Figure 3.7      The effect of concentrations of PTR extracts on the viability of K562 cells determined by trypan blue exclusion method was expressed as the relative % surviving cells, mean  $\pm$ S.D. (n=5), against the log concentration of extracts. Different letters represent the significant difference between the means of the number of cells in control group and treatment group by Student's t-test (\*  $p < 0.05$ , #  $p < 0.01$ )----- 75



Figure 3.8	The effect of PTR extracts on the proliferation of HL-60 cells determined by BrdU incorporation method was expressed as the % proliferating cell against the log concentration employed. Different letters represent the significant difference between the number of cells in control group and treatment group according to t-test (* $p < 0.05$ , # $p < 0.01$ ) -----	81
Figure 3.9	The effect of PTR extracts on the proliferation of K562 cells determined by BrdU incorporation method was expressed as the % proliferating cell against the log concentration employed. Different letters represent the significant difference between the number of cells in control group and treatment group according to t-test (* $p < 0.05$ , # $p < 0.01$ ) -----	82
Figure 3.10	Representative cytograms showing the effect of CEP at 300 $\mu\text{g/ml}$ on the cell-cycle phases ( $G_0/G_1$ , S, and $G_2/M$ ) and apoptosis (Sub- $G_1$ peak) of HL-60 cells at 24, 48 and 72 hours -----	90
Figure 3.11	Representative cytograms showing the effect of CEP at 300 $\mu\text{g/ml}$ on the cell-cycle phases ( $G_0/G_1$ , S, and $G_2/M$ ) and apoptosis (Sub- $G_1$ peak) of K562 cells at 24, 48 and 72 hours -----	91
Figure 3.12	Representative cytograms showing the effect of EDP at 400 $\mu\text{g/ml}$ on the cell-cycle phases ( $G_0/G_1$ , S, and $G_2/M$ ) and apoptosis (Sub- $G_1$ peak) of HL-60 cells at 24, 48 and 72 hours -----	93
Figure 3.13	Representative cytograms showing the effect of EDP at 300 $\mu\text{g/ml}$ on the cell-cycle phases ( $G_0/G_1$ , S, and $G_2/M$ ) and apoptosis (Sub- $G_1$ peak) of K562 cells at 24, 48 and 72 hours -----	94
Figure 3.14	Representative cytograms showing the effect of HWE1 at 400 $\mu\text{g/ml}$ on the cell-cycle phases ( $G_0/G_1$ , S, and $G_2/M$ ) and apoptosis (Sub- $G_1$ peak) of HL-60 cells at 24, 48 and 72 hours -----	96

Figure 3.15	Representative cytograms showing the effect of HWE1 at 300 $\mu\text{g/ml}$ on the cell-cycle phases ( $G_0/G_1$ , S, and $G_2/M$ ) and apoptosis (Sub- $G_1$ peak) of K562 cells at 24, 48 and 72 hours -----	97
Figure 3.16	Bivariate PI/annexin V analysis of the (a) untreated and (b) PTR HWE2-treated (200 $\mu\text{g/ml}$ ) HL-60 cells-----	99
Figure 3.17	Representative cytograms showing the effect of HWE2 at 200 $\mu\text{g/ml}$ on the cell-cycle phases ( $G_0/G_1$ , S, and $G_2/M$ ) and apoptosis (Sub- $G_1$ peak) of HL-60 cells at 24, 48 and 72 hours -----	100
Figure 3.18	Representative cytograms showing the effect of HWE2 at 200 $\mu\text{g/ml}$ on the cell-cycle phases ( $G_0/G_1$ , S, and $G_2/M$ ) and apoptosis (Sub- $G_1$ peak) of K562 cells at 24, 48 and 72 hours -----	101
Figure 3.19	Representative cytograms showing the effect of HWE3 at 200 $\mu\text{g/ml}$ on the cell-cycle phases ( $G_0/G_1$ , S, and $G_2/M$ ) and apoptosis (Sub- $G_1$ peak) of HL-60 cells at 24, 48 and 72 hours -----	103
Figure 3.20	Representative cytograms showing the effect of HWE3 at 100 $\mu\text{g/ml}$ on the cell-cycle phases ( $G_0/G_1$ , S, and $G_2/M$ ) and apoptosis (Sub- $G_1$ peak) of K562 cells at 24, 48 and 72 hours -----	104
Figure 3.21	(a) The Bcl-2 and Bax expressions in HL-60 cells incubated with CEP at 300 $\mu\text{g/ml}$ for 24, 48 and 72 h with the relative density of the band measured by densitometer. $\beta$ -actin was used as the loading control. (b) The corresponding ratio of the relative density of Bax/Bcl-2 in CEP-treated HL-60 cells -----	108
Figure 3.22	(a) The Cdk1, Bcl-2 and Bax expressions in HL-60 cells incubated with EDP at 400 $\mu\text{g/ml}$ for 24, 48 and 72 h with the relative density of the band measured by densitometer. $\beta$ -actin was used as the loading control. (b) The corresponding ratio of the relative density of Bax/Bcl-2 in EDP-treated HL-60 cells -----	109



Figure 3.22	(c) The relative expression of Cdk1 in EDP-treated HL-60 cells----	110
Figure 3.23	(a) The Bcl-2 and Bax expressions in HL-60 cells incubated with HWE1 at 400 µg/ml for 24, 48 and 72 h with the relative density of the band measured by densitometer. β -actin was used as the loading control. (b) The corresponding ratio of the relative density of Bax/Bcl-2 in HWE1-treated HL-60 cells -----	111
Figure 3.24	(a) The cyclin E, Cdk2, Bcl-2 and Bax expressions in HL-60 cells incubated with HWE2 at 200 µg/ml for 24, 48 and 72 h with the relative density of the band measured by densitometer. β -actin was used as the loading control. (b) The corresponding ratio of the relative density of Bax/Bcl-2 in HWE2-treated HL-60 cells -----	112
Figure 3.24	The relative expression of (c) cyclin E and (d) Cdk2 in HWE2-treated HL-60 cells -----	113
Figure 3.25	The Bcl-2 and Bax expressions in HL-60 cells incubated with HWE3 at 100 µg/ml for 24, 48 and 72 h with the relative density of the band measured by densitometer. β -actin was used as the loading control. (b) The corresponding ratio of the relative density of Bax/Bcl-2 in HWE3-treated HL-60 cells -----	114



## Abbreviations

ATCC	American Type Culture Collection
AP	Alkaline phosphatase
Bax	Bcl-2-associated X protein
Bcl-2	B-cell lymphoma-2
BrdU	Bromodeoxyuridine
BSA	Bovine serum albumin
Cdks	Cyclin-dependent kinases
Cdkis	Cyclin-dependent kinase inhibitors
CEP	Crude extracellular polysaccharides
DMEM	Dulbecco's Modified Eagle's Medium
DMSO	Dimethyl sulfoxide
EDP	Endo-polysaccharides
ELISA	Enzyme linked immunosorbent assay
FBS	Fetal bovine serum
FITC/ FLUOS	Fluorescein isothiocyanate
G <sub>1</sub> phase	Gap1 phase
G <sub>2</sub> phase	Gap2 phase
GC	Gas chromatography
HepG2	human hepatocellular carcinoma
HL-60	human acute promyelocytic leukemia
HPLC	High pressure liquid chromatography
Hs68	Human normal foreskin
HWEs	Hot water extracts
K562	Human chronic myelogenous leukemia
M phase	Mitotic phase
MCF-7	Human breast carcinoma
MTT	3-(4,5-dimethylthiazol-2-yl)-2,5-diphenyl tetrazolium bromide
MW	Molecular weight
PBS	Phosphate buffered saline
PI	Propidium iodide

PS -----	Phosphatidylserine
PSP -----	Protein-bound polysaccharides
PTR -----	<i>Pleurotus tuber-regium</i>
Rb -----	Retinoblastoma
RPMI -----	Roswell Park Memorial Institute
S phase -----	Synthesizing phase
SCP -----	Sclerotial polysaccharides
SDS-PAGE -----	Sodium dodecyl sulphate-polyacrylamide gel electrophoresis
SEC -----	Size exclusion chromatography
TDS -----	Total dissolved solutes
Vero -----	Monkey normal kidney

# **Chapter 1      INTRODUCTION**

## **1.1    Cancer treatment and potential novel antitumor agents**

It has been generally approved that surgery, radiotherapy and chemotherapy are the major treatments of cancer. However, a series of side effects was found on the patients who are subjected to these treatments, such as increasing the mortality and morbidity, lowering appetite, destroying the immune system. This is because they are not only toxic to cancer cells but also to normal cells and tissues as well (Boivin, 1990). Innovation of other non-invasive treatments is essential to alleviate the suffering of cancer patients.

An understanding of the occurrence of cancer helps to develop effective antitumor agents. As cancer originates from normal cell, the action of antitumor agents must be tumor-selective in order that no harmful effects act on normal cells but effectively eliminate the tumor ones (Mizuno, 1999). Due to the impaired proliferation and death machinery, tumor cells are unable to stop dividing or undergo death process (Schwartz & Shah, 2005). Therefore, developing a compound which could restore the balance between cell growth and cell death by controlling the cell cycle progression and/or inducing apoptosis might become a novel agent in cancer treatment.

## **1.2    History of mushroom polysaccharides in medical uses**

Mushrooms have been used in traditional oriental medical treatments for



many years. The medicinal effects of mushrooms have been documented in the Chinese and Japanese medical books, such as 'Sen Nong Ben Cao Jing' and 'Ben Cao Gang Mu' in China and 'Nihon Shoki' in Japan (Mizuno *et al.*, 1995). *Ganoderma lucidum*, *Coriolus versicolor*, *Lentinus edodes*, *Grifola frondosa* are some of the examples of medicinal mushrooms employed since ancient times (Mizuno *et al.*, 1995; Ooi, 2000). They were reported to have various health-beneficial properties. *G. lucidum* and *C. versicolor* were described to promote longevity and good health while *L. edodes* was used for treatment of cold. *G. frondosa* had the function of calming the nerve and the mind (Ooi, 2000). In the past, mushrooms were usually boiled in water and the hot water extracts were used as medicine. Mushroom polysaccharides were certainly one of these water-soluble components (Wassar, 2002). In the 1960's, the medicinal effect of mushrooms and their corresponding bioactive components were demonstrated by scientific and medical studies (Mizuno, 1995). The polysaccharides isolated from mushrooms have also been identified to be the most potent and active substance carrying the antitumor and immunomodulating properties (Wassar & Weis, 1999; Wassar, 2002). Hence, mushroom polysaccharides have drawn much attention in cancer therapy since then.

Numerous mushrooms, particularly those belong to the class Basidiomycetes and Ascomycetes, have been proved to consist of antitumor polysaccharides derived from different developmental stages, including the fruiting bodies, sclerotia, mycelia and its culture filtrates (Ooi and Liu, 2000). Nowadays, some of the mushroom polysaccharides are validated to be used as nutraceuticals and even as medicine in Japan, China, Russia, U.S. and Canada (Mizuno, 1999; Wassar, 1999; Smith *et al.*, 2003). The most famous ones are lentinan extracted from the fruiting body of *Lentinus edodes*; schizophyllan obtained from the culture medium of *Schizophyllum*

*commune*; and PSK isolated from the mycelium of *Coriolus versicolor* (Mizuno, 1996; Miles & Chang, 1997; Wassar, 1999).

### 1.3 Life cycle of mushroom

Mushrooms refer to macrofungi consisting of a mycelial network and a large enough distinctive fruiting body which can be seen by naked eyes. They usually belong to the Class Basidiomycetes and some are Ascomycetes (Ooi & Liu, 2000). In the class Basidiomycetes, 'club-like' spores called basidia are produced in the cap of fruiting body. Germination of the spores gives hyphae that extend at the tip and form a primary mycelium. At the same time, secondary mycelium is formed from hypha produced by fusion of two compatible hyphae. Some of the hyphae would grow at some other regions leading to branching. A bunch of hyphae and mycelia are fused together to form a mycelial network. The network becomes larger and larger and finally a new macroscopic fruiting body is germinated. New spores would then be produced by the mature fruiting body and dispersed to begin a new life cycle (Fig. 1.1) (Stamets, 1983; Wassar & Weis, 1999; Chang & Miles, 2004).

A special morphological form, sclerotia, could be developed under stressful conditions, for example, starvation, unfavorable humidity or temperature for germination. The most common sclerotium is from *Poria cocos* (also called 'Fuling' in China) that is widely used in Chinese soups. It is a compact mass of mycelia and its thickened wall and the nutrient- and chemical-rich inner part allow it to overcome the undesirable situations and even survive for many years (Hoffman, 1999). When the conditions become favorable, sclerotia may form fruiting bodies (Fig. 1.2), producing and dispersing spores, continuing the life cycle (Carlile *et al.*, 2001).



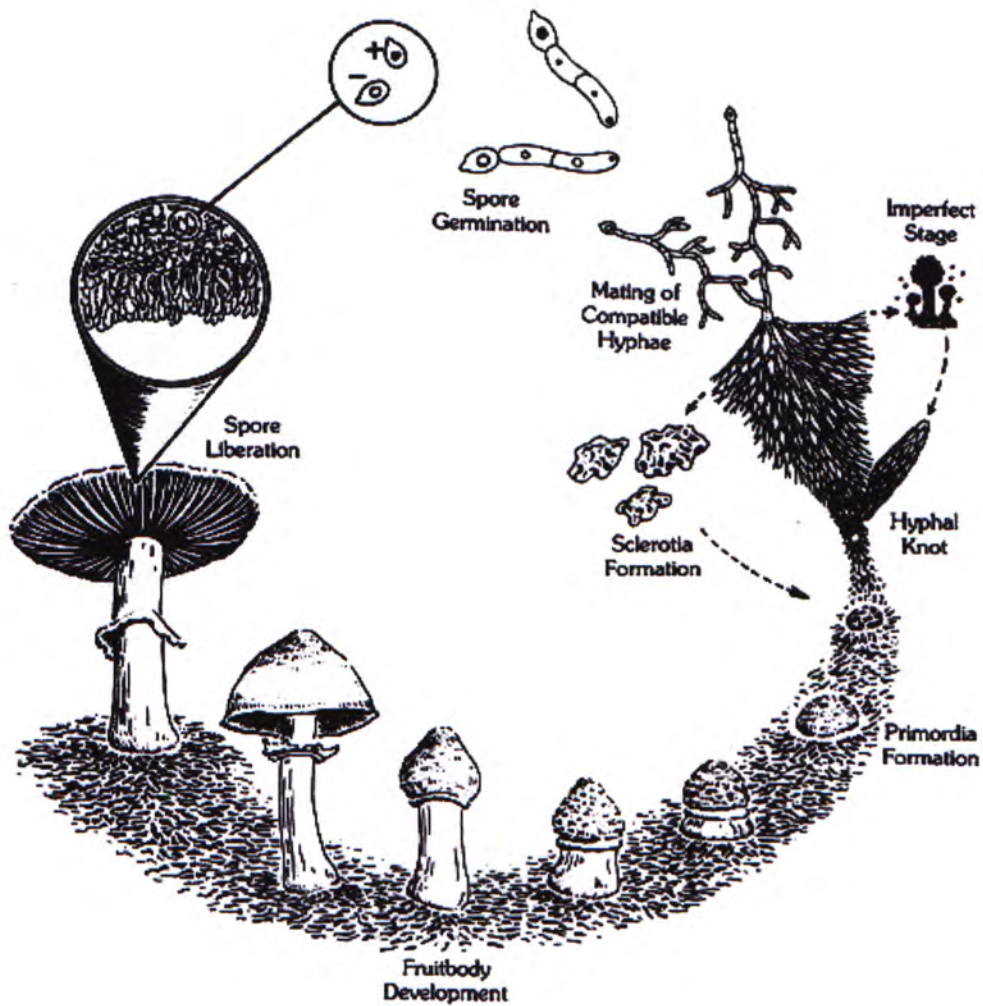


Fig. 1.1 The typical life cycle of mushroom including the stages of mycelial hypha, sclerotium and fruiting body (Stamets, 2000).



Fig. 1.2 A fruiting body on the top of a sclerotium of *Pleurotus tuber-regium* (PTR).

## 1.4 Classification of antitumor mushroom polysaccharides

Polysaccharides are macromolecules which are made up of numerous monosaccharides interconnecting together by glycosidic linkages. They may be linear or highly branched as one monosaccharide can join to more than two other monosaccharides (Daba & Ezeronye, 2003). Owing to this, several terms have been derived from the structure of polysaccharides such as glucans and glycans. Glucan is a polysaccharide that consists of glucose only, and only glucose is yielded by acid hydrolysis (Mizuno, 1999; Daba & Ezeronye, 2003). Glycan means the polysaccharide that consists of monosaccharides other than glucose (Daba & Ezeronye, 2003).

Cell wall of mushroom is mainly made up of protein, chitin and polysaccharide such as glucans and mannans (Wu *et al.*, 2004). By applying different extraction methods, various antitumor polysaccharides originating from the cell wall can be obtained. These polysaccharides could be divided into three major groups according to the monosaccharide constituents:  $\beta$ -glucans, heteropolysaccharides and polysaccharide-protein complexes (Mizuno, 1999).

### 1.4.1 $\beta$ -glucans

Antitumor polysaccharides of mushroom are mostly  $\beta$ -glucans. In particular, they are commonly (1 $\rightarrow$ 3)-  $\beta$ -D-glucopyranans with (1 $\rightarrow$ 6)-  $\beta$ -D-glucosyl branches, having an average molecular weight of  $5 \times 10^5$  and  $20 \times 10^5$  (Mizuno *et al.*, 1989). These  $\beta$ -D-glucans are oriented in a right triple helical form as indicated by NMR



analysis and x-ray diffraction (Marchessault *et al.*, 1977).

$\beta$ -glucans are existed in the forms of triple helix, single helix or random coil. They could exist as different conformations in different states (solid or liquid state) resulted from different preparations. Aqueous-soluble branched (1 $\rightarrow$ 3)-  $\beta$ -glucans are single-helix by coordinating with water molecules (Ohno, 2005), but mostly, in triple-helical structure (Mizuno *et al.*, 1995). They form a gel or even agar-like structure during prolonged storage because of their intermolecular interaction (Ohno, 2005). Low-molecular linear (1 $\rightarrow$ 3)-  $\beta$ -glucans are readily soluble in aqueous solution and are maintained in random coil (Yadomae and Ohno, 1996). However, those having high molecular weight are not soluble in aqueous solution, and could form gel due to their long chain length whereas those having intermediate chain length form precipitate (Mizuno *et al.*, 1995). On the other hand, the gel formed by linear and branched (1 $\rightarrow$ 3)-  $\beta$ -glucans are in single helix and triple helix conformations (Mizuno *et al.*, 1995). Their solubilities could be improved under alkaline condition or in DMSO solution because of the conversion of their helical conformations to random coil. The original secondary structure could be resumed back to either single helix or triple helix after adding HCl for neutralization (Mizuno *et al.*, 1995). However, recovery of the helical conformation was not achievable in some cases, such as schizophyllan, even after neutralization of the alkali treatment (Hobbs, 2005).

For instance, lentinan and schizophyllan, isolated from *Lentinus edodes* and *Schizophyllum commune*, having a high molecular weight of  $5 \times 10^5$  and  $4.5 \times 10^5$ , respectively, have been revealed to have a main chain of (1 $\rightarrow$ 3)- $\beta$ -D-glucan with (1 $\rightarrow$ 6)-linked branch at an interval of three main chain units (Mizuno *et al.*, 1995).



Other antitumor polysaccharides isolated from the fruiting bodies of *Ganoderma lucidum*, *Coriolus versicolor*, *Poria cocos* and *Grifola frondosa* are also  $\beta$ -glucans (Mizuno *et al.*, 1995).

#### 1.4.2 Heteropolysaccharides

Apart from  $\beta$ -glucans, heteropolysaccharides have also been reported to have antitumor activities. Glucuronic acid, galactose, mannose, arabinose or xylose, or the combinations of them, is usually the main monosaccharide in the side chain of a  $\beta$ -glucan main chain (Mizuno *et al.*, 1995). In heteroglycans, side chains usually contain arabinose, mannose, fucose, galactose, xylose, glucuronic acid and glucose or different combinations of them (Wassar, 2002). A large number of the heteropolysaccharides have been shown to be effective against tumors (Ooi and Liu, 1999), for example, antitumor glucomannan isolated from the mycelia of *Agaricus blazei* (Tsuchida *et al.*, 2001). Several heteroglycans have been extracted from the fruiting bodies of *Ganoderma lucidum* (Wassar and Weis, 1999). Also, exocellular heteropolysaccharides (glucuronoxylomannan) have been obtained from *Tremella mesenterica* (Vinogradov *et al.*, 2004).

#### 1.4.3 Polysaccharide-protein complexes

Besides the above two classes, polysaccharides with bound protein is the third class of antitumor mushroom polysaccharides which is called polysaccharide-protein complex or protein bound polysaccharides. PSK and PSP derived from the

mycelia of *Coriolus versicolor* (Tsukagoshi *et al.*, 1984) are the polysaccharide-protein complexes being most extensively studied. PSK which was a product of Japan was isolated from the strain CM101 of *C. versicolor* whereas PSP was produced in China, isolated from the strain COV-1 (Ng, 1998). They are branched (1→3)- $\beta$ -, (1→4)- $\alpha$ -glucans and are rich in aspartic acid and glutamic acid in their polypeptide moieties (Ng, 1998; Lau *et al.*, 2004). PSP consists of mainly arabinose, rhamnose, galactose, mannose and xylose while the polysaccharides of PSK has fucose, galactose, mannose and xylose in their side chains (Cui and Chisti, 2003). They showed *in vitro* direct cytotoxicity on numerous tumor cell lines including leukemia (HL-60), lymphoma, (Lau *et al.*, 2004), hepatoma (HepG2) (Dong *et al.*, 1996) and breast cancers (MCF-7) (Dong *et al.*, 1997). Moreover, PSP exerted strong immunomodulatory activities by increasing the level of  $\gamma$ -interferon, interleukin-1 $\beta$ , -2 and -6 and the proliferation of T-cells (Ng, 1998; Hsieh *et al.*, 2002). These cytokines and T-cells are responsible for the enhancement of the immune system.

### 1.5 Structure-activity relationship of mushroom polysaccharides

Polysaccharides can be made up of different monosaccharides together with other components like proteins and they have different linkages, branching and conformations and hence different molecular mass and water solubility. The potency of antitumor activity of mushroom polysaccharides varies, but it has been suggested that it is associated with their own structural characteristics, including molecular mass, degree of branching and substitution, conformation, presence of bound protein, chemical modification and water solubility (Kiho *et al.*, 1989; Adachi *et al.*, 1990; Chihara, 1992; Mischnick, 1995; Ohno *et al.*, 1995; Wassar, 2002; Surenjav *et al.*,



2006).

### 1.5.1 Lentinan as typical example

It is generally suggested that antitumor mushroom polysaccharides rely on the basic structure of a triple-helical (1→6) branched (1→3)-β-D-glucan with high molecular mass (Wassar, 2002). A recent research analyzing the structural effects of (1→3)-β-D-glucans from *Lentinus edodes* is a good example to illustrate this point (Surenjav *et al.*, 2006). Two triple helical and protein bound (1→3)-β-D-glucans (L-I<sub>2</sub> and L-I<sub>3</sub>) with molecular weights  $1.57 \times 10^6$  and  $1.51 \times 10^6$ , respectively were isolated from two different strains of fruiting bodies of *Lentinus edodes*. Several derivatives were produced including their deproteinized fractions (LNP-I<sub>2</sub> and LNP-I<sub>3</sub>), fractions with lower molecular weight (LU-I<sub>2</sub> and LU-I<sub>3</sub>) and those with single flexible chain (LSC-I<sub>2</sub> and LSC-I<sub>3</sub>) which were produced by dissolving the native fractions in DMSO solvent which can break the intra- and intermolecular hydrogen bonds. They had significant inhibitory effects on the growth of Sarcoma 180 (S-180) solid tumor in Kunming mice (Surenjav *et al.*, 2006). L-I<sub>2</sub> and L-I<sub>3</sub> inhibited S-180 tumor with a range of inhibition % from 25.9 to 70.0 at a daily dose of 20 to 60 mg per kg body weight of the mice. However, LNP-I<sub>2</sub> and LNP-I<sub>3</sub> could only have a tumor inhibition % about 40. LU-I<sub>2</sub> and LU-I<sub>3</sub> also exhibited a growth inhibition on S-180 tumor smaller than 30% in Kunming mice. Besides, the inhibitory effects of LSC-I<sub>2</sub> and LSC-I<sub>3</sub> were sharply decreased, ranging from only 0.6% to 16.7%. All these results suggested that bound protein content, high molecular weight and triple helix of the polysaccharides are important structural parameters for the antitumor potency of polysaccharides (Surenjav *et al.*, 2006).

### 1.5.2 Molecular weight

Polysaccharides having molecular weight higher than  $2 \times 10^5$  are suggested to have more potent antitumor activity (Bohn and BeMiller, 1995). Two water-soluble heteropolysaccharides which isolated from *Poria cocos* by 0.9% sodium chloride and then hot water, with high molecular weight of  $2.6 \times 10^5$  and  $8.9 \times 10^5$ , respectively demonstrated significant *in vivo* and *in vitro* antitumor activities (Jin *et al.*, 2003). They inhibited the growth of S-180 tumor by 56.0% and 66.8% in BALB/c mice, respectively. Also, their significant cytotoxicities against HL-60 leukemic cells and HepG2 liver cancer cells were observed (Jin *et al.*, 2003). It is noteworthy that these heteropolysaccharides are mainly consisted of  $\alpha$ -D-glucose, mannose and galactose (Jin *et al.*, 2003), implying that polysaccharides other than  $\beta$ -glucans could give promising antitumor activities as well.

In spite of this, polysaccharides with low molecular weight also demonstrated significant antitumor activities. A water-soluble  $\alpha$ -glucan isolated from the mycelia of *Pleurotus ostreatus* had molecular weight smaller than  $1 \times 10^4$ , exerting significant inhibitory effect of 93.75% on HT-29 colon cancer cells by apoptotic induction via upregulating the expression of pro-apoptotic Bax and cytochrome *c* (Lavi *et al.*, 2006). It indicated that not only  $\beta$ -glucans with high molecular weight, but also low-molecular-weight  $\alpha$ -glucan could show significant antiproliferative activity.

### 1.5.3 Conformation

Besides, not all the polysaccharides with high molecular could enhance the



antitumor activities. The *in vivo* and *in vitro* antitumor activities of the fractions derived from Lentinan by different degree of ultrasonication were highly affected by their molecular weight and also the conformation (Zhang *et al.*, 2005). The triple helical fractions having moderate molecular weight of  $14.9 \times 10^4$  and  $18.4 \times 10^4$  exerted the highest inhibition ratios on the growth of S-180 solid tumor in BALB/c mice at a high dose of 60 mg/kg and a low dose of 20 mg/kg, respectively. However, the tumor inhibitory effects was decreased substantially (to 16.8%) after their conformations were changed to single flexible coil (Table 1.1). In contrast, the fraction with lower molecular weight exhibited the strongest % inhibition towards S-180 cells *in vitro*. Therefore, triple-helical polysaccharides having moderate and low molecular weight had the strongest *in vivo* and *in vitro* antitumor effects among the fractions derived from Lentinan.

#### 1.5.4 Chemical modification

Chemical modification also enhances the water solubility of the polysaccharides and their antitumor activities. Carboxymethylation, formylmethylation, aminethylation and sulfation can introduce an ionic group to the polysaccharides so as to improve their water solubility (Ooi and Liu, 2000). The polysaccharides that are relatively water-soluble usually have stronger antitumor activities. Huang *et al.*, (2006) demonstrated that sulfation could enhance the antitumor activities to  $\alpha$ -glucans isolated from *Poria cocos* mycelia. Six water-soluble sulfated  $\alpha$ -glucans with various molecular weights were modified from the native water-insoluble  $\alpha$ -glucans extracted from *Poria cocos* mycelia by introducing the hydrophilic sulfogroups on the backbone of glucan. The antitumor activities of

these fractions were tested against Sarcoma 180 tumor cells in BALB/c mice *in vivo*. The inhibition ratio of native fraction was 7.41% while that of the six sulfated derivatives was ranged from 32.2% to 52.0%, showing that all the sulfated fractions were effective in suppressing the S180 tumor cell growth (Huang *et al.*, 2006). *In vitro* antitumor activities of the native and sulfated fractions at three concentrations (0.005, 0.05 and 0.5 mg/ml) were also investigated with the help of HepG2 and Sarcoma 180 cells. The native fraction could not inhibit both cell lines; however, all the sulfated derivatives inhibited the growth of two cell lines significantly with an inhibition ratio of 50% (Huang *et al.*, 2006). It therefore indicated sulfation can enhance both *in vivo* and *in vitro* antitumor activities of mycelial  $\alpha$ -glucans extracted from *Poria cocos*.

Furthermore, a water-insoluble (1 $\rightarrow$ 3)- $\beta$ -glucan isolated from the sclerotia of *Poria cocos* was chemically modified by sulfation, carboxymethylation, methylation, hydroxyethylation and hydroxypropylation to produce five water-soluble fractions with molecular weight of  $3.8 \times 10^4$ ,  $18.9 \times 10^4$ ,  $16.0 \times 10^4$ ,  $76.8 \times 10^4$  and  $224.3 \times 10^4$ , respectively (Wang *et al.*, 2004). The resulted sulfated, carboxymethylated and methylated fractions were highly soluble in water. Their *in vitro* antiproliferative activities against MKN-45 and SGC-7901 gastric cancer cells showed a dose-dependent manner (0.5 mg/ml, 1 mg/ml and 2 mg/ml). These three modified fractions exhibited a 30% higher inhibition ratio at 2 mg/ml than that of the native fractions and other chemically modified ones (Wang *et al.*, 2004). Also, the *in vivo* antitumor activity of all the chemically modified fractions against S-180 solid tumor in BALB/c mice was higher than the native fractions, among which the sulfated, carboxymethylated and methylated fractions showed a ten-fold stronger inhibition than the native one. It is believed that the higher the water solubility the



polysaccharides had, the stronger the antitumor activity they could exert. Therefore, chemical modification might enhance the antitumor activity together with a moderate molecular weight of polysaccharides.

#### 1.5.5 Degree of branching

Degree of branching is also a determining factor for the antitumor property of polysaccharides. Polysaccharides with high molecular weight ( $1 \times 10^5$ - $2 \times 10^5$ ) and with the degree of branching between 0.20 and 0.33 were observed to have most remarkable antitumor activities (Bohn and BeMiller, 1995). Lentinan and schizophyllan have an average degree of branching of 0.33 (Bohn and BeMiller, 1995). For those with degree of branching smaller than 0.25, they also showed strong activities if they had no ordered structure and their molecular weights were lower than  $2 \times 10^4$  (Bohn and BeMiller, 1995). In some cases, antitumor activities of polysaccharides could be enhanced after debranching. This was illustrated by Pachyman and its debranched derivative named Pachymaran (Chihara *et al.*, 1970). Pachyman is a  $\beta$ -glucan with (1 $\rightarrow$ 6)  $\beta$ - branches obtained from the sclerotia of *Poria cocos* with no antitumor activity. After debranching by Smith degradation, Pachymaran was formed as a straight chain  $\beta$ -glucan with potent antitumor activity (Chihara *et al.*, 1970).

From the above, it could be realized that the relationship between degree of branching and antitumor activity of polysaccharides is very complicated. In summary, moderate branching was essential for the polysaccharides with high molecular weight (Ohno, 2005) and low degree of branching might be favorable for those with

lower molecular weight. However, antitumor activities sometimes could only be obtained from those without branch chain.

The structure-activity relationship of mushroom polysaccharides is still controversial as shown by many contradictory results. It was due to the huge variability in the chemical structure of antitumor polysaccharides and difficulties in the identification of the bio-active components (Table 1.2). For instance, although the most well-known antitumor mushroom polysaccharides, Lentinan and Schizophyllan are  $\beta$ -(1 $\rightarrow$ 3)-glucans, antitumor polysaccharides with other structures such as those mentioned above,  $\alpha$ -glucans isolated from culture filtrates of *Pleurotus ostreatus* (Lavi *et al.*, 2006) and sulfated  $\alpha$ -glucans isolated from *Poria cocos* mycelia (Huang *et al.*, 2006), undoubtedly also had prominent *in vitro* antitumor activities. Thus, this diversity makes the confirmation of the structure-activity relationship of polysaccharides more challenging.



Table 1.1 The conformation, molecular weight and *in vivo* and *in vitro* antitumor activities of the polysaccharide fractions derived from *Lentinan*\*

Fraction	Conformation	MW x10 <sup>4</sup>	% Inhibition on S-180 solid tumor in BALB/c mice with administration of		% Inhibition on S-180 cell lines at 500µg/ml <i>in vitro</i>
			20 mg/kg x 8days	60 mg/kg x 8days	
L-FV-IB11	Triple helix	28.3	19.0	34.0	30
L-FV-IB12	Triple helix	21.6	23.0	34.6	25
L-FV-IB21	Triple helix	18.4	31.2	36.3	30
L-FV-IB31	Triple helix	14.9	28.6	49.5	35
L-FV-IB41	Triple helix	11.4	22.1	27.6	-
L-FV-IB32	Triple helix	9.79	23.5	26.0	40
L-FV-IB52	Triple helix	5.71	27.2	38.2	45
L-FV-IB73	Triple helix	3.57	27.7	35.4	40
L-FV-IB21D	Single flexible chain	5.59	12.8	16.8	-
L-FV-IB31D	Single flexible chain	4.37	8.1	14.3	-

-: did not mention in the paper

\* Modified from Zhang *et al.*, (2005)

Table 1.2 Examples of antitumor mushroom polysaccharides isolated from different developmental stages \*

Mushroom	Fruiting body	Mycelium	Culture medium
<i>Agaricus blazei</i>	$\beta$ -glucan, Insoluble $\beta$ -glucan, Hetero- $\beta$ -glucan	Glucomannan-protein	Mannan-protein
<i>Coriolus versicolor</i>	$\beta$ -glucan	$\beta$ -glucan (PSP, PSK)	-
<i>Ganoderma lucidum</i>	$\beta$ -glucan, Hetero- $\beta$ -glucan	-	$\beta$ -glucan
<i>Grifola frondosa</i>	Grifolan ( $\beta$ -glucan), Acidic $\beta$ -glucan, Hetero- $\beta$ -glucan, xyloglucan, mannoglucan, fucomannoglucan	Mannogalatofucan, heteroxylan, fucoxylan, galactomannoglucan	-
<i>Lentinus edodes</i>	$\beta$ -glucan	$\alpha$ -Mannan-peptide	Hetero-glucan protein

-: No polysaccharides were recorded

\* Adapted from Mizuno et al., (1995); Wassar and Weis, (1999)

## 1.6 Antitumor mushroom polysaccharides obtained from different developmental stages

As mentioned in 1.3, mushroom can exist in different morphological forms during the life cycle. Polysaccharides extracted from the different stages of the same mushroom have not only different chemical characteristics and also different antitumor potency.

It could be observed that the number of polysaccharides isolated from the fruiting body of mushroom was more than those from mycelium and culture medium. Twenty-nine, six and one polysaccharides were successful isolated from the fruiting body, mycelium and culture medium of *Ganoderma tsugae* (Wasser, 2002). This phenomenon was also commonly found in other mushroom such as *Grifola frondosa*, *Ganoderma lucidum* and *Pleurotus ostreatus* (Table 1.2) (Mizuno *et al.*, 1995; Wassar and Weis, 1999).

*Ganoderma tsugae* is a mushroom having fruiting bodies, mycelia and culture medium from which polysaccharides have been isolated and investigated. From its fruiting body, 14 water-soluble polysaccharides belonged to protein-containing glucogalactans with mannose and fucose, and 15 water-insoluble protein-containing (1→3)- $\beta$ -glucans with different proportions of protein were successfully isolated, among which seven glycans exhibited strong antitumor activities (Wang *et al.*, 1993).

Six water-soluble polysaccharides having different structural characteristics were extracted from the mycelium of *G. tsugae* (Peng *et al.*, 2005), including heteropolysaccharide-protein complexes,  $\beta$ -D-glucans, polysaccharides with both



(1→3)- $\beta$ -D-glucans and (1→4)-  $\alpha$ -D-glucans, and (1→6)branched (1→3) - $\beta$ -D-glucans, as revealed by  $^{13}\text{C}$ NMR and IR spectra. Their molecular weights were ranged from  $62.8 \times 10^4$  to  $468 \times 10^4$ . The fractions which were found to be heteropolysaccharide-protein complexes and mixtures of (1→3) - $\beta$ -D-glucans and (1→4)-  $\alpha$ -D-glucans possessed significant potent antitumor activity (>50% inhibition ratio) against the Sacroma 180 *in vivo*. It was suggested that the antitumor activity might be associated with the protein and galactose content as well as the lower molecular weight of the heteropolysaccharide-protein complexes (Peng *et al.*, 2005).

Besides, a crude extracellular polysaccharide and its two fractionated derivatives were obtained in the culture filtrate of *G. tsugae* (Peng *et al.*, 2003). Although all three polysaccharides had similar monosaccharide composition, the two fractionated derivatives existed as compact coil chain and slightly expended coil chain, respectively. The molecular weight of all the two fractionated derivatives of extracellular polysaccharides ( $8.35 \times 10^4$  and  $23.8 \times 10^4$ ) was much lower than the crude one ( $92.0 \times 10^4$ ). The crude extracellular polysaccharide showed a significantly higher *in vivo* tumor inhibition (60.44%) injected peritoneally at a daily dose of 5 mg per kg body weight in response to Sacroma 180 solid tumor grown in BALB/c mice. This might be due to its high protein content (23.1%) which implied a protein-bound polysaccharide (Peng *et al.*, 2003).

Apart from the developmental stage, the mushroom antitumor polysaccharides isolated from the same stage but different strains might not be structurally identical. PSK isolated from the strain CM101 and PSP from the strain COV-1 of *Coriolus versicolor* is a good example. They have the same proportion of

polysaccharide but with different protein moiety and different monosaccharide profile. PSK consisted of fucose whereas PSP had rhamnose and arabinose (Ng, 1998).

The chemical components used in the culture media of mycelium affect the mycelial polysaccharides produced. The water-soluble heteropolysaccharides extracted from a wild strain and a cultivated strain of *Poria cocos* mycelia cultured in two media containing bran extract and corn steep liquor respectively were unique in their chemical compositions and molecular weights (Jin *et al.*, 2003). Their *in vivo* antitumor activities against Sacroma 180 in BALB/c mice and *in vitro* growth inhibitory effect on HL-60 and HepG2 cell lines varied. The heteropolysaccharides isolated from the wild stain cultured in corn steep liquor, containing more mannose and galactose and protein, showed stronger *in vivo* antitumor activities. Although from different strains, the heteropolysaccharides isolated from the mushroom cultured in corn steep liquor inhibited the growth of HL-60 and HepG2 cells more significantly.

Interestingly, structural characteristics of even the same type of polysaccharides obtained from the same strain of mushroom might be slightly different due to the different degree of maturity. Water-soluble glucans were extracted from the fruiting bodies of *Agaricus blazei* (*Agaricus brasiliensis*) in different levels of maturity including those cap-closed immature with no spores, cap-opened mature with immature spores and cap-opened with mature spores (Camelini *et al.*, 2005).  $^{13}\text{C}$  NMR spectra showed that the polysaccharides isolated from all the mature stages contained (1→2)- $\beta$ -glucans, (1→6)- $\beta$ -glucans, (1→3)- $\beta$ -glucans



and (1→6)-  $\alpha$  - glucans. However, only cap-opened fruiting bodies contained (1→4)-  $\alpha$  -glucans, which was rather abundant in those with mature spores. Except (1→2)-  $\beta$  - glucans and (1→4)-  $\alpha$  -glucans, all mushroom polysaccharides obtained above were proven to have antitumor activities (Mizuno *et al.*, 1990; Fujimiya *et al.*, 1998). Moreover, the growth inhibitory effect of PSP (1 mg/ml), which was isolated from the mycelium of *Coriolus versicolor*, on Molt 4 leukemic cells was increased with an increase in the cultivation time and the maturity of the mycelia (Lee *et al.*, 2005). Thus, even in the same developmental stage, mushrooms with different maturity would have slightly differences in both their chemical characteristics and their antitumor efficacies.

#### **1.7 Mechanisms of *in vitro* antitumor activity of mushroom polysaccharides: cell cycle arrest and apoptotic induction**

Most of the mushroom polysaccharides are suggested to be biological response modifiers (BRM) (Wassar and Weis, 1999) of which actions are host-mediated that via the immune response (Wassar, 2002). BRM is a substance inhibits the tumor without harming or adding extra stress on the host, but help the host to adapt various environmental and biological stresses so as to minimize the sufferings brought from the disease (Wassar and Weis, 1999). Immunomodulatory effect of mushroom polysaccharides has been accepted to be the mechanism of their antitumor activities that the polysaccharides activate the immune system of the host rather than direct killing the cancer cells (Wasser, 2002). However, in recent years, many mushroom polysaccharides have been suggested to have direct cytotoxicity towards various cancer cell lines and hence a new mechanistic approach has been aroused.



Cell-cycle arrest and apoptosis are recently used to study the mode of actions of cancer treatment since cancer cells, unlike normal ones, have uncontrolled proliferation and defective death machinery as mentioned earlier in 1.1. The mushroom polysaccharides were proposed to modify the regulation of cell cycle and the molecules involved in apoptosis. As a result, the cancer cells would stop further proliferation and undergo programmed cell death.

### 1.7.1 Cell cycle regulation

Defined by Howard and Pelc (1953), cell cycle involves DNA synthesizing S phase and mitotic M phase. These two phases are separated by Gap1 ( $G_1$ ) and Gap2 ( $G_2$ ) (Fig 1.3). Most cells are non-dividing in human body and stay in a quiescent state classified as  $G_0$  during which cellular growth still occurs (Schwartz & Shah, 2005). When a cell is stimulated by growth factors, it must pass through  $G_1$ , S,  $G_2$  and M phases sequentially to complete the cell division that produces two offsprings (Fig 1.3). The cell cycle is tightly regulated by cyclins, cyclin-dependent kinases (Cdk), cyclin-dependent kinase inhibitors (Cdk<sub>i</sub>) and tumor suppressor proteins (Sherr, 2000). Cyclins in each phase when associated with their corresponding cdk<sub>s</sub> can activate them. The activated cyclin-cdk complexes in one phase drives the cell to pass to the next phase of cell cycle. Cyclin D/ Cdk4 or 6 complex is important in the progression of  $G_1$  phase. Cyclin E/Cdk2 is responsible for the  $G_1$ /S transition. Cyclin A/Cdk2 is necessary for S phase progression while cyclin A/Cdk1 helps the cell to move through  $G_2$  phase. Cyclin B/Cdk1 governs the occurrence of M phase (Baguley, 2002; Schwartz & Shah, 2005).

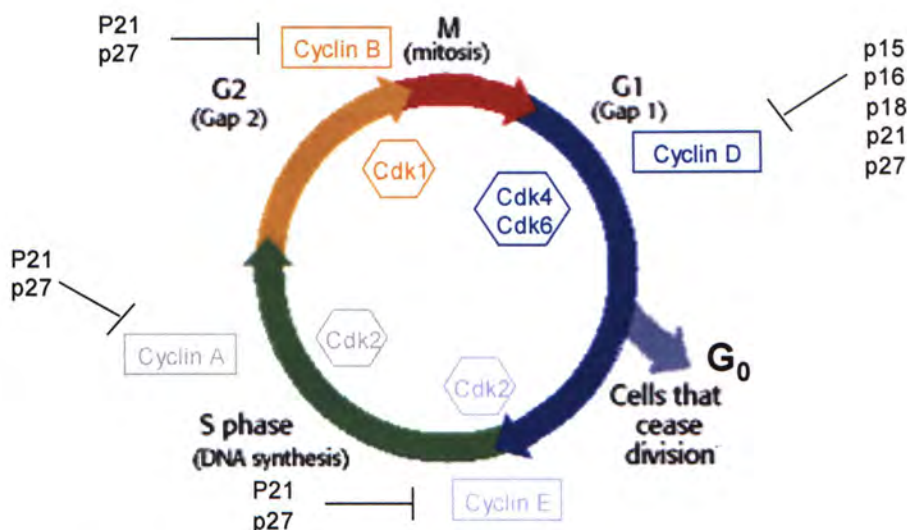


Fig 1.3 The key regulators in the cell cycle (adapted from Sherr, 2000; Schwartz & Shah, 2005)

When the cell is activated in response to the growth factors, it enters the cell cycle in G<sub>1</sub> phase and passes through the restriction point. Stimulation of growth factors leads to the induction of cyclin D production in mid- G<sub>1</sub> phase. Cyclin D would bind to and activate Cdk4 and Cdk6 (Sherr, 1995). Cyclin D/Cdk4(6) complex, together with cyclin E/Cdk2 complex, phosphorylates and inactivates tumor suppressor protein Rb so that E2F transcription factor would no longer be bound (Malumbres and Barbacid, 2001). This would result in the transcription of several essential proteins for S phase and the cell is ready to enter S phase (Sherr, 2000). In the G<sub>1</sub>/S boundary, Cdk2 would bind to cyclin A and this complex is responsible for the progression of S phase where DNA replication is being performed. When the DNA synthesis is completed correctly, cyclin A would bind to Cdk1 instead of Cdk2, facilitating the G<sub>2</sub> phase progression. Cyclin B would be formed in late- G<sub>2</sub> phase but



remains inactive in cytoplasm until mitosis begins. When the cell is ready for cell division, cyclinB/Cdk1 complex is activated by phosphatase cdc25 and is relocated into the nucleus to drive the cell to M phase and undergo mitosis (Schwartz & Shah, 2005).

There are three cell cycle checkpoints located in G<sub>1</sub>/S boundary, S phase and G<sub>2</sub> which ensure the cell in the cell cycle completed the process of earlier stage without errors (Pommier *et al.*, 2002). The G<sub>1</sub> checkpoint is closely related to the tumor suppressor proteins p53 and pRb. They govern the pathways that downregulate the cyclin D/Cdk4(6) and cyclin E/Cdk2 complexes and cause G<sub>1</sub> arrest in response to DNA damage. The p53 protein has been regarded as 'the guardian of the genome' as it also involves in apoptotic pathway. When there is DNA damage, it can either stop the cell cycle in order to allow the repair of DNA or trigger apoptosis to kill the DNA-damaged cell (Eastman, 2004).

S-phase checkpoint is also called the replication checkpoint that monitors the DNA synthesis and the cell progression during S phase (Schwartz & Shah, 2005). The mechanism of S-phase checkpoint pathway is not fully discovered, but it is thought to involve the inhibition of Cdk2 and further block the loading of CDC45 onto DNA. As a result, DNA polymerase would not be recruited and so no DNA replication was initiated (Kastan and Bartek, 2004). On the other hand, when there is DNA damage occurred in G<sub>2</sub> phase or those unrepaired DNA damage from previous S or G<sub>1</sub> phase, G<sub>2</sub> checkpoint would be initiated. It is also greatly dependent on p53 pathway to suppress the activity of cyclin B/Cdk1 complex in order to halt the cell (Kastan and Bartek, 2004).



Deregulation of either one of the proteins involved in cell cycle leads to unlimited cell growth. For instance, p53 and pRb proteins are usually lost in human cancers and so repair mechanism cannot take place (Kastan and Bartek, 2004). Targeting these proteins in cell cycle and hence restore the cell cycle checkpoints are the possible new strategy in cancer treatment.

### 1.7.2 Induction of apoptosis

Apoptosis is a programmed cell death for removing the unwanted cells in which their contents would be absorbed by neighboring tissue, so no inflammatory response results (Baguley, 2002; Fesik, 2005). During apoptosis, a series of biochemical and morphological changes were occurred. Biochemically, it involves an extrinsic death receptors-dependent pathway and an intrinsic mitochondria-dependent pathway (Fig 1.4). Both two pathways rely on caspases to transmit the signals in the cell and carry out the morphological changes of apoptosis (Cory and Adams, 2002; Okada and Mak, 2004). Due to a series of changes in biochemical pathway, it is typical to observe nuclear shrinkage and chromatin condensation in the early stage of apoptosis. DNA would become fragmented in the presence of DNA fragmentation factors. In late apoptosis, cell fragmentation, membrane blebbing, formation of apoptotic bodies which are finally engulfed by phagocytosis would be resulted (Igney and Krammar, 2002).

Mitochondria is an integral part in the intrinsic pathway of apoptosis which is controlled by the Bcl-2 family proteins and other mitochondrial proteins such as

cytochrome *c* (Fig 1.4) (Lavi *et al.*, 2006). Bcl-2 family proteins are key regulators in apoptosis that involve antiapoptotic and proapoptotic proteins. Bcl-2 family proteins are divided into three subfamilies according to their conserved Bcl-2 homology (BH) domains, including anti-apoptotic Bcl-2 family, pro-apoptotic Bax family and BH3-only family (Cory and Adams, 2002). Anti-apoptotic Bcl-2 family consists of Bcl-2, Bcl-w and Bcl-xL that inhibit the induction of apoptosis by blocking the activation of pro-apoptotic Bax family proteins. Pro-apoptotic Bax family involves Bax, Bak and Bok which promote apoptosis by disrupting the mitochondrial membrane and lead to the release of cytochrome *c*. BH3-only family, such as Bid, Bim, Bad and Bik, functions like a DNA-damage sensor that can only promote apoptosis in the presence of Bax family proteins and help to inhibit the Bcl-2 family (Cory and Adams, 2002; Fesik, 2005). Among the Bcl-2 family proteins, antiapoptotic Bcl-2 and proapoptotic Bax are the most important and highly investigated regulatory proteins (Oltvai *et al.*, 1993).

When DNA damage is detected, tumor suppressor protein p53 would be activated and its downstream product, Bax, translocates from the cytosol to the mitochondrial membrane, neutralizing the antiapoptotic Bcl-2 (Fig 1.4). The inactivation of Bcl-2 protein was further inhibited by binding with BH3-only protein, such as Bid. As a result, the release of cytochrome *c* from the mitochondria was induced. Together with Apaf-1 and procaspase 9, apoptosome is formed. Finally, caspase 3 was activated and apoptosis results (Cory and Adam, 2002; Okada and Mak, 2004).

The balance of antiapoptotic and proapoptotic proteins cannot be neglected.



Bax/Bcl-2 ratio is usually used to study the mechanism of apoptosis since it determines the susceptibility of cells to apoptosis and the therapeutic response to the chemotherapy (Raisova *et al.*, 2001). However, apoptosis is counteracted if the level of Bcl-2 is too high (Oltvai *et al.*, 1993), therefore, cells with higher Bax/Bcl-2 ratio is susceptible to apoptosis.

In the extrinsic pathway, when there is death signal received by the cell surface bound death receptor, the death domain would recruit adaptor molecule, which further interact with two caspase 8 (Fig 1.4). The activation of caspase 8 would further cleave and activate the downstream effector caspases, such as, caspase 3, and finally apoptosis was initiated and a series of morphological changes would be observed (Cory and Adams, 2002; Okada and Mak, 2004). The two apoptotic pathways would be converged to produce an amplified action by cleaving the Bid by caspase 8. The cleaved Bid would bind to Bax and activate the intrinsic pathway as described above (Fesik, 2005).



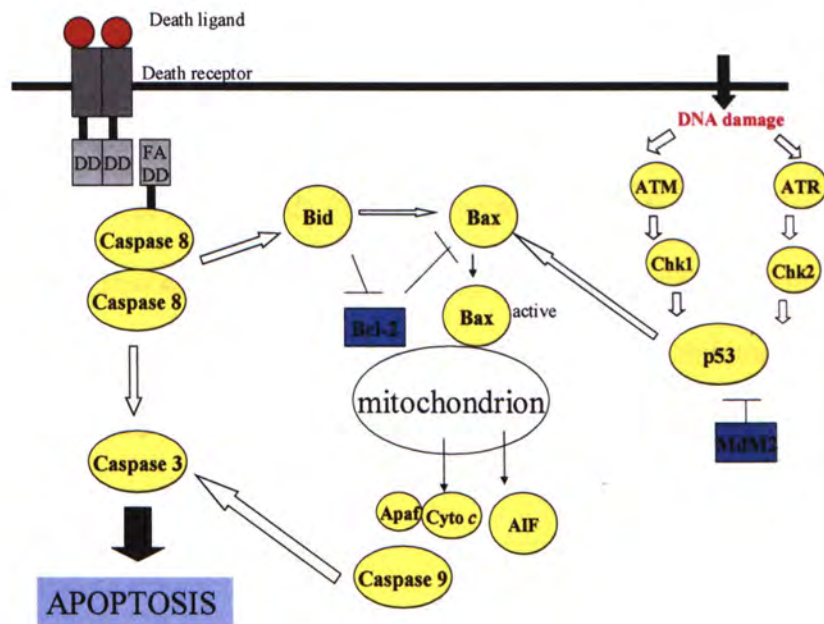


Fig 1.4 Simplified main apoptotic pathways: the extrinsic death receptors-dependent pathway (left) and the intrinsic mitochondria-dependent pathway (right) (adapted from Fesik, 2005; Igney and Krammar, 2002).

## 1.8 The novel strategies for cancer treatment

Unlike normal cells, cancer cells have uncontrolled growth and proliferation. Cancer cells strive for alive by disrupting the apoptotic pathway and deregulating the cell cycle (Fesik, 2005). Moreover, a lethal disease, metastasis, would be developed in the late stage of cancer. It refers to a group of cell detached from the original site and passed through the blood circulation to reach another site to initiate growth again. Finally, cancers are found in more than one organs (Gibbs, 2003). Thus, the recent

approach by balancing the growth and death of cancer cells can be done by controlling their cell cycle and promoting apoptosis.

PSP derived from the mycelia of *Coriolus versicolor*, (Chow *et al.*, 2003; Lau *et al.*, 2004; Yang *et al.*, 2005; Hui *et al.*, 2005), protein-bound polysaccharides (PL) isolated from *Phellinus linteus* (Li *et al.*, 2004) and  $\beta$ -glucan extracted from mycelia of *Poria cocos* (Zhang *et al.*, 2006b) all have *in vitro* growth inhibitory effects resulted from arresting cell cycle or induction of apoptosis. In particular, PSP was being most extensively investigated.

The polysaccharide-peptide (PSP) isolated from *Coriolus versicolor* inhibited the breast cancer cells (MDA-MB-231) upon 24 hour incubation and it was believed to be via apoptosis by upregulating the p21 expression and decrease cyclin D1 expression (Chow *et al.*, 2003). An ethanol extract derived from *G. versicolor* inhibited the growth of human B-cell lymphoma Raji and promyelocytic leukemic HL-60 and NB-4 cell significantly, with the proliferation of HL-60 cells being suppressed the most (Lau *et al.*, 2004). The antiproliferative activity of the ethanol extract was suggested that to be due to the induction of apoptosis as the induction of nucleosome production in a dose-dependent manner was demonstrated (Lau *et al.*, 2004).

Also, PSP exerted antiproliferative activity on HL-60 cells significantly by apoptotic induction and the mechanism involving the apoptotic pathway had been extensively investigated (Yang *et al.*, 2005). Bcl-2/Bax ratio and cytochrome *c* were significantly reduced after PSP treatment (100-400  $\mu$ g/ml) on HL-60 cells,



consistently with the decrease in mitochondrial membrane potential. PSP-treated cell population with activation of caspase-3, -8 and -9 was increased dose- and time-dependently (Yang *et al.*, 2005). Moreover, low doses of PSP (25 µg/ml) could arrest the HL-60 cells at S and G<sub>2</sub>/M phase with elevation of cyclin E expression (Hui *et al.*, 2005). This was consistent with another study that PSP inhibited the growth of Molt 4 leukemic cells via S-phase arrest and apoptosis (Lee *et al.*, 2005).

Protein-bound polysaccharides (PL) isolated from *Phellinus linteus* inhibited the growth of SW480 human colon cancer cells significantly. Flow cytometry had shown that there was an accumulation of G<sub>2</sub>/M cells and an increment of sub-G<sub>1</sub> peak dose dependently when various concentrations of PL was incubated with SW480 cells (Li *et al.*, 2004). PL-induced apoptosis was further confirmed by TUNEL assay which indicated an increased number of apoptotic stained cells in a dose-dependent manner as well. Results from the western blotting suggested that its inhibitory activity was correlated with the decrease of the Bcl-2 level and increase of the cytochrome *c* level which promoted the occurrence of apoptosis and a decrease of cyclin B1 expression so as to delay the G<sub>2</sub> to M progression (Li *et al.*, 2004). Therefore, PL inhibited the growth of SW480 cells by inducing G<sub>2</sub>/M cell-cycle arrest and apoptosis.

An alkaline-soluble β-glucan extracted from the mycelium of *Poria cocos* was reported to have antiproliferative activity on human breast cancer cell line (MCF-7) in our laboratory recently (Zhang *et al.*, 2006b). The proliferation and viability of MCF-7 cells were significantly retarded by the β-glucan. Flow cytometry analysis suggested that the β-glucan caused cell-cycle arrest at G<sub>1</sub> phase and



apoptotic induction. It was further revealed by immunoblotting that cyclin D1 and E expressions were reduced whereas Bax/Bcl-2 ratio was elevated in  $\beta$ -glucan-treated MCF-7 cells.

## 1.9 Literature Review on *Pleurotus tuber-regium*

In this study, a both edible and medicinal mushroom, *Pleurotus tuber-regium* (PTR), which belongs to the Class *Basidiomycetes* was investigated. Depending on the environmental and culture conditions, PTR can exist in the stage of mycelium, fruiting body and sclerotium (Fig 1.5) which is a solid mass of hyphae in its life cycle (Ooi, 2000). It is commonly used as an ingredient of soup and sausage and had been claimed to have certain medicinal effects such as alleviating headache, stomach pain, fever, cold, chest pain, dropsy and smallpox (Zoberi, 1973; Oso, 1977; Ude *et al.*, 2001). Antiviral activity of sclerotial PTR polysaccharides, for instance, sulfated  $\beta$ -glucans had been reported (Zhang *et al.*, 2004a). However, antitumor activity of PTR polysaccharides which was found to be the most remarkable bioactivity had been extensively investigated (Zhang *et al.*, 2001, 2004b,c, 2006a).

It has been reported that the fruiting body of PTR was high in protein (Kadiri & Fasidi, 1990) whereas its sclerotium (Fig 1.5) has over 80% of dietary fiber (Cheung & Lee, 1998). Among the various morphological forms of PTR, the structure and *in vitro* antiproliferative activity of sclerotium has been studied most. Previous studies have revealed that the hot-alkali sclerotial polysaccharide had a main chain of (1 $\rightarrow$ 3)- $\beta$ -glucan with every third unit having a (1 $\rightarrow$ 6)- $\beta$ -D-

glucopyranosyl branch on average (Deng, 2000; Zhang *et al.*, 2001). Glucose was the major monosaccharide in all sclerotial fractions, including hot-alkali, hot-water and sonicated ones (Deng *et al.*, 2000; Zhang *et al.*, 2001; Zhang *et al.*, 2004c), the efficacy of their *in vitro* antiproliferation was similar but the carboxymethylated hot-alkali sclerotial fraction was the most effective fraction in suppressing the growth of HL-60 cells.

Hot-alkali fractions were extracted from the sclerotia of PTR having molecular weight of a range from  $1.0 \times 10^4$  –  $42.2 \times 10^4$ . The fractions with moderate molecular weight ( $5.8 \times 10^4$  –  $17.1 \times 10^4$ ) that existed as a random coil had antiproliferation towards HL-60 and HepG2 cancer cell lines (Zhang *et al.*, 2001). It was shown that the fraction having molecular weight of  $17.1 \times 10^4$  inhibited the cell growth most, showing more than 40% inhibition on HK-60 at 50  $\mu\text{g/ml}$  and more than 60% inhibition on HepG2 cells at 100  $\mu\text{g/ml}$  (Zhang *et al.*, 2001). However, the hot-water and sonicated fractions having a molecular weight of  $43.5 \times 10^4$  and  $4.01 \times 10^4$ , respectively had only a inhibitory % of less than 40% against the HL-60 cell at 200  $\mu\text{g/ml}$  (Zhang *et al.*, 2004c). Besides, the carboxymethylated derivatives of the above hot-alkali (1 $\rightarrow$ 3)- $\beta$ -glucans were water soluble had higher molecular weight, ranging from  $2.08 \times 10^4$  –  $53.2 \times 10^4$ . All the carboxymethylated fractions possessed higher *in vitro* antiproliferative activity towards HL-60 cells (Zhang *et al.*, 2004b). Recently, the mechanism for the *in vitro* antiproliferative activity of this carboxymethylated  $\beta$ -glucan against MCF-7 breast cancer cell line was shown to be via G<sub>1</sub> arrest by down-regulating cyclin D1 and cyclin E expressions and apoptotic induction by lowering Bcl-2 expression and increasing the Bax/Bcl-2 ratio (Zhang *et al.*, 2006a).



The water-soluble polysaccharides isolated by hot water and ultrasonication from PTR mycelia have also been evaluated from their antitumor activity (Zhang *et al.*, 2004c). Both mycelial fractions were found to have lower carbohydrate content but higher protein content than the sclerotial fractions. Nevertheless, they were mainly consisted of glucose. The hot-water and sonicated mycelial fractions had higher molecular weight ( $76.2 \times 10^4$  and  $4.27 \times 10^4$  MW, respectively) than the corresponding sclerotial fractions and also gave stronger growth inhibitory effect more than 50% inhibition at 200  $\mu\text{g/ml}$  on HL-60 cells (Zhang *et al.*, 2004c).



Fig1.5 Sclerotia of *Pleurotus tuber-regium* (PTR)



## 1.10 Objectives

Besides the biological response modifying properties, studies on the direct *in vitro* inhibition on cancer cell growth by mushroom non-starch polysaccharides have been increasing. Polysaccharides extracted from *Lenitnus edodes*, *Ganoderma lucidum*, *Coriolus versicolor* and *Poria cocos* have been shown to have strong antiproliferative activities against different cancer cell lines *in vitro* (Hui *et al.*, 2005; Jiang *et al.*, 2004; Surenjav *et al.*, 2006; Zhang *et al.*, 2006b). Although the mechanisms behind these observations still need further investigation, they might be related to the pathway controlling the cell-cycle arrest and apoptosis that regulate the balance between cell death and cell proliferation so as to eliminate the cancer cells without harming the host.

Previous findings have demonstrated that hot alkali-soluble polysaccharides and its carboxymethylated derivatives, as well as hot water-soluble mycelial polysaccharides from PTR had potent *in vitro* antiproliferative activities. However, the mechanism was poorly understood. Characterization and bioactivity of polysaccharides extracted from fruiting body and culture medium of PTR have not yet been examined.

In this project, the chemical composition of the extracts from PTR fruiting body was evaluated and compared with that of the PTR sclerotial, mycelial and crude extracellular extracts investigated previously (Wong, 2004; Zhang *et al.*, 2004c). Besides, the *in vitro* antiproliferative activity of the extracts isolated from PTR mycelium, fruiting body and culture medium were studied in order to elucidate the plausible mechanism(s) involved which might be associated with cell cycle and/or

apoptotic pathways. An *in vitro* comparative study was carried out to explain the structure-activity relationship involved in these mushroom extracts and tumor cell antiproliferation.



### 2.1 Materials

#### 2.1.1 Assay kits

The protein assay kit was purchased from Sigma (Catalog number: P 5656). The cell proliferation ELISA BrdU incorporation assay kit (chemiluminescent) (Catalog number: 11669915001) and the annexin-V-FLUOS staining kit (Catalog number: 11988549001) were purchased from Roche Applied Science.

#### 2.1.2 Mushroom samples

Fruiting bodies of *Pleurotus tuber-regium* (PTR) (Fig 2.1) were obtained from the Sanming Mycological Institute in Fujian of China. PTR mycelia (Fig 2.1) were obtained from the submerged fermentation in a 8L fermentor using a basal medium that contained 4g/L yeast extract, 1g/L  $\text{KH}_2\text{PO}_4$ , 0.6g/L  $\text{MgSO}_4 \cdot 7\text{H}_2\text{O}$  and 30g/L glucose described previously (Wong, 2004).



Fig 2.1 Fruiting body (left) and mycelia (right) of *Pleurotus tuber-regium* (PTR)

### 2.1.3 Cell lines and their subculture

Human acute promyelocytic leukemia HL-60 (ATCC no. CCL-240), human chronic myelogenous leukemia K562 (ATCC no. CCL-243), human breast cancer MCF7 (ATCC no. HTB-22), human hepatocellular carcinoma HepG2 (ATCC no. HB-8065) and monkey normal kidney Vero (ATCC no. CCL-81) cell lines were purchased from the American Type Culture Collection (ATCC). Human foreskin Hs68 (ATCC no. CRL-1635) was provided by Professor Y.S. Wong of the Department of Biology at CUHK.

The HL-60, MCF-7, HepG2 and Vero cells were grown in Roswell Park Memorial Institute (RPMI) 1640 medium (Sigma) (1.5 g/L sodium bicarbonate was added, pH was adjusted to 7.4) while the K562 and Hs68 cells were grown in Dulbecco's Modified Eagle's Medium (DMEM) (GIBCO) (2 g/L sodium bicarbonate was added, pH was adjusted to 7.4). Both media were supplemented with 10% fetal bovine serum (FBS) (GIBCO) and 1% antibiotics (100 units/ml penicillin and 100 µg/ml streptomycin) (GIBCO). The cells were incubated in a 5% carbon dioxide humidified incubator at 37°C. Cells with a density of at least  $2.5 \times 10^5$  cells were cultured in a 25 cm<sup>2</sup> tissue-culture flask.

They were subcultured about every three days according to the ATCC guidelines. There were a few differences between the procedure of subculture for suspension and adherent cancer cell lines. For the suspension HL-60 and K562 cancer cells, a part of the cells was transferred into a new tissue-culture flask with addition of 7 ml of fresh medium when subculture. For the adherent MCF-7, HepG2,



Vero and Hs68 cancer cells, the medium in the tissue-culture flask was first removed and washed with phosphate buffered saline (PBS) (pH 7.4) to remove the remaining medium that contained trypsin inhibitor. The cells were trypsinized with 1 ml of trypsin-EDTA solution (2% EDTA and 2.5 % trypsin solution were diluted by sterile PBS) for about 2 minutes until they were all detached from the bottom of the tissue-culture flask. Together with 4 ml of the corresponding medium, they were subject to centrifugation at 1000 rpm for 5 minutes. Cell pellets were resuspended in fresh medium and a part of the cell suspension was transferred to new tissue-culture flasks which containing 7 ml of fresh medium.

#### 2.1.4 Antibodies

Purified mouse anti-human monoclonal antibodies purchased from BD Biosciences Pharmingen and Sigma Chemical as listed below. Goat anti-mouse secondary antibody was from an Immun-Star Goat Anti-Mouse (GAM)-AP Detection Kit purchased from Bio-Rad Laboratories.

Table 2.1 The antibodies used in determination of expression of proteins

Primary Antibody	Brand	Catalog Number	Approximate molecular weight (kDa)	Dilution applied
Anti-Cyclin E	BD Biosciences Pharmingen	551160	50	1:250
Anti-Cdk1/Cdc2		610037	34	1:2500
Anti-Cdk2		610145	33	1:2500
Anti-Bcl-2		610539	26	1:500
Anti-Bax		610983	21	1:250
Anti-β-actin	Sigma Chemical	A5316	42	1:5000



## 2.2 Extraction of mushroom polysaccharides

### 2.2.1 Hot-water extracts from mushroom fruiting body

The PTR fruiting bodies were first milled into powder a mechanical grinder (MF10, IKA) to a particle size of 0.5 mm and were kept in distilled water (1:25 w/v) at 95 °C for 2 hours with stirring (Fig 2.2). The extraction mixture was centrifuged at 14000 rpm for 40 minutes and the supernatant was then dialyzed against ultrapure water until the total dissolved solute (TDS) was below 10 µg/ml so as to remove molecules with molecular weight smaller than 6000-8000 daltons. The retentate was lyophilized by a freeze-drier (LABCONCO 7960013, Freezone). The above extraction was repeated twice to obtain a total of three hot water extracts from PTR fruiting body designated as HWE1, HWE2 and HWE3, respectively.

### 2.2.2 Hot-water extracts from mushroom mycelia

The hot-water PTR mycelial extracts were obtained by procedures previously described (Wong, 2004). In brief, the mycelium of PTR was homogenized with distilled water (1:25 v/v) using a Waring laboratory blender (WARING 8011) at high speed and the homogenate was boiled for one hour. The supernatant was obtained after centrifugation. The above process was repeated twice to obtain a total of three supernatants. They were pooled together and mixed with four volumes of 95% ethanol overnight to precipitate the polysaccharides. The mixture was centrifuged at 4800rpm for 5 minutes and then the precipitates were re-dissolved in distilled water

and dialysed against distilled water until the total dissolved solute (TDS) was below 10 µg/ml to remove any small molecules. The retentate containing the PTR mycelial hot-water soluble extract was lyophilized and was coded as EDP (Fig 2.3a).

### 2.2.3 Exo-polysaccharides from submerged fermentation medium

Exo-polysaccharides contained in the culture medium of PTR mycelia was concentrated and purified by ultrafiltration using a Pall Gelman Maximate System with a cassette of MW 10,000 cut off. About 1000 ml of culture medium was concentrated by ultrafiltration and then about 4L of distilled water was added to the concentrate for washing. The above process was repeated for eight times until the TDS was below 5 µg/ml and the solution was finally concentrated to about 500ml (Wong, 2004). After lyophilization, the solid powder containing the PTR exo-polysaccharide was coded as CEP (Fig 2.3b).

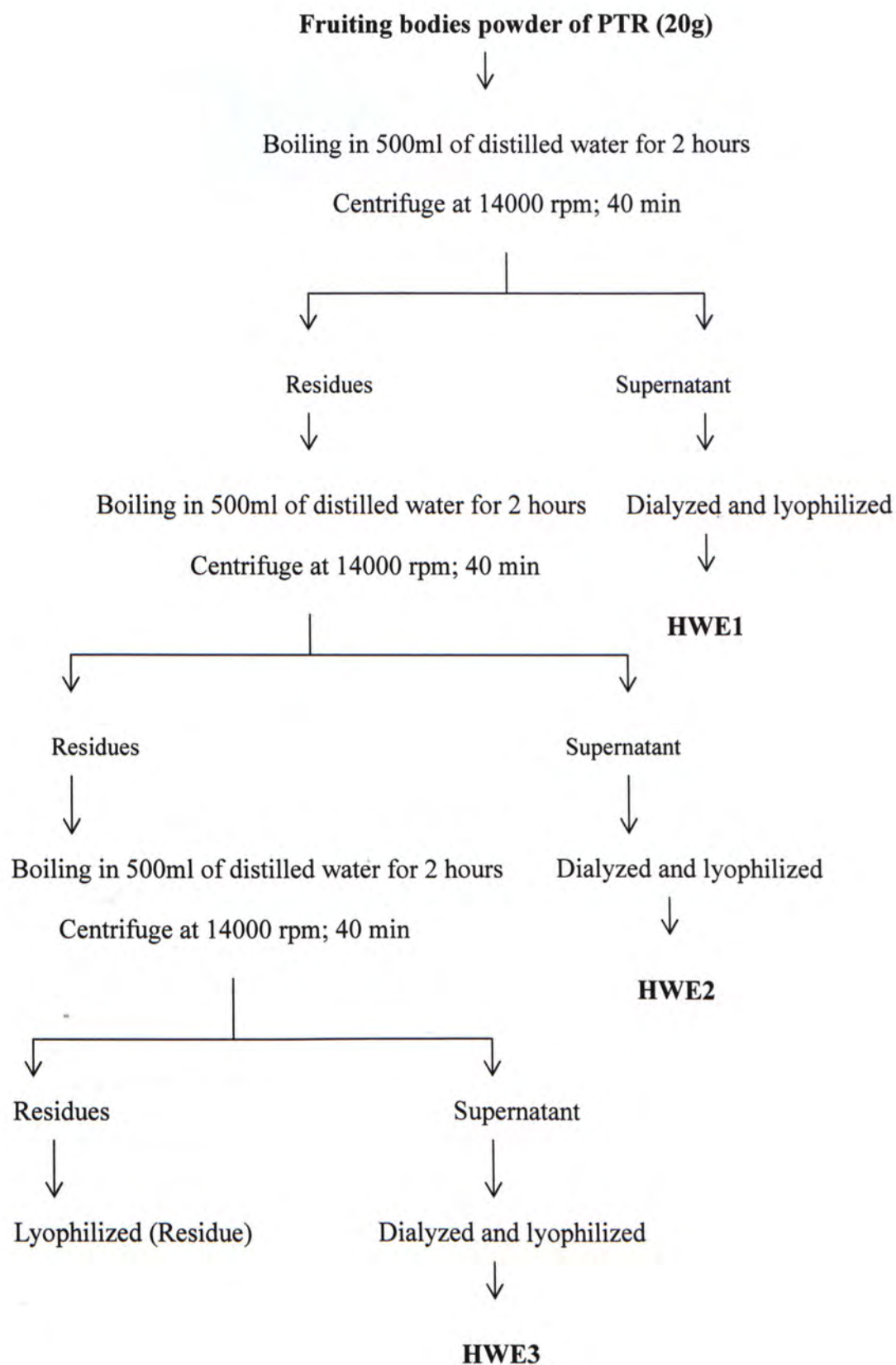


Fig 2.2 Hot water extraction scheme of fruiting bodies of PTR



(a)



(b)



Fig 2.3 The freeze-dried powder of PTR extracts from (a) mycelium and (b) culture medium.

## 2.3 Chemical and physio-chemical composition of PTR extracts

### 2.3.1 Neutral monosaccharides

The sugars inside the PTR extracts were first acid hydrolyzed and were then converted into alditol acetate derivatives (3.3.1.1 and 3.3.1.2). The neutral sugar derivatives of the PTR extracts were separated and analyzed quantitatively by gas chromatography (GC) (3.3.1.3) (Blakeney *et al.*, 1983). Besides, the content of acidic sugars was measured by a colorimetric method (3.3.2) based on the Official Methods of Analysis (AOAC) method (Theander *et al.*, 1995).

#### 2.3.1.1 Acid Depolymerization

About 15 mg of PTR sample was mixed with 0.7 ml of 12M concentrated sulphuric acid at 35 °C for one hour with occasional vortex. The mixture was diluted

to 2M sulphuric acid by adding 3.5 ml of distilled water. The acid hydrolysate of the sample extract was produced after boiling the mixture at 95 °C for one hour with occasional vortex and cooled under tap water to room temperature. Two standard sugar mixtures (1.5 ml of each; Standard I: 0.2005 g of arabinose, 0.2006 g of fucose, 0.2004 g of galactose, 0.2006 g of galactosamine, 0.2001 g of glucosamine; Standard II: 0.2003 g of glucose, 0.2000 g of mannose, 0.2001 g of rhamnose, 0.2000 g of ribose and 0.2003 g of xylose) were prepared and undergone similar acid hydrolysis as the PTR samples.

#### 2.3.1.2 Neutral sugar derivatization

Three milliliters of the above acid hydrolysates were transferred into new test tubes and were cooled in ice followed by the addition of 1 ml of internal standard, allose (1 mg/ml). Appropriate amount of 12M and 2M of ammonia were added into samples and standards, respectively with thorough vortex-mixing to ensure their alkalinity. Five microliters of octan-1-ol which acted as an anti-foaming reagent was added to the test tubes. The reduction of the hydrolyzed monosaccharides was done by adding 0.2 ml of freshly prepared sodium borohydride (200 mg/ml in 2M ammonia) and the mixture was kept at 40 °C for 30 minutes. The mixture was vortex-mixed with 0.4 ml of glacial acetic acid. An aliquot of the acidified mixture (0.2 ml) was transferred to another test tube and was incubated at room temperature for 10 minutes together with 0.3 ml of 1-methylimidazole and 2ml of acetic anhydride for acetylation. The excess acetic anhydride was degraded by adding 5 ml of distilled water with vortex-mixing. After the mixture was cooled to room temperature, 1 ml of dichloromethane was added and the mixtures were stood for 10 minutes for phase



separation. After the upper layer was removed, the lower layer was washed twice with 1 ml of distilled water. The lower layer containing the alditol acetates derivatives was dried with anhydrous sodium sulphate and then stored in a vial at -20°C before GC analysis.

#### 2.3.1.3 Determination of neutral sugar composition by GC

The alditol acetates derivatives of the neutral sugars were measured by a GC chromatograph (Hewlett-Packard 6890, USA) with an Alltech DB-225 capillary column (15 m x 0.25 mm i.d., 0.25 µm film) and an oven temperature program of initial temperature 170°C, followed by a temperature rise of 2°C/min to 220°C with a final hold of 10 minutes. The injector and detector temperature was set at 270°C. Helium was used as carrier gas and the alditol derivatives were detected by flame ionization detector. Calibration was made with the ten monosaccharides mentioned above. N-acetylglucosamine was detected as glucosamine because the N-acetyl group at C-2 was deacetylated during the sulphuric acid hydrolysis (Pazur, 1994). The amount of sugar standards detected was compared with the internal standard to monitor recovery because of the losses during the processes of acid hydrolysis and derivatization as well as to correct for the different response factors (Rf) of the flame ionization detector to individual monosaccharides. The values for monosaccharides were expressed as polysaccharide residues (anhydro-sugars) by multiplying the amounts of pentoses with a factor of 0.88, hexoses with a factor of 0.90 and deoxypentoses with a factor of 0.89.



$$\text{Amount of individual monosaccharide in sample (mg)} = \frac{\text{Peak area of individual monosaccharide in sample} \times (1\text{mg/ml} \times 1\text{ml})^*}{\text{Peak area of allose in sample}}$$

$$R_f = \frac{\text{Individual monosaccharide concentration in standard (mg/ml)} \times 1.5\text{ml}^{**} \times \text{Peak area of allose in standard}}{(1\text{mg/ml} \times 1\text{ml})^* \times \text{Peak area of monosaccharide in standard}}$$

\* Allose concentration in standard tube (1mg/ml) x Volume of internal standard added

\*\* Volume of external standard added

$$\text{Individual monosaccharides \%} = \frac{R_f \times \text{coefficient} \times \text{amount of individual monosaccharides (mg)} \times 100\%}{\text{Sample weight (mg)}}$$

$$\text{Normalized individual monosaccharide \%} = \frac{\% \text{ individual monosaccharide} \times 100}{\text{Total \% monosaccharide in the sample}}$$

### 2.3.2 Uronic acid (acidic monosaccharides) content

The uronic acid content was determined by a AOAC colorimetric method (AOAC, 1996). Acid hydrolysate of the PTR sample (0.3 ml), which was obtained from the acid depolymerisation (2.3.1.1), was vortex-mixed with sodium chloride / boric acid solution (0.3 ml, 2 g sodium chloride and 3 g boric acid were dissolved in 100 ml distilled water). Five milliliters of 18M concentrated sulphuric acid was added to the mixture with vortex mixing. The mixture was kept at 70 °C for 40 minutes. After cooling the mixture to room temperature, 0.2 ml of dimethylphenol (0.1 g 3,5-dimethylphenol was dissolved in 100 ml glacial acetic acid) was added with vortex-mixing and the mixtures stood at room temperature for 10 minutes. Glucuronic acid of concentrations at 10µg/ml, 50µg/ml, 100µg/ml, 200µg/ml and 500µg/ml were used as standards. The reagent blank was 2M sulphuric acid. Absorbance of the sample solutions at 400 nm and 450 nm against the reagent blank were measured. The reading at 400 nm was subtracted from 450 nm to correct for the interference from hexoses. The formula for calculating the % acidic monosaccharides was shown below:

% Acidic monosaccharides

$$= \frac{\text{Acidic monosaccharide content derived from standard curve } (\mu\text{g/ml}) \times 4.2\text{ml}^*}{\text{Sample weight } (\mu\text{g})} \times 100\%$$

\* total volume of acid hydrolysate

### 2.3.3 Total carbohydrate content

The phenol-sulphuric acid method was applied to measure the total carbohydrate content of the PTR polysaccharides (Dubois *et al.*, 1956). Acid hydrolysate of the PTR samples from 2.3.1 was first diluted 50 times in 2 M concentrated sulphuric acid and 0.5 ml of the diluted sample was vortex-mixed with 0.5 ml of 5% phenol in water. Concentrated sulphuric acid (18M, 2.5 ml) was added rapidly and the mixture was allowed to stand for 30 minutes at room temperature. The absorbance of the sample was measured by a spectrophotometer (Genesys G5, Spectronic) at 490nm and the total carbohydrate content was quantified in reference to glucose standards with concentration of 12.5 µg/ml, 25 µg/ml, 50 µg/ml and 100 µg/ml.

% Total carbohydrate content

$$= \frac{\text{Carbohydrate content derived from standard curve (}\mu\text{g/ml)} \times 4.2\text{ml}^* \times 50^{**}}{\text{Sample weight (}\mu\text{g)}} \times 100\%$$

\* total volume of acid hydrolysate

\*\* dilution factor

### 2.3.4 Protein content

Protein content of the PTR samples was quantified by the Lowry assay (Lowry *et al.*, 1951) using a protein assay kit (Sigma). Briefly, protein standard



solutions (BSA) were prepared for a range from 25 to 200 µg/ml by distilled water. PTR samples were diluted 4 times and made up to a final volume of 1ml solution with distilled water. Lowry Reagent Solution (1ml) was mixed with 1 ml of aqueous sample solution. The mixture was stood at room temperature for 20 minutes before Folin & Ciocalteu's phenol reagent (0.5 ml) was then added to the mixture. The blank (distilled water only) and the protein standards were treated similarly to the PTR samples. After a 30-minute incubation period, the absorbance of the purple-color solution was measured by a spectrophotometer (Genesys G5, Spectronic) at a wavelength of 750nm. The protein content of the PTR samples was calculated from a standard curve of BSA.

% Protein

$$= \frac{\text{protein content derived from standard curve } (\mu\text{g/ml}) \times 1\text{ml}^* \times 4^{**}}{\text{Sample weight } (\mu\text{g})} \times 100\%$$

\* Total volume of sample solution

\*\* dilution factor

### 2.3.5 Molecular weight and the homogeneity

The molecular weight and the homogeneity of the PTR extracts were estimated by high pressure liquid chromatography (HPLC) (Waters 600E, Waters). Diluted sodium chloride (0.2M) was used as the eluent which was degassed prior injection. The samples were dissolved in 0.2M sodium chloride, filtered by the 0.22µm Millipore filter, and were then passed through a size exclusion column TSK-

Gel G3000 PW (30 cm x 7.5 mm i.d.; Supelco, Catalog Number: 8-05762) and TSK-Gel G5000 PW (30 cm x 7.5 mm i.d.; Supelco, Catalog Number: 8-05764) separately, with a PWH Guard column (7.5cm x 1.5mm i.d.; Supelco, Catalog Number: 8-06762). The flow rate of the eluent (0.2M sodium chloride) was 3.0 ml/min and the column was kept at 30 °C. The retention time of the PTR extracts and pullulan standards (Shodex Standard P-82, Showa Denko) were obtained by the Empower software (Waters). Molecular weight of PTR extracts was calculated from a calibration curve obtained from the retention time of pullulan standards against the log value of their sizes. Refractive index and ultraviolet absorbance at 280 nm were used for monitoring the amount of polysaccharides and protein in the PTR samples, respectively.

## 2.4 *In vitro* growth inhibitory effects

### 2.4.1 Trypan blue dye exclusion method

Trypan blue dye exclusion method (Zhang *et al.*, 2004c) was applied for suspension cells (HL-60 and K562 cancer cells). Cell viability is measured according to the ability of viable cells to exclude the dye. Cells were seeded ( $2.5 \times 10^3$  cells/well) on a 96-well microplate. The PTR extracts at concentrations of 12.5, 25, 50, 100, 200 and 400 µg/ml were added, followed by a 72-hour incubation. The living cells that excluded the trypan blue dye were counted using a hemacytometer. The treatment groups were compared with control having no PTR extracts added. The experiments were carried out in five replicates.

The above results were expressed as relative % surviving cells calculated as:

$$\text{Relative \% surviving cells} = \frac{\text{Viable cell number of treatment group}}{\text{Viable cell number of control}} \times 100\%$$

#### 2.4.2 Colorimetric 3-(4,5-dimethylthiazol-2-yl)-2,5-diphenyl tetrazolium bromide (MTT) assay

MTT assay was applied for adherent cells (MCF-7, HepG2, Vero and Hs68 cells). Reduction of MTT salt by mitochondrial succinate dehydrogenase gives a purplish-blue formazan product, of which amount is measured and reflects the cell viability indirectly (Mosmann, 1983). Cells were seeded ( $2.5 \times 10^3$  cells/well) on a 96-well microplate. The PTR samples at concentrations of 12.5, 25, 50, 100, 200 and 400  $\mu\text{g/ml}$  were added after the cell attachment and incubated for 72 hours. The cell viability was detected by a microplate reader (SpectraMAX 250) at 570nm as described by Mosmann (1983). The treatment groups were compared with controls without adding any PTR samples. The experiments were carried out in five replicates.

The above results were expressed as relative % proliferating cells calculated as:

$$\text{Relative \% proliferating cells} = \frac{\text{Absorbance of treatment group}}{\text{Absorbance of control}} \times 100\%$$



## 2.5 *In vitro* cell proliferation assay

An ELISA BrdU incorporation assay (chemiluminescent) which is based on the incorporation of pyrimidine analogue, BrdU, into the DNA in the S phase of proliferating cells was used to measure cell proliferation. The procedures were generally based on an ELISA BrdU kit (Roche Applied Science; Catalog number: 11669915001). In brief,  $1 \times 10^3$  cells/well were seeded on a 96-well microplate. The PTR samples at concentrations of 12.5, 25, 50, 100, 200 and 400  $\mu\text{g/ml}$  were added, followed by 72-hour incubation. Ten microliters of BrdU labeling solution was added in each well and the plate was incubated for 2 hours at  $37^\circ\text{C}$  to allow BrdU incorporated into the DNA-synthesizing cells. The solutions in each well were discarded and the wells were dried in  $60^\circ\text{C}$  oven for an hour. After that, cells were fixed and denatured with 200  $\mu\text{l}$  FixDenat solution for 30 minutes and were then incubated with 100 $\mu\text{l}$ /well of anti-BrdU-POD working solution for 90 minutes at room temperature. The cells in each well were washed by 200 $\mu\text{l}$  washing solution three times to remove the excess antibody conjugates. After removing the washing solution, the cells were incubated with the 100  $\mu\text{l}$  substrate component solution in dark for three minutes with shaking. The chemiluminescent light emitted was measured by a luminometer (ML3000 microtiter® plate luminometer, Dynatech Laboratories). The treatment groups were compared with controls without treatments. The experiments were carried out in five replicates.

The results were expressed as relative % proliferating cells calculated as:

$$\text{Relative \% proliferating cells} = \frac{\text{Chemiluminescence of treatment group}}{\text{Chemiluminescence of control}} \times 100\%$$

## 2.6 Cell-cycle analysis

The effect of the PTR extracts on the cells was assessed by flow cytometry which can quantify the cell-cycle phase distribution. Various cell densities were grown in 25 cm<sup>2</sup> culture flasks for 24 hours, 48 hours or 72 hours. The treatment groups were co-incubated with PTR samples at an appropriate concentration according to the results in 3.5. After the incubation, cells were collected into a test tube and centrifuged at 300 g for 10 minutes. The medium was discarded and the cell pellet was washed with 2 ml of PBS twice followed by centrifugation at 300 g for 10 minutes in between and then fixed in 70% cold ethanol. The fixed cell pellet was stored at -20 °C until the day before analysis.

Prior for the cell-cycle analysis, the ethanol inside the test tube was removed after centrifuging at 300 g for 10 minutes and then washed with 2 ml of PBS twice as described above. The cell pellet was then resuspended in 1 ml of solution containing 0.005 g/100 ml propidium iodide (PI) and 0.001 g/100 ml RNase A (0.121 g/100 ml of Tris-base was added; pH 8.0). The test tube was kept at 4 °C overnight. The PI-stained cell was transferred to a specific tube by filtering the cell clumps by a piece of nylon mesh placing on the mouth of the specific tube. Cell-cycle of the treated cells was detected by a EPICS-XL flow cytometer (Beckman Coulter, Miami, FL) with cell debris being excluded. Cell-cycle distribution was analyzed using the multicycle software from Phoenix Flow Systems, San Diego, CA. A DNA histogram with sub-G<sub>1</sub>, G<sub>0</sub>/G<sub>1</sub>, S and G<sub>2</sub>/M phases was constructed.



## 2.7 Apoptotic determination

Annexin V/PI staining assay can distinguish and divide cells into early apoptosis, late apoptosis and viable by detecting the changes of cell membrane permeability and the presence of phosphatidylserine (PS) on the cell surface (Engeland *et al.*, 1998). The procedures were based on an Annexin-V-FLUOS Staining Kit followed with some modifications. The density of the cells used and the general procedures were the same as cell cycle analysis (2.6). After co-incubated with the PTR extracts, the cells were counted by a hemacytometer. An amount of  $1 \times 10^6$  cells was added into three centrifuge tubes separately, followed by washing with PBS twice and an addition of 100  $\mu$ l of Annexin-V-Fluos labeling solution, fluorescein (FITC) solution and PI solution, respectively. The mixtures were kept in dark for 15 minutes and then centrifuged at 300 g for 5 minutes to obtain the cell pellets, which was then resuspended in 0.5 ml of Incubation Buffer. Positive controls were prepared for calibration by adding 3% formaldehyde into a flask of cultured cells and incubated for 10 minutes. In the culture flask, an amount of  $1 \times 10^6$  cells was added to three centrifuge tubes separately. The positive controls were treated and stained similarly as the samples. After removing the cell clumps by a piece of nylon mesh, the apoptotic cells were determined by the EPICS-XL flow cytometer using 488 nm excitation and 515 nm and  $>600$  nm bandpass filters for FITC and PI detection, respectively.

## 2.8 Expression of proteins involved in apoptosis and cell-cycle

Western blot was employed to determine the protein expression in the cells



treated with PTR extracts. Proteins isolated from the treated cells were separated by sodium dodecyl sulphate-polyacrylamide gel electrophoresis (SDS-PAGE). The protein of interest was detected by western blot (Mini-PROTEAN 3 Electrophoresis System; Bio-rad Laboratories).

#### 2.8.1 Preparation of cell lysates

A density of  $2.5 \times 10^5$  cells/ml cells was cultured in a 75 cm<sup>2</sup> tissue-culture flask and was co-incubated with the PTR extracts at the same concentration used in flow cytometry for the 24, 48 and 72 hours. The cells were centrifuged at 300 g for 10 minutes and the cell pellet was washed with PBS twice. The cell pellet was then lysed by 0.1 ml of ice-cold lysis buffer containing 2 µl of protease inhibitor cocktail (BD Biosciences Pharmingen; Cat No.: 554779) for one hour at 4°C with occasional vortexing. The cell lysate was transferred into a 1.5 ml microtube and subjected to centrifugation at 12,000 rpm for 5 minutes. The supernatant was transferred to a new microtube and was kept at -20°C before determination of protein concentration.

#### 2.8.2 Determination of protein concentrations

The protein content in the cell lysate was quantified by the BCA protein assay using BSA protein standard through the measurement of absorbance at 562nm by a microplate reader. A set of BSA standards at concentration of 12.5, 25, 50, 100, 200 and 400 µg/ml was prepared. The sample was diluted by distilled water 50-fold. One hundred microliters of working reagent from the BCA protein assay kit was added

(50 parts of reagent A was vortex-mixed with one part of reagent B) into both sample and BSA protein standards. The microplate was incubated at 37°C for 30 minutes and the absorbance was then measure by the mircoplate reader (SpectraMAX 250, Gene Co. Ltd.) at 562 nm. The protein concentration was compared and calculated in comparison with the BSA standard curve as follows.

Actual protein concentration ( $\mu\text{g}/\mu\text{l}$ ) in sample

= Protein concentration ( $\mu\text{g}/\text{ml}$ ) derived from the standard curve  $\times 50^* \times 1000^{**}$

\*dilution factor

\*\* conversion factor

### 2.8.3 Western blot

Thirty to sixty micrograms of protein from cell lysate was required. The loading in each lane of samples consisted of 10  $\mu\text{l}$  of 2x loading dye and a calculated volume of desired protein amount. Distilled water was added to make up the final loading volume to 20  $\mu\text{l}$ . The sample was heated for 5 minutes at 95°C in a Thermomixer comfort (Eppendorf, company) before loading.

The proteins in the cell lysate were packed on 5% stacking gel and electrophoresed on 12% SDS separating gel. The two glass plates were washed with water and 70% ethanol, respectively. The glass plates were held by the casting frame. Around 5 ml of 12% SDS separating gel was first added in between the two plates. The bubbles inside the glass plates were removed by gently knocking the glass plate. The gel was covered and flattened by isopropanol. After 40 minutes for gel



polymerization, isopropanol was poured off and absorbed by filter paper. After that, 5% stacking gel was added on the top of the separating gel and the comb was inserted. The gel was stood for 15 minutes.

After the gel was polymerized, the comb was removed and the glass plates were put into the tank for western blotting. The center of the tank was fully filled with 1x running buffer (14.4 g glycine, 3.03 g Tris-base and 1 g SDS were dissolved in 1L of distilled water) to ensure the wells were covered by it. Ten microliters of Precision Plus Protein dual color standards (Bio-Rad Laboratories) and 20  $\mu$ l of sample were loaded into the wells using fine-tipped pipettes. The standard marker and the sample were migrated on the stacking gel at 60V and were separated on the separating gel at 120V until the end-point of the electrophoresis which was determined by the pre-stained protein standard marker.

The separated proteins on the polyacrylamide gel were transferred to the Immuno-Blot™ PVDF membrane, 0.2  $\mu$ m for protein blotting (Bio-rad Laboratories, Catalog: 162-0177). The membranes were first pre-wetted by methanol. Then, the sponges, filter papers and the pre-wetted membranes were shaken in freshly-prepared 1x transfer buffer (14.4g glycine and 3.03g Tris-base were dissolved in 800 ml of distilled water, followed by an addition of 200 ml of methanol). The membrane sandwich was assembled based on the kit instructions with the following sequence from the negative side to the positive side: sponge, filter paper, gel, membrane, filter paper, and then sponge. Bubbles were squeezed out from the membrane sandwich with the help of a test tube. After placing it and the ice block into the transfer tank, it was fully filled with 1x transfer buffer. The transfer process was carried out at 110V for one hour on a hot-plate with continuous stirring to keep a constant heat flow. The



membrane was then shaken in the freshly-prepared blocking buffer (0.5% Auora milk powder and 0.5% Tween 20 were dissolved in 1x PBS) for one hour.

The membrane was kept in a 50 ml centrifuge tube, probing with 3 ml of the corresponding primary antibody which was diluted by the blocking buffer according to the recommendation (Table 3.1). The centrifuge tube was rotated in a hybridization oven kept at 4 °C overnight. The membrane was then washed by PBST (0.5% Tween-20 was dissolved in 1x PBS) on a shaker for 15 minutes. It was then probed with 3 ml of the goat anti-mouse secondary antibody conjugated to alkaline phosphatase (AP) which was diluted by the blocking buffer (dilution: 1:3000) for an hour at room temperature. After washing the membrane by PBST on a shaker for 30 minutes, it was kept in the PBST until the detection process was performed.

The protein of interest was visualized by the chemiluminent protein detection system. One milliliter of detection substrate buffer from the Immun-Star Goat Anti-Mouse (GAM)-AP Detection Kit (Bio-Rad Laboratories) was added on the membrane for 5 minutes. Finally, in the dark room, the membrane was covered by an X-ray film in a film cassette with an optimal time and the film was developed by the X-ray film processor (Kodak).

Anti- $\beta$ -actin antibody was used as a loading control. After the membrane was rinsed by PBST, it was then placed into a sealed box and was shaken in the stripping buffer at 50°C for 20 minutes in an orbital shaker. The membrane was then rinsed by PBST again to remove the remaining stripping buffer. After that, it was shaken in the blocking buffer for one hour. It was re-probed with anti- $\beta$ -actin primary antibody and detection was made according to the procedures described above.

The western blot was scanned and quantified with the software LumiAnalysis 3.1 of Lumi-Imager (Roche Molecular Biochemicals). The integrated values for each band were taken and their ratios against  $\beta$ -actin were calculated.

$$\text{Relative quantity of the band for sample} = \frac{\text{integrated value of band for sample}}{\text{integrated value of band for } \beta\text{-actin}}$$

$$\text{Normalized band value for sample(\%)} = \frac{\text{Relative quantity of the band for sample}}{\text{Relative quantity of the control band}} \times 100\%$$

## 2.9 Statistics

Data in all the assays were statistically assessed by Student's t-test and differences with a *p*-value of less than 0.05 were considered significant. The dose-response curves were plotted using the GraphPad PRISM® software.

### 3.1 Yield of extract samples isolated from different developmental stages of PTR

Hot-water extraction is commonly used since hot water extracts obtained from other edible mushrooms usually have exhibited strong antitumor activities (Chihara, 1969; Ikekawa, 1968, 1969), particularly those extracted from the fruiting bodies and mycelia (Reshetnikov, 2001). Hot water extract of *Agaricus bisporus* inhibited the growth of S180 and Ehrlich sarcoma cells by 90% and 100% *in vitro*, respectively (Ying *et al.*, 1987). Intravenous administration of insoluble (1→3)- $\beta$ -D-glucans from yeast cell wall had raised many side effects such as hepatoplenomegaly (Riggi & Di Luzio, 1962), granuloma formation (Williams *et al.*, 1985), micro-embolization and enhanced endotoxin sensitivity (Browder *et al.*, 1987). Hot water extracts would not cause these problems and therefore facilitate their medicinal and clinical applications (Zhang *et al.*, 2004b). Moreover, the conformation of polysaccharides which is believed to be necessary for antitumor activity would be retained more easily than other treatments like alkaline extraction (Hobbs, 2005).

Why made 3 extracts? The yield of the three hot-water extracts (HWEs) obtained from the fruiting bodies of PTR, HWE1, HWE2 and HWE3, was 7.65%, 2.04% and 2.08%, respectively (Table 3.1). The yield was comparatively higher than that of three hot-water extracts sequentially isolated from the fruiting body of *Agaricus blazei* at 121 °C for two hours (Ohno *et al.*, 2001), of which was 3.2%, 0.5% and 0.4%, respectively. Usually, most water-soluble molecules are extracted preferentially in the first round of extraction. The yield of all the PTR extracts,



including the sclerotial one (SCP) investigated previously, was below 10% (Table 3.1). The low yield of hot-water extraction (less than 10% dry weight) is common in other mushroom polysaccharides as well. Since polysaccharides have high molecular weight with different conformations and degree of branching, they can form gel or precipitate in aqueous solutions easily (Mizuno *et al.*, 1995). Increase in the extraction temperature could enhance the degree of solubility of polysaccharides in aqueous solutions. However, extraction temperature of 95 °C was still employed in this project because excessive heating would reduce the molecular weight of polysaccharides and disrupt their conformation which could not be regained after cooling (Hobbs, 2005). The triple helix structure of Schizophyllan was lost after heating above 135 °C (Brant *et al.*, 1997).

The yield of mycelial extract of PTR (EDP) (4.38% dry weight) was consistent with that obtained previously (4% dry weight) (Zhang *et al.*, 2004c) (Table 3.1). The relatively higher yield of EDP obtained might be due to the fact that the mycelia were extracted twice more than the previous study. On the other hand, the yield of EDP was high when comparing with the mycelial polysaccharides extracted from *Poria cocos* of various strains and culture media by hot water, ranging from only 1.7% to 3.1% only (Jin *et al.*, 2003).

The yield of extracellular extract of PTR (CEP) was only 0.091g dry weight per liter of culture medium of PTR mycelial fermentation (Table 3.1), which was much lower than those obtained from *Ganoderma lucidum* and *Ganoderma tsugae*, which were 0.85g and 0.5g per liter of culture medium, respectively (Sone *et al.*, 1985, Peng *et al.*, 2003).

Table 3.1 The yield, total carbohydrate and protein content of the PTR extracts. <sup>a</sup>

<i>Developmental stage</i>	<i>PTR extracts</i>	<i>Yield</i>	<i>Total carbohydrate content</i>	<i>Protein content</i>
Culture medium*	CEP	0.091 <sup>b</sup>	83.4±1.30	15.9±0.19
Mycelium*	EDP	4.38	87.2±4.73	3.24±0.14
Fruiting body	HWE1	7.65	42.4±2.90	35.4±0.80
	HWE2	2.04	45.3±0.69	30.4±0.88
	HWE3	2.08	32.0±3.36	36.1±0.10
Sclerotium **	SCP	3.60	77.0	5.10

<sup>a</sup> % dry weight , <sup>b</sup> g dry weight/L

\* data from Wong, 2004

\*\* data from Zhang *et al.*, 2004c

### 3.2 Chemical characteristics of hot-water extracts isolated from different stages of PTR

#### 3.2.1 The total carbohydrate and protein content of PTR extracts

The carbohydrate content of PTR extracts was determined by using glucose as standard in the phenol-sulphuric assay while their protein content was determined by the Lowry method using BSA protein as reference. Both CEP and EDP were high in total carbohydrate content, which were accounted for 83.4% and 87.2%, respectively (Table 3.1). This was concomitant with their low protein content, which were 15.9% and 3.24%, respectively (Table 3.1). Therefore, polysaccharides were the major constituent in these two extracts, with protein as the minor component.



The water-soluble mycelial polysaccharides of PTR isolated from previous study had 51% of carbohydrate and 10.7% of protein (Zhang *et al.*, 2004c). The small variations in the chemical composition between the present results with those obtained previously was reasonable as different extraction process and conditions were adopted. In previous study, the powder mycelia was first defatted and suspended in 0.9% sodium chloride solution, followed by boiling at 100°C for 3 hours once. The mycelial polysaccharide was obtained after dialysis and lyophilization. However, in the present study, the mycelia were extracted by hot water three times and then ethanol-precipitated before dialysis. It is believed that the extraction conditions applied in the present study could isolate the mycelial extract with higher carbohydrate content and comparatively larger amount of polysaccharides. Water soluble sclerotial polysaccharides (SCP) of PTR was also high in carbohydrate content (77%) but only small amount of protein (5.1%) was found (Zhang *et al.*, 2004c) (Table 3.1), matching its high content of dietary fiber (>80%) (Cheung & Lee, 1998).

On the contrary, the three HWEs isolated from the fruiting body had a comparatively lower total carbohydrate content ranged from 32.0% to 46.1% but much higher protein content of over 30% (Table 3.1). These results were reasonable as it has been revealed that the fruiting body of PTR was high in protein (around 10g/100g) (Akindahunsi and Oyetayo, 2006; Kadiri & Fasidi, 1990). While the total carbohydrate content, in descending order, was HWE2, HWE1 and HWE3. The protein content in decreasing order showed an opposite trend of HWE3, HWE1 and HWE2 (Table 3.1). Therefore, the difference between carbohydrate and protein amounts was the largest in HWE2. However, similar amounts of total carbohydrate and protein (ratio in terms of % dry weight: 0.9:1) was observed in HWE3



### 3.2.2 The monosaccharide composition of PTR extracts

The monosaccharides in PTR extracts (except acidic monosaccharides which was analyzed by a colorimetric method separately) could be separated and detected by gas chromatography (GC). Based on the result of GC, although glucose was dominant in HWEs, a considerable percentage of mannose and galactose, and a minor amount of ribose were obtained. This suggested that there might be more than one monosaccharide made up the backbone of the polysaccharides of HWEs. When comparing the three HWEs, the proportion of glucose and uronic acids was increasing from HWE1 to HWE3 but other monosaccharides, including mannose, galactose and ribose, were decreasing (Table 3.2). It was suggested that more than one type of polysaccharides might present in the HWEs.

N-acetylglucosamine, derived from chitin which is a structural cell wall polysaccharide in fungi, was only found in CEP and EDP. Obviously, glucose was the major monosaccharides in EDP, suggesting glucan was probably the main type of polysaccharides in the PTR mycelium. Similarly, water-soluble mycelial polysaccharides investigated previously found glucose was the major sugar (73.1%), with small amount of galactose, mannose, glucosamine and uronic acid (14.3%, 9.4%, 3.1% and 0.5%, respectively) (Table 3.2). The mycelial polysaccharides isolated from wild strain *Poria cocos* (a sclerotium-forming mushroom similar to PTR) cultivated in a medium containing corn steep liquor was also glucose-dominant (70.7%) (Jin *et al.*, 2003). On the other hand, mannose was the main monosaccharides in CEP. It was common that high mannose content was found in exo-polysaccharides, such as that isolated from the *Poria cocos* mentioned above,

consisted of 61.7% mannose (Jin *et al.*, 2003).

The content of acidic monosaccharides, for instance, glucuronic acid and galacturonic acid, were estimated by the total amount of uronic acids. Despite of the fact that CEP had 3.25% of uronic acids which was the highest, all of the PTR extracts consisted of less than 1% of uronic acids (Table 3.2). Thus, the content of acidic monosaccharides in PTR extracts was considered as low and insignificant.

In summary, three kinds of monosaccharides involving glucose, mannose, and galactose were detected in all fractions but in different proportions. Except the mannose-rich CEP, glucose was most dominant in three HWEs, EDP and SCP (Zhang *et al.*, 2004c) but the amount of mannose and galactose in the HWEs was also very substantial.

Table 3.2 The monosaccharide composition of the PTR extracts <sup>a</sup>

Monosaccharide composition	PTR extracts					
	EDP*	CEP*	SCP **	HWE1	HWE2	HWE3
Rhamnose	0.55	n.d. <sup>b</sup>	n.d.	n.d.	n.d.	n.d.
Fucose	0.14	0.30	n.d.	n.d.	n.d.	n.d.
Ribose	0.06	n.d.	n.d.	7.66	6.48	4.24
Arabinose	0.08	n.d.	n.d.	n.d.	n.d.	n.d.
Xylose	0.09	0.29	n.d.	n.d.	n.d.	n.d.
Mannose	4.76	76.0	7.70	26.9	21.8	20.4
Galactose	3.35	5.37	6.90	16.3	15.4	14.8
Glucose	87.3	7.10	85.4	49.2	56.3	60.5
Glucosamine	2.69	4.68	n.d.	n.d.	n.d.	n.d.
Galactosamine	n.d.	2.99	n.d.	n.d.	n.d.	n.d.
Uronic acids	0.95	3.25	n.d.	0.29	0.58	0.70

<sup>a</sup> % monosaccharide of total carbohydrate

<sup>b</sup> n.d. not detectable

\* data from Wong, 2004

\*\* data from Zhang *et al.*, 2004c

### 3.3 Molecular weight distribution of PTR extracts

In order to determine the structure of PTR extracts, their molecular weight distributions and homogeneities were examined by HPLC. A TSK-Gel G5000PW and a G3000PW columns were chosen in HPLC for analyzing the water-soluble PTR extracts. The hydrophilic resin has excellent chemical and mechanical stability between pH2 and 12. The G5000PW column has a particle size of 17µm with pore size of 1000Å whereas G3000PW has a particle size of 10µm with pore size of 200Å.



There two columns were employed so that a broad range of molecular weight distribution could be determined.

The molecular weight of PTR HWEs was estimated by the TSK3000PW column. Two peaks of  $0.10 \times 10^4$  and  $1.32 \times 10^4$ , and another peak of larger than  $21.2 \times 10^4$  were detected by the RI detector (Data not shown). The SEC chromatogram indicated that all small molecules were successfully removed by extensive dialysis. Also, TSK3000PW was not efficient enough to separate and analyze the polymers of larger molecular weight because the pullulan standards P200-P800 were overlapping (Fig 3.1). When analyzing by G5000PW column, the pullulan standards were well separated (Fig 3.2). Three obvious fractions were determined in the three HWEs chromatograms with molecular weight ranging from  $0.5 \times 10^4$  to  $185.5 \times 10^4$  in reference to pullulan standards (Table 3.3). It was not surprising that more than one fraction was found in PTR HWEs since they were only crude water extracts. Polysaccharides in the fruiting bodies of mushroom are usually very heterogeneous. However, the molecular weight of Fraction 3 was much lower than those of polysaccharides isolated from other mushrooms which were well-known for their antitumor activities. For example, Lentinan and Schizophyllan had a MW of  $50 \times 10^4$  and  $45 \times 10^4$  (Mizuno *et al.*, 1995). Thus, only Fractions 1 in HWEs was considered as the most potential antiproliferative polysaccharides. UV detector was specified for the presence of protein. Obviously, strong UV absorbance was observed in fraction 1 and 3 of all three PTR HWEs (Fig 3.3b, 3.4b and 3.5b), implying certain amount of protein was associated with the polysaccharides which was consistent with the high protein content of PTR HWEs (3.2.1).

In the chromatograms of all PTR HWEs, fraction 1 of HWE2 had highest

molecular weight ( $185.5 \times 10^4$  MW). Besides, the major fraction in HWE3 was the high-molecular-weight fraction 1. It might be that the polysaccharides obtained are mainly originated from the cell wall of mushroom. Those compounds with small molecular weight were easily released out and was extracted preferentially in the first extraction. By applying a longer boiling time, the cell wall would be further fragmented and therefore those with higher molecular weight which located in the inner cell wall could be isolated in the subsequent extraction. Besides, it might be possible that the three fractions obtained in three HWEs had different degree of branching. Evidence showed highly-branched  $\beta$ -glucans are located at the outer cell surface while linear  $\beta$ -glucans are linked with chitin covalently (Beelman *et al.*, 2003). Therefore, more branched polysaccharides might exist in fraction 2 and 3 whereas fraction 1 might contain more linear polysaccharides. Interestingly, HWE2 has the highest molecular weight among the three PTR extracts, suspecting that HWE2 might have a more expanded conformation and therefore a higher molecular weight was measured by the SEC HPLC. Further investigation was required for confirmation.

CEP had the smallest molecular weight of  $4.41 \times 10^4$  (Wong, 2004) whereas the molecular weight of HWEs was the largest. EDP and SCP consisted of two major fractions, but mainly composed of that with higher molecular weight ( $50.9 \times 10^4$  MW and  $43.5 \times 10^4$  MW, respectively) (Wong, 2004; Zhang *et al.*, 2004c). Two fractions were also detected from mycelial polysaccharides isolated previously from PTR and the molecular weight of the major one was  $76.2 \times 10^4$  (Zhang *et al.*, 2004c). Such phenomenon commonly occurred as different extraction conditions was used and so different polysaccharides would be isolated. For example, lentinan isolated from *Lentinus edodes* was a (1 $\rightarrow$ 3)  $\beta$ -D -glucan with MW of about  $5 \times 10^5$  (Mizuno *et al.*,



1989) whereas a polysaccharides isolated from similar process mainly consisted of D-glucose had MW of  $20.3 \times 10^4$  (Zheng *et al.*, 2005), and an ethanol-based extract of *L. edodes* which had molecular weight of a  $1.4 \times 10^4$  revealed by SEC HPLC (Gu, 2005).

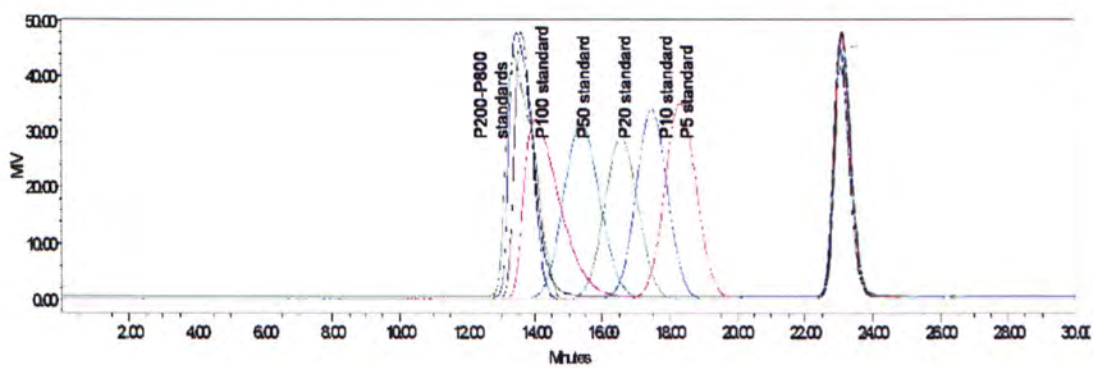


Fig 3.1 The SEC profile of pullulan standards by a TSK3000PW column at 30°C with sodium chloride (0.2M) at a flow rate of 3.0 ml/min and RI detection.

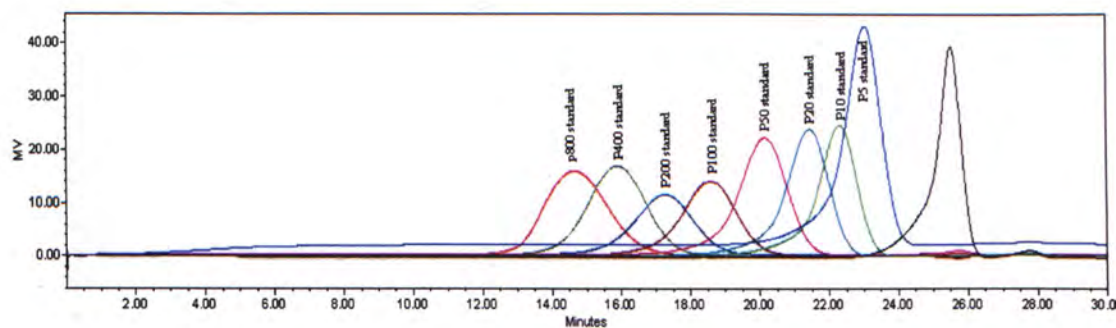


Fig 3.2 The SEC profile of pullulan standards by a TSK5000PW column at 30°C with sodium chloride (0.2M) at a flow rate of 3.0 ml/min and RI detection.



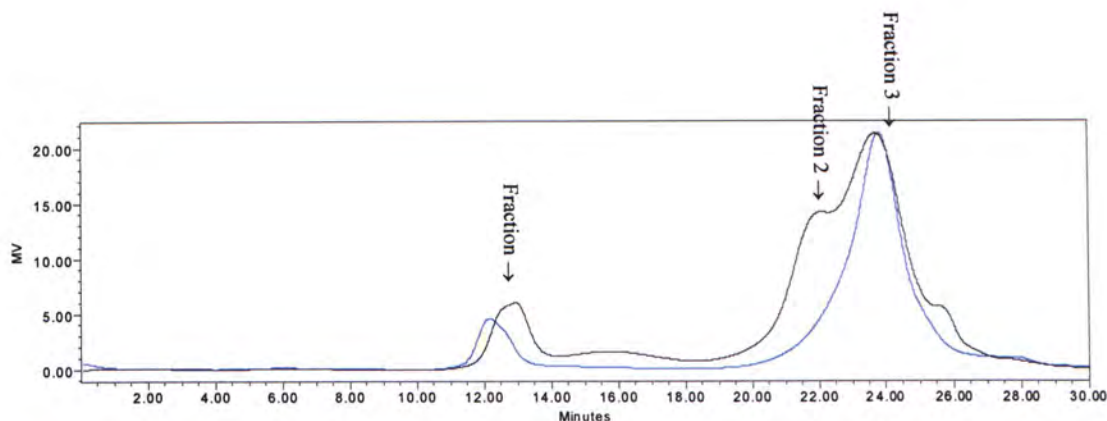


Fig 3.3 The HPLC chromatogram of HWE1 obtained by a TSK5000 column with detection by refractive index (black line) alone and together with UV absorbance (blue line). The eluent was 0.2M sodium chloride at a flow rate of 3.0 ml/min and the column was kept at 30°C.

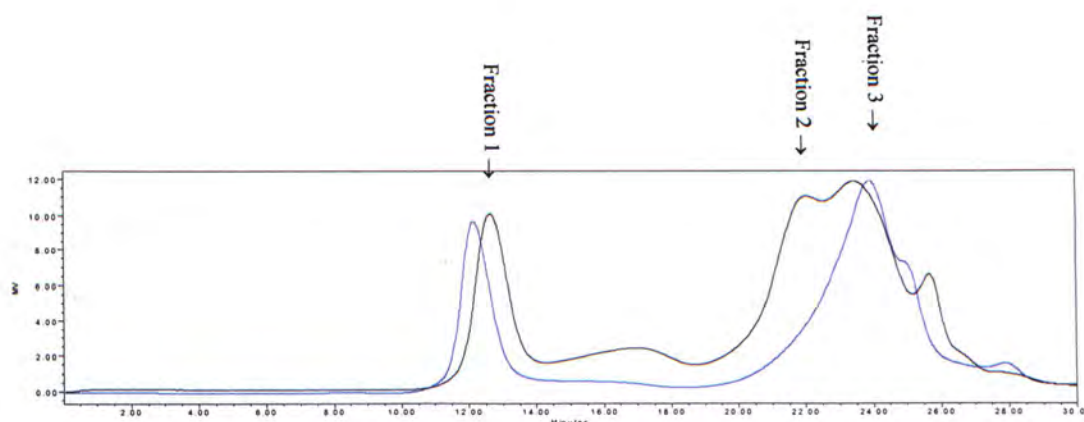


Fig 3.4 The HPLC chromatogram of HWE2 obtained by a TSK5000 column with detection by refractive index (black line) alone and together with UV absorbance (blue line). The eluent was 0.2M sodium chloride at a flow rate of 3.0 ml/min and the column was kept at 30°C.

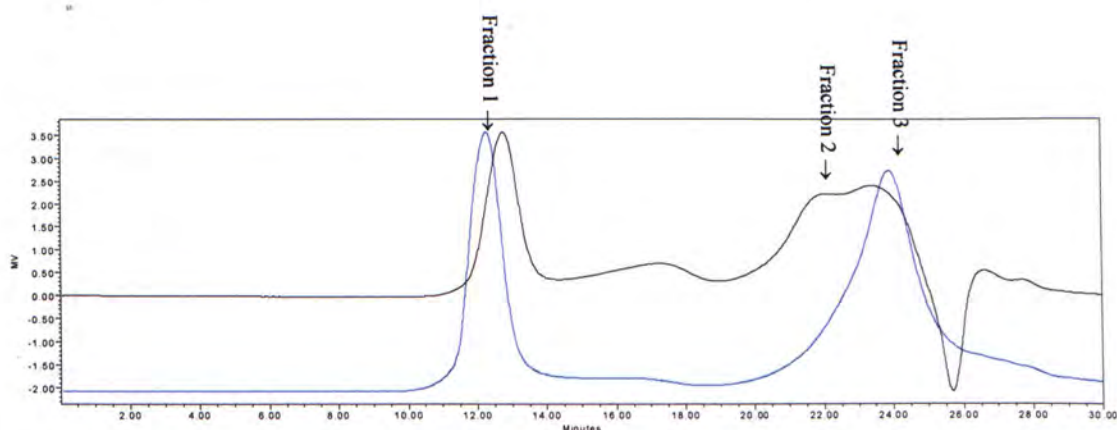


Fig 3.5 The HPLC chromatogram of HWE3 obtained by a TSK5000 column with detection by refractive index (black line) alone and together with UV absorbance (blue line). The eluent was 0.2M sodium chloride at a flow rate of 3.0 ml/min and the column was kept at 30°C.

Table 3.3 The molecular weight ( $M_w$ ) of the PTR HWE1, HWE2 and HWE3.

<i>Sample</i>	<i>Fraction 1</i>		<i>Fraction 2</i>		<i>Fraction 3</i>	
	$M_w \times 10^4$	<i>Peak area %</i>	$M_w \times 10^4$	<i>Peak area %</i>	$M_w \times 10^4$	<i>Peak area %</i>
HWE1	156.4	6.76	1.2	26.47	0.5	60.94
HWE2	185.5	18.87	1.2	29.87	0.6	41.83
HWE3	174.9	29.98	1.2	26.22	0.6	29.20

### 3.4 Chemical characterization of PTR extracts

PTR extracts isolated from different developmental stages varied considerably both in terms of chemical composition and molecular weight. Based on the chemical characterization of PTR extracts, their possible structures could be deduced.

Previous study found that EDP and CEP had very high carbohydrate content but low in protein content (Wong, 2004). It is believed that they belonged to different types of polysaccharides according to their monosaccharide profile. Glucose was the major monosaccharides obtained in EDP and whereas CEP was rich in mannose, so they were proposed to be glucan and mannan, respectively (Wong, 2004). Three HWEs contained substantial amount of protein and the fraction 1 and fraction 3 were found along with strong UV absorbance in HPLC analyses, suggesting the polysaccharide might couple with protein and they were therefore likely to be polysaccharide-protein complexes. Fraction 2 of PTR HWEs was speculated to be pure glycan. It is believed that the polysaccharide portions were made up of glucose, mannose and galactose. GC results showed that % glucose and % uronic acid were



increased while % mannose and % galactose were decreased from HWE1 to HWE3. Meanwhile, fraction 1 was the major fraction in HWE3 while fraction 3 was dominant in HWE1, speculating that fraction 1 was made up of glucose and fraction 3 was made up of mannose and galactose. It suggested that fraction 1 and fraction 3 of HWEs might be glucan and mannan/galactan/mannogalactan, respectively.

The hot-alkali sclerotial polysaccharides have been revealed to be a glucose-rich (1→3)-  $\beta$ -glucan with every third unit having a (1→6)- $\beta$ -D-glucopyranosyl branch on average (Deng, 2000; Zhang *et al.*, 2001). It seemed that the water-soluble sclerotial polysaccharide was also glucans as the percentage of glucose was over ten-fold of that of mannose and galactose.

The chemical composition and molecular weight of PTR extracts was totally different from each other. HWEs from fruiting body, having the highest molecular weight and protein content, contained three fractions. EDP and sclerotial polysaccharides with moderate molecular weight ( $50.9 \times 10^4$  MW and  $43.5 \times 10^4$  MW, respectively) were rich in glucose (Wong, 2004; Zhang *et al.*, 2004c). CEP with relatively low molecular weight was rich in mannose (Wong, 2004). According to the present results, HWEs were assumed to be polysaccharide-protein complexes composed of different monosaccharides, EDP and CEP was speculated to be glucan and mannan, respectively.



### 3.5 Cytotoxic effect of PTR extracts on various cell lines *in vitro*

Four human cancer cell lines were employed to assess the *in vitro* cytotoxicity and antiproliferative activities of PTR extracts. They were originated from different organs and cancer types, including acute promyelocytic leukemia (HL-60), chronic myelogenous leukemia (K562), breast cancer (MCF-7) and liver cancer (HepG2). All of them are model cell lines used by Drug Research and Development of the National Cancer Institute in screening for potential antitumor agents and studying cell cycle and apoptosis pathway (Hui *et al.*, 2005). Besides, two normal cell lines, one from monkey kidney (Vero) and one from human foreskin (Hs68) were applied to test the cytotoxicity of PTR extracts on normal cells, if any.

#### 3.5.1 Effect of PTR extracts on HL-60 cell viability

In general, all the PTR extracts from a concentration of 12.5 µg/ml to 400 µg/ml could inhibit the HL-60 cells significantly (Fig 3.6). PTR HWEs reduced the cell viability significantly in a dose dependent manner, however, HWE1 was less effective than HWE2 and HWE3 in terms of LC<sub>50</sub> value of the growth inhibitory effect of HWE1, HWE2, and HWE3 estimated 50% at 100 µg/ml, 25 µg/ml and 50 µg/ml, respectively.

On the contrary, the number of HL-60 surviving cells remained high in CEP and EDP treatment from 12.5 µg/ml to 200 µg/ml (Fig 3.6). However, CEP lowered the relative surviving HL-60 cells sharply from 78.8% at 200 µg/ml to 13.0% at 400 µg/ml (Fig 3.6). The relative surviving HL-60 cells was also reduced by EDP from

65.7% at 200 µg/ml to 34.9% at 400 µg/ml. These suggested that their cytotoxicity was most effective at 400 µg/ml among the concentrations tested. The estimated LC<sub>50</sub> value of CEP and EDP was both about 300 µg/ml. Water-soluble PTR mycelial polysaccharides had been shown to have 80% inhibition (20% surviving cells) on HL-60 cells at 200 µg/ml previously (Zhang *et al.*, 2004c). The difference in the inhibitory effect of EDP obtained from the present result and the previous study might be due to the difference in their molecular weight distribution. The mycelial polysaccharides extracted previously consisted of a major peak of  $76.2 \times 10^4$  MW whereas EDP consisted of a major peak of  $50.9 \times 10^4$  MW. Polysaccharides with higher molecular weight usually possess enhanced antitumor activities (Bohn and BeMiller, 1995). Besides, water-soluble sclerotial polysaccharides exhibited less than 40% growth inhibition (more than 60% surviving cells) on HL-60 cells at 200 µg/ml (Zhang *et al.*, 2004c) as compared with other PTR extracts.

In summary, cytotoxicity of PTR extracts towards HL-60 cells varied. HWEs could significantly reduce the percentage of viability of HL-60 cells in a dose-dependent fashion, among which HWE2 was the most potent. Cell viability was only reduced sharply only at high concentration of CEP and EDP.

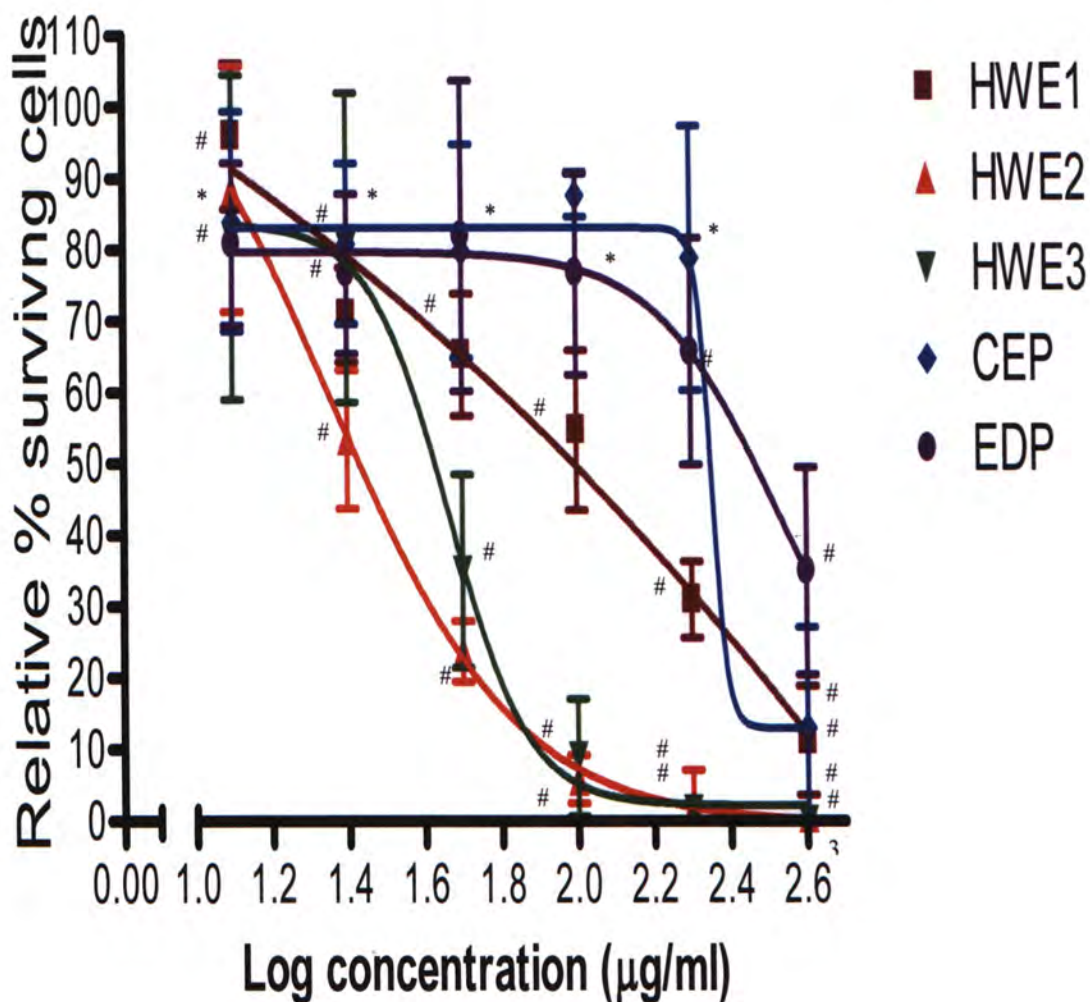


Fig 3.6 The effect of concentrations of PTR extracts on the viability of HL-60 cells determined by trypan blue exclusion method was expressed as the viability %, mean  $\pm$  S.D. (n=5), against the log concentration of extracts. Different letters represent the significant difference between the means of the number of cells in control group and treatment group by Student's t-test (\*  $p < 0.05$ , #  $p < 0.01$ ).



### 3.5.2 Effect of PTR extracts on K562 cell viability

Obviously, the relative % of surviving K562 cells was reduced the most by CEP and HWE2, in which the relative % of surviving cells was found to be smaller than 20% at all tested concentrations (Fig 3.7). Strong growth inhibitory effects was maintained even at 12.5  $\mu\text{g/ml}$  for CEP- and HWE2-treated cells, suggesting the bioactive components were very potent and a lower concentration might also give significant inhibition on K562 cells if tested. Although HWE3 could not retard the K562 cell viability as much as HWE2 and CEP, the relative % of surviving cells was decreased from 52.9 % at 12.5  $\mu\text{g/ml}$  to 27.0 % at 400 $\mu\text{g/ml}$ . The estimated  $\text{LC}_{50}$  value of HWE3 was 12.5  $\mu\text{g/ml}$ . The percentage of K562 surviving cells was the least affected by HWE1 and EDP which has a relative % of surviving cells of 63.3% and 82.6% at 400  $\mu\text{g/ml}$ , with less than 50% inhibition being found in all concentrations tested.

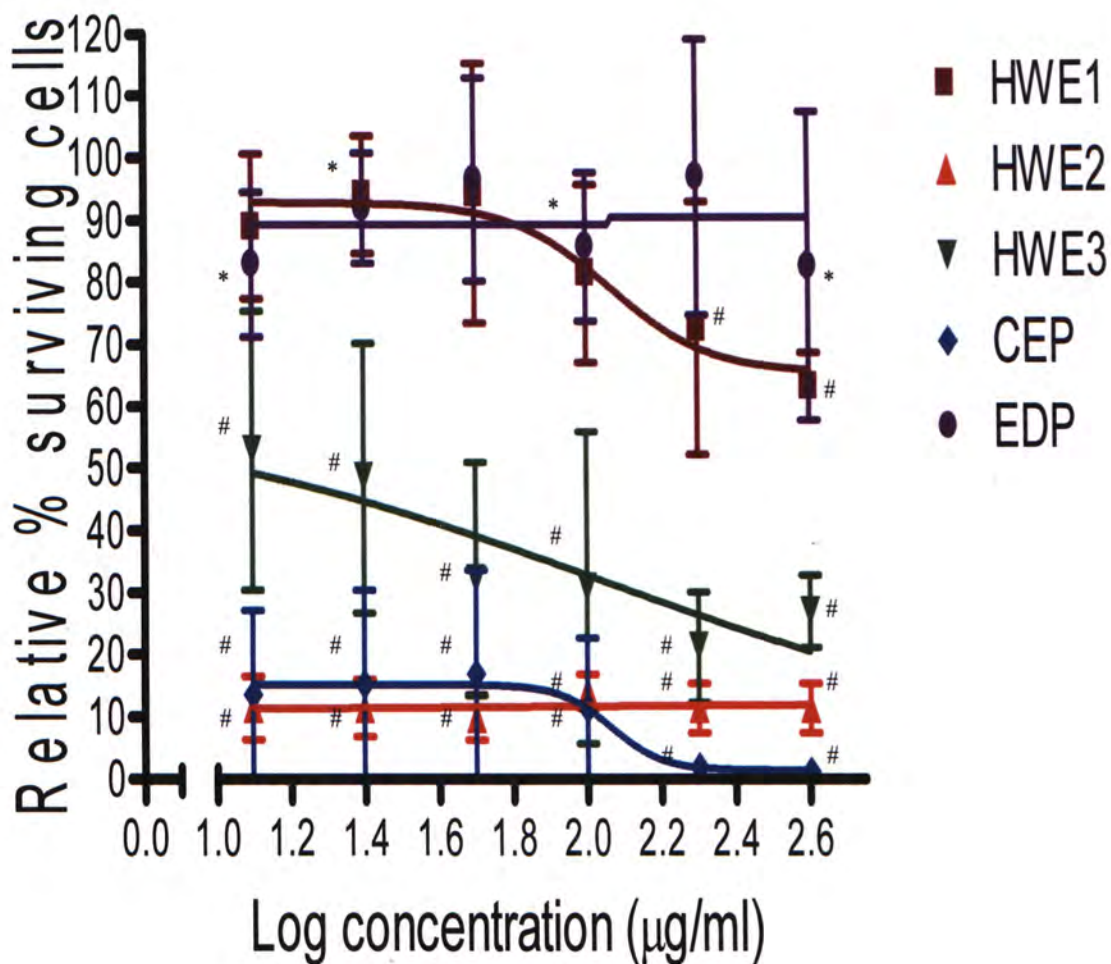


Fig 3.7 The effect of concentrations of PTR extracts on the viability of K562 cells determined by trypan blue exclusion method was expressed as the relative % surviving cells, mean  $\pm$  S.D. (n=5), against the log concentration of extracts. Different letters represent the significant difference between the means of the number of cells in control group and treatment group by Student's t-test (\*  $p < 0.05$ , #  $p < 0.01$ ).

### 3.5.3 Effect of PTR extracts on MCF-7 cell proliferation

Not all the PTR extracts could inhibit MCF-7 cell proliferation significantly. EDP, HWE1 and HWE3 only had a relative % of proliferating cells of 88.7%, 60.5% and 71.9%, respectively even at 400 µg/ml. Higher concentration of PTR extracts might demonstrate a stronger inhibition, however, PTR extracts were not completely soluble in the medium and a very viscous solution with precipitates would be formed if the concentration of the extracts was too high. This would greatly hinder the cell culture experiments to be carried out effectively. In comparison, CEP and HWE2 gave a stronger inhibition of which the relative % of proliferating cells was 19.6% and 39.8% at 400 µg/ml, respectively (Table 3.4).

### 3.5.4 Effect of PTR extracts on HepG2 cell proliferation

All the PTR extracts had no inhibitions on HepG2 cells in all tested concentrations except in 400 µg/ml at which the relative % of surviving cells was all higher than 60% (Table 3.5). Therefore, PTR extracts were less effective in exerting *in vitro* cytotoxicity against HepG2 cells.



Table 3.4 The effect of concentrations of PTR extracts on the proliferation of MCF-7 cells determined by MTT method was expressed as relative % of proliferating cells (mean±S.D., n=5).

PTR extract	Concentration (µg/ml)				
	12.5	25	50	100	400
CEP	- <sup>a</sup>	-	53.0±7.12 <sup>#</sup>	71.6±3.18 <sup>#</sup>	19.6±2.04 <sup>#</sup>
EDP	-	-	-	-	88.7±7.84 <sup>*</sup>
HWE1	83.8±9.23	73.8±7.55 <sup>#</sup>	65.2±6.25 <sup>#</sup>	68.9±4.51 <sup>#</sup>	60.5±6.22 <sup>#</sup>
HWE2	76.4±7.84 <sup>b</sup>	89.9±3.12	69.1±6.90 <sup>#</sup>	64.3±8.93 <sup>#</sup>	38.8±8.52 <sup>#</sup>
HWE3	82.6±9.59 <sup>a</sup>	85.3±11.4 <sup>*</sup>	81.5±11.7 <sup>*</sup>	-	71.9±6.18 <sup>*</sup>

Different letters represent the significant difference between the mean of the number of cells in control group and treatment group by Student's t-test (<sup>\*</sup>  $p < 0.05$ , <sup>#</sup>  $p < 0.01$ ).

<sup>a</sup>: no inhibition was found

Table 3.5 The effect of concentrations of PTR extracts on the proliferation of HepG2 cells determined by MTT method was expressed as relative % of proliferating cells (mean±S.D., n=5).

PTR extract	Concentration (µg/ml)				
	12.5	25	50	100	400
CEP	- <sup>a</sup>	-	-	-	63.1±9.77 <sup>#</sup>
EDP	-	-	-	-	67.6±5.38 <sup>#</sup>
HWE1	-	-	-	-	76.2±14.4 <sup>*</sup>
HWE2	-	-	-	-	80.5±15.4 <sup>*</sup>
HWE3	-	-	-	70.2±5.49 <sup>*</sup>	66.5±10.2 <sup>*</sup>

Different letters represent the significant difference between the mean of the number of cells in control group and treatment group by Student's t-test (<sup>\*</sup>  $p < 0.05$ , <sup>#</sup>  $p < 0.01$ ).

<sup>a</sup>: no inhibition was found

### 3.5.5 Effect of PTR extracts on normal cell proliferation

The tumor specificity of the cytotoxic effect of PTR extracts was evaluated by two normal cell lines, human Hs68 and monkey Vero. No significant inhibitions were found from 12.5 µg/ml to 400 µg/ml, suggesting their cytotoxicity was specific against cancer cells only (data not shown). This selectivity implicated that the PTR extracts might be used as potential antiproliferative agents to cancer cells.

## 3.6 Effect of PTR extracts on the proliferation rate of various cell lines *in vitro*

Apart from assessing the relative % surviving cells of the cancer cell lines by PTR extracts, the proliferation rate of the cells is another specific parameter to determine the effectiveness of these potential antitumor agents. The proliferation was measured by BrdU incorporation assay which was based on the incorporation of pyrimidine analogue, BrdU, into the DNA of proliferating cells during the S phase (Roche Applied Sciences, 2003). The relative % proliferating cells of the cancer cell lines was examined after 72-hour treatment of PTR extracts in comparison to that of control group. Lower percentage of the relative proliferating cells suggested that the extract could reduce the proliferation of the cell effectively and had higher antiproliferative activity.

### 3.6.1 Effect of PTR extracts on HL-60 cell proliferation

In general, the relative % of proliferating cells decreased with increasing



concentrations of PTR extracts applied. All PTR extracts showed significant antiproliferative activities on HL-60 cells at 400 µg/ml, among which HWE2 reduced the relative % of proliferating cells the most, up to 7.11%. HWE1, HWE3 and CEP demonstrated steady antiproliferative activities from 25 to 100 µg/ml but the % of proliferating cells was reduced to 45.9%, 46.1% and 22.2% by HWE1, HWE3 and CEP at 400 µg/ml, respectively, indicating their antiproliferative activities were only effective at 400 µg/ml (Fig 3.8). It was clear that the antiproliferative activities of other PTR extracts were weaker than HWE2 at 400µg/ml and the estimated IC<sub>50</sub> values from the curve were 200µg/ml for CEP, 400µg/ml for HWE1 and HWE2, and 300 µg/ml for HWE3.

However, a slight proliferative effect was observed in the case of EDP, which reflected that it could not reduce the HL-60 cell proliferation effectively (Fig 3.8). The antiproliferative activity was regarded as unremarkable because very large number of proliferating cells (>70%) still remained up to 400 µg/ml.

### 3.6.2 Effect of PTR extracts on K562 cell proliferation

Similar antiproliferative effect of PTR extracts on K562 cells was observed at all tested concentrations and that they all lowered the relative % of proliferating cells the most at 400µg/ml. CEP, HWE1 and HWE2 showed significant ( $p<0.01$ ) antiproliferative activities towards K562 cells at 400µg/ml with a relative % of proliferating cells of 22.9%, 15.7% and 6.37% was found, respectively. HWE3 significantly ( $p<0.01$ ) retarded the proliferation of K562 cells in a dose-dependent manner, keeping at about 30% proliferating cells at 400 µg/ml. EDP showed more



than 50% relative proliferating cells at all tested concentrations, suggesting its antiproliferative activity was the least effective among the PTR extracts (Fig 3.9). The estimated  $IC_{50}$  values were 300  $\mu\text{g/ml}$  for CEP and HWE1, 400  $\mu\text{g/ml}$  for EDP, 200  $\mu\text{g/ml}$  for HWE2 and 100  $\mu\text{g/ml}$  for HWE3. Therefore, it was deduced that HWE2 and HWE3 were more potent in reducing the proliferation of K562 cells than HWE1, EDP and CEP.

### 3.6.3 Effect of PTR extracts on MCF-7 cell proliferation

Only HWE1, EDP and CEP lowered the relative % of proliferating cell in MCF-7 cells at 200  $\mu\text{g/ml}$  and 400  $\mu\text{g/ml}$ , however, their values were higher than 50% which were regarded as unremarkable results. No antiproliferations were found in HWE2 and HWE3-treated cells (Table 3.6). To conclude, no substantial antiproliferative activities of PTR extracts were observed in MCF-7 cells.

### 3.6.4 Effect of PTR extracts on HepG2 cell proliferation

Similar to MCF-7 cells, the proliferation of HepG2 cells could not be lowered by PTR extracts in general. EDP and CEP showed significant ( $p < 0.01$ ) inhibition only at high concentration (400  $\mu\text{g/ml}$ ), with relative % of proliferating cells of 31.7% and 17.7%, respectively (Table 3.7).

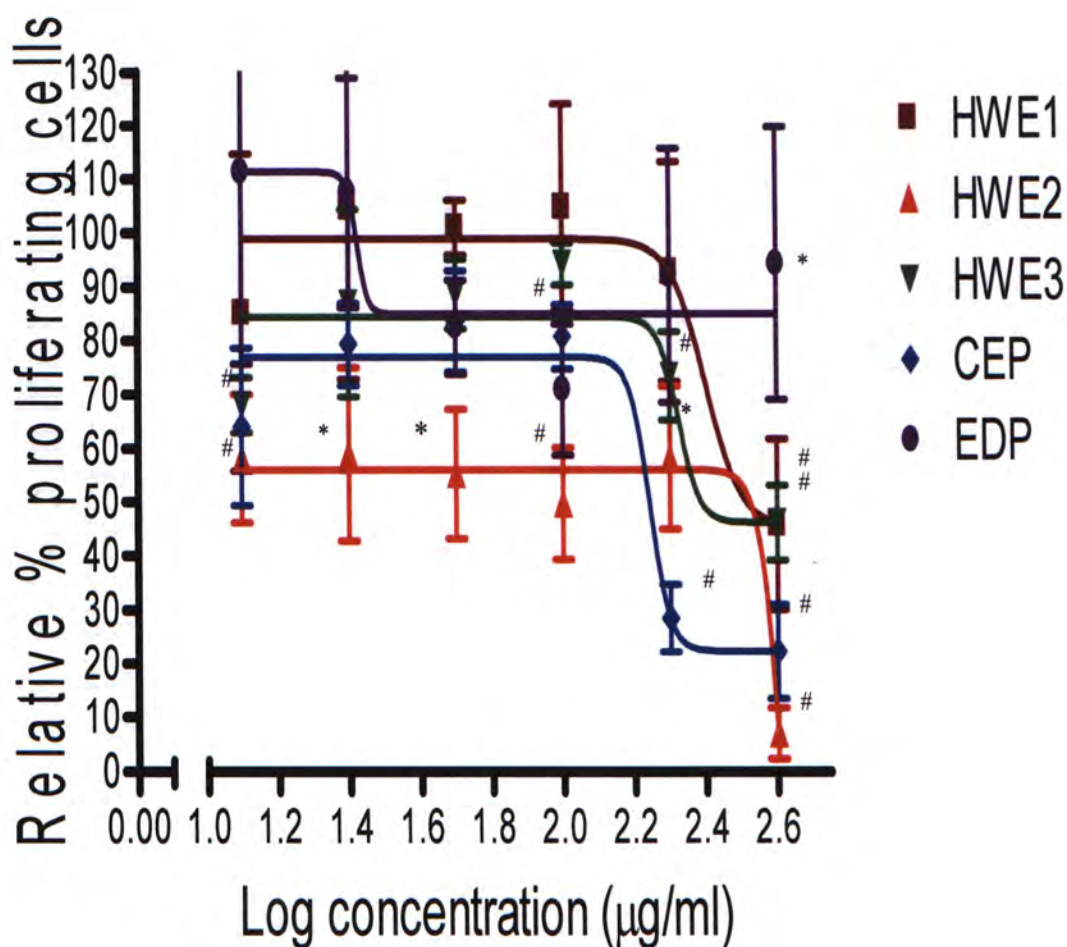


Fig 3.8 The effect of PTR extracts on the proliferation of HL-60 cells determined by BrdU incorporation method was expressed as the % proliferating cell against the log concentration employed. Different letters represent the significant difference between the number of cells in control group and treatment group according to t-test (\*  $p < 0.05$ , #  $p < 0.01$ ).

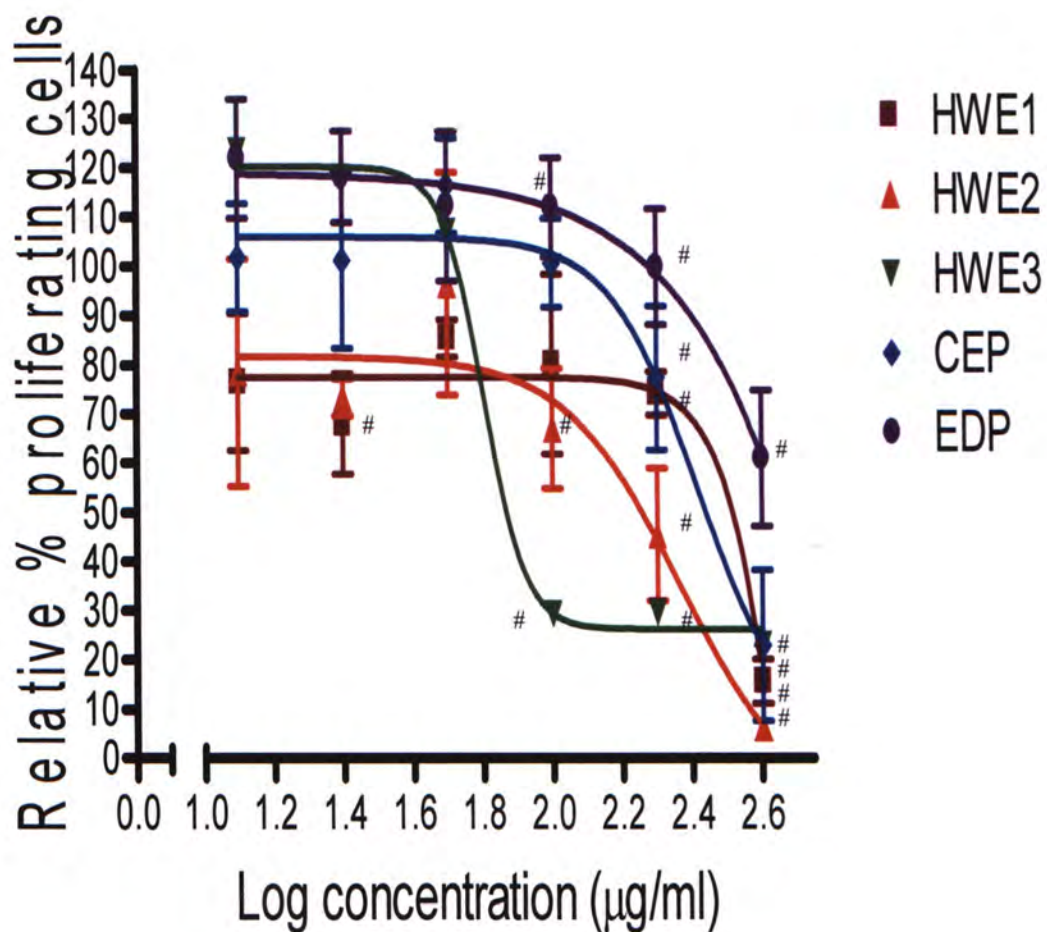


Fig 3.9 The effect of PTR extracts on the proliferation of K562 cells determined by BrdU incorporation method was expressed as the % proliferating cell against the log concentration employed. Different letters represent the significant difference between the number of cells in control group and treatment group according to t-test (\*  $p < 0.05$ , #  $p < 0.01$ ).



Table 3.6 The effect of concentrations of PTR extracts on the proliferation of MCF-7 cells determined by BrdU incorporation method was expressed as relative % of proliferating cells (mean±S.D., n=5).

PTR extract	Concentration (µg/ml)					
	12.5	25	50	100	200	400
CEP	93.4±7.65	- <sup>a</sup>	94.9±9.46	93.6±5.99	82.7±6.25 <sup>*</sup>	77.1±8.72 <sup>#</sup>
EDP	91.9±11.4	80.0±15.0	82.5±12.0	78.1±3.57 <sup>*</sup>	72.6±9.47 <sup>*</sup>	74.2±4.72 <sup>#</sup>
HWE1	-	-	-	-	90.3±5.68	52.5±4.89
HWE2	-	-	-	-	-	-
HWE3	-	-	-	-	-	-

Different letters represent the significant difference between the mean of the number of cells in control group and treatment group by Student's t-test (<sup>\*</sup>  $p<0.05$ , <sup>#</sup>  $p<0.01$ ).  
<sup>a</sup>: no antiproliferation was found

Table 3.7 The effect of concentrations of PTR extracts on the proliferation of HepG2 cells determined by BrdU incorporation method was expressed as relative % of proliferating cells (mean±S.D., n=5).

PTR extract	Concentration (µg/ml)					
	12.5	25	50	100	200	400
CEP	- <sup>a</sup>	-	-	93.2±8.46	61.4±11.5	17.7±8.21 <sup>#</sup>
EDP	-	-	-	-	-	31.7±13.3 <sup>#</sup>
HWE1	-	-	-	-	-	-
HWE2	-	-	-	-	-	-
HWE3	73.98±19.2	-	-	95.5±17.8	55.5±18.1	66.8±12.5

Different letters represent the significant difference between the mean of the number of cells in control group and treatment group by Student's t-test (<sup>\*</sup>  $p<0.05$ , <sup>#</sup>  $p<0.01$ ).  
<sup>a</sup>: no antiproliferation was found

### 3.6.5 Effect of PTR extracts on normal cell proliferation

The tumor specificity of the antiproliferative activity of PTR extracts was examined by the two normal cell lines, human Hs68 and monkey Vero cells. No significant changes in relative % of proliferating cells were found from 12.5 µg/ml to 400 µg/ml, suggesting that their antiproliferative activities were tumor-selective (data not shown).

## 3.7 Summary of the cytotoxic and antiproliferative activities exhibited by PTR extracts

A compound is considered to be a potent antitumor agent if it has substantial cytotoxic and/or antiproliferative activities specific to tumor cells and not normal cells. In the present experiments, both the relative number of surviving cells and proliferating cells in treatment group were measured in order to give a more comprehensive screening for the effectiveness of PTR extracts.

PTR extracts possessed different growth inhibitory and antiproliferation efficacies towards the four different human cancer cell lines. The retardation of growth and proliferation of HL-60 and K562 cells by PTR extracts were more significant than those of MCF-7 and HepG2 cells at all tested concentrations. HWE2 showed the strongest inhibition on HL-60, K562 and MCF-7 cell among the three HWEs. CEP was the best PTR extract against MCF-7 cell proliferation but all the PTR extracts could not reduce the HepG2 cell proliferation effectively. In general,



EDP could not retard the viability and proliferation of all cell lines as effective as other PTR extracts.

HWE2 (approximate  $LC_{50}$  value: 25  $\mu\text{g/ml}$ ) possessed the strongest cytotoxicity while CEP (approximate  $IC_{50}$  value: 200  $\mu\text{g/ml}$ ) had the most potent antiproliferative effect on HL-60 cells. Meanwhile, substantial cytotoxicity was found in HWE2- and CEP-treated K562 cells while HWE3 (approximate  $IC_{50}$  value: 100  $\mu\text{g/ml}$ ) reduced the relative % of proliferating K562 cells effectively. Also, similar antiproliferative activities exerted by HWE2 retarding the proliferation of HL-60 (7.11%) and K562 (6.37%) cells at 400  $\mu\text{g/ml}$  were observed. It seemed that CEP and HWE2 were the two most promising samples among all the PTR extracts. It is interesting that three HWEs exhibited different *in vitro* cytotoxic and antiproliferative efficacies, suggesting HWE2 might have some unique bioactive components or favorable chemical structure, such as more expanded conformation as mentioned in 3.3, to improve its activity.

On the other hand, it is inevitably that the cell survival and cell proliferation of the cancer cells were not completely the same. It was due to the differences in the principles, measuring target and specificity of the methods applied. Trypan blue exclusion dye method is a simple method that estimates the cell viability by direct counting the number of viable cells which has intact membrane to exclude the dye (Zhang *et al.*, 2004c). MTT method employed in this study measures the cell proliferation based on the metabolic activity of the cells to reduce the MTT salt to a colored formazan product (Mosmann, 1983). In BrdU incorporation assay, anti-BrdU-peroxidase (POD) would be bound to the incorporated BrdU during S phase. The relative number of proliferating cells was quantified by the light emitted by the



reaction product between POD and the substrate solution containing luminol (Roche Applied Sciences, 2003). Only a portion of cells was counted in the trypan blue exclusion dye method which might increase the measurement errors. In addition, MTT method assumes all the cells have the same metabolic activity which also might increase the measurement errors. On the contrary, BrdU incorporation assay is an ELISA method which would be more specific and is assumed to be more accurate than either trypan blue exclusion method or MTT assay.

HL-60 and K562 cells were more sensitive to the PTR extracts than MCF-7 and HepG2 cells. Cell cycle-mediated drug resistance has recently reported that the sensitivity of a cell to a cytotoxic agent would be affected by the position of the cell in the cell cycle or the activation of the cell cycle checkpoint (Schwartz and Shah, 2005). The efficacy of the agent would be reduced if the treated-cell was arrested at a phase which is not the most effective one for the agent. It was thereby hypothesized that the difference in the response between the cell lines, such as different cell cycle checkpoints elicited, led to different sensitivity to the PTR extracts. Comparing with MCF-7 and HepG2 cells, HL-60 and K562 cells might be arrested at a certain phase at which PTR extracts were more effective.

### 3.8 Analysis of the effect of PTR extracts on the cell-cycle phases of HL-60 and K562 cells

The *in vitro* growth inhibitory mechanism(s) of the PTR extracts were investigated by the cell cycle distribution of HL-60 and K562 cell lines in terms of cell cycle arrest and apoptosis determined by flow cytometry. The approximate IC<sub>50</sub> values of PTR extracts estimated from the BrdU method (3.6) were used to find out the effective concentrations which could exert significant effect on cell cycle and apoptosis by several trials. Three time points were applied (24 hours, 48 hours, and 72 hours) in order to observe the trend in the change of cell cycle and apoptosis mediated by the PTR extracts.

Propidium iodide (PI), a fluorochrome that intercalates with DNA molecules, can determine the DNA content by flow cytometry. The DNA content in the G<sub>2</sub>/M phase of the cells is doubled to that of the G<sub>1</sub> phase. The cells in S phase were synthesizing their DNA at the time when they were fixed, the DNA content was intermediate between those of the G<sub>1</sub> and G<sub>2</sub>/M phase. DNA fragmentation is typical phenomenon in apoptosis so that the DNA content in apoptotic cells was below that of the G<sub>1</sub> phase (Vermes *et al.*, 2000).

#### 3.8.1 Effect of CEP on cell-cycle phases of HL-60 and K562 cells

When CEP at 300 µg/ml was incubated with HL-60 cells, an approximate 3-fold increment of Sub-G<sub>1</sub> (apoptotic) peak was observed in a time-dependent manner when compared with the controls (Fig 3.10 and table 3.8). The apoptotic peak was



significantly ( $p<0.01$ ) increased from control of 4.16% cells to 15.5% cells at 72 hours after CEP treatment. However, there was no significant change in the other phases of the cell cycle of the HL-60 cells (Table 3.8). When CEP at 300  $\mu\text{g/ml}$  was incubated with K562 cells, significant increase in the apoptotic peak (20.2%) was only observed after 72 hours. There was no significant effect of CEP on the cell cycle phases at the three time points, suggesting that CEP could only trigger apoptosis in K562 cells after 72 hours (Fig 3.11 and table 3.9).

In both HL-60 and K562 cell lines, the apoptotic peak was observed without any significant changes in each cell-cycle phase, suggesting that apoptosis was related to the cytotoxicity of CEP and cell-cycle arrest might not be responsible for its triggering. In addition, significant apoptotic peak (2.8-fold of control) was readily induced in HL-60 cells upon 24-hour incubation (Table 3.8) while it was only observed at 72 hours in K562 cells (1.3-fold of control) (Table 3.9). It might be explained by the characteristics of the two cell lines. Overexpression of the antiapoptotic Bcl-2 and Bcl-x<sub>L</sub> was observed in HL-60 and K562 cells, respectively, preventing the release of cytochrome *c* and the initiation of apoptosis (Martins *et al.*, 1997). Nevertheless, HL-60 was known to be apoptotic-proficient that can induce apoptosis when it was treated with various chemotherapeutic drugs (Cao *et al.*, 2004). In opposite, K562 was an apoptotic-resistant cell lines that many chemotherapeutic drugs were not effective enough to eliminate it. It is because it contains the Philadelphia chromosome expressing the bcr-abl protein, resulted from a reciprocal translocation that the abl gene on chromosome 9 is transferred to chromosome 22 that includes the bcr gene (Yassin *et al.*, 2003). The bcr-abl protein in K562 cells was thought to be the main reason for their resistance to apoptosis (Yassin *et al.*, 2003).



Delayed apoptosis in K562 cells after exposure to other agents has been reported. An antimitotic agent, docetaxel, at  $10^{-8}$  M induced DNA fragmentation in HL-60 cells less than 6 hours and apoptotic bodies was observed at 24 hours, while apoptotic characteristics of K562 cells became obvious at 48 hours and DNA fragmentation was evident at 24 hours (Cao *et al.*, 2004). Using a DNA-damaging agent, etoposide at 10  $\mu$ M, 35% and 90% apoptotic cells were detected in treated-HL-60 cells at 6 hours and 24 hours, respectively, but no significant apoptotic cells was observed in K562 cells at both time points. DNA fragmentation was only observed when K562 cells were treated with 100  $\mu$ M of etoposide for 24 hours (Ritke *et al.*, 1994). Therefore, the delayed apoptotic induction in K562-treated cells with lower extent might be due to the presence of bcr-abl protein to allow the cells to have enough time to repair the damaged DNA to develop drug resistant ability.

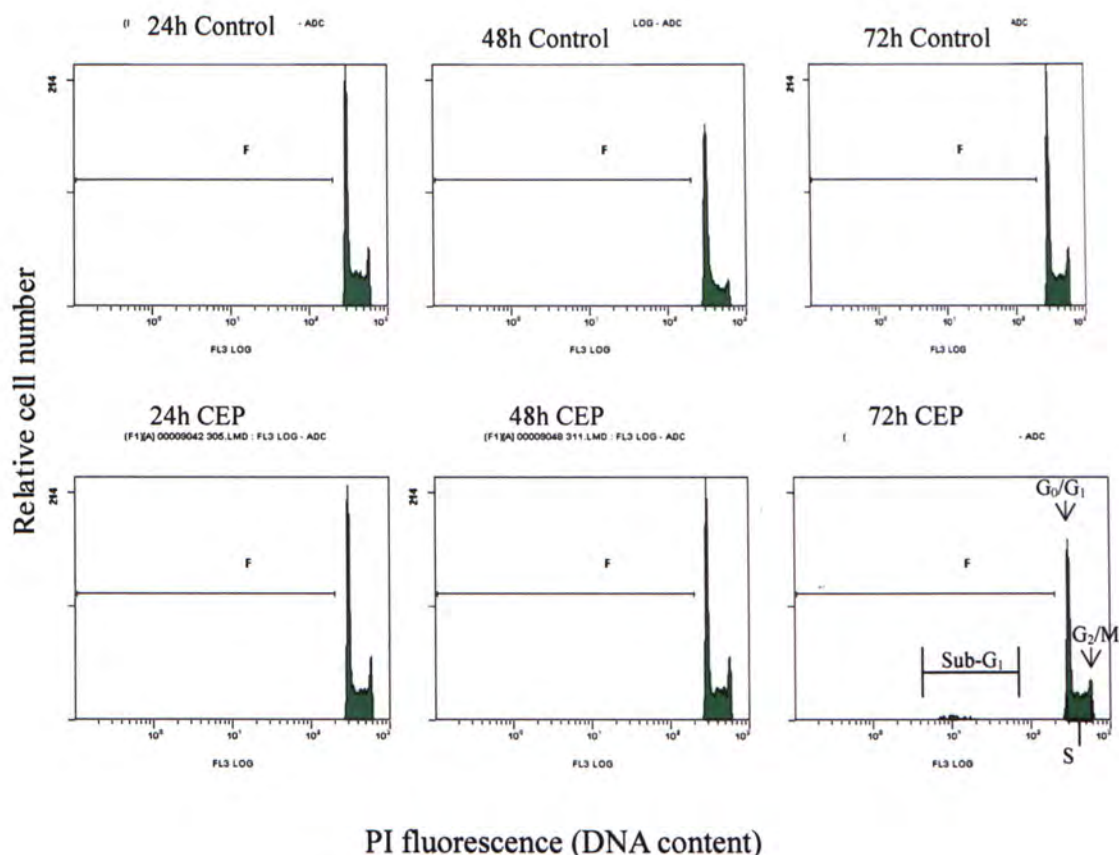


Fig. 3.10 Representative cytograms showing the effect of CEP at 300 µg/ml on the cell-cycle phases (G<sub>0</sub>/G<sub>1</sub>, S, and G<sub>2</sub>/M) and apoptosis (Sub-G<sub>1</sub> peak) of HL-60 cells at 24, 48 and 72 hours.

Table 3.8 Numeric expression of the relative cell number on the cell-cycle phases and apoptosis of HL-60 cells by CEP at 300 µg/ml.

Group	% Apoptotic cells (Sub-G <sub>1</sub> )	% Non-apoptotic cells		
		G <sub>0</sub> /G <sub>1</sub>	S	G <sub>2</sub> /M
24h control	2.90±0.36	39.2±0.42	49.7±0.31	11.2±0.12
24h CEP	8.04±1.19 <sup>#</sup>	41.2±1.29	49.1±1.89	9.77±0.60
48h control	3.91±1.52	44.5±2.23	45.2±2.20	10.3±0.35
48h CEP	8.95±1.03 <sup>#</sup>	44.7±1.13	44.7±0.84	10.6±0.26
72h control	4.16±0.70	44.8±1.30	45.8±1.00	9.37±0.45
72h CEP	15.5±2.69 <sup>#</sup>	42.4±1.97	47.8±1.34	9.80±1.73

Different letters represent the significant difference between the relative number of cells in control group and treatment group by Student's t-test (\*  $p < 0.05$ , <sup>#</sup>  $p < 0.01$  and @  $p < 0.001$ ).

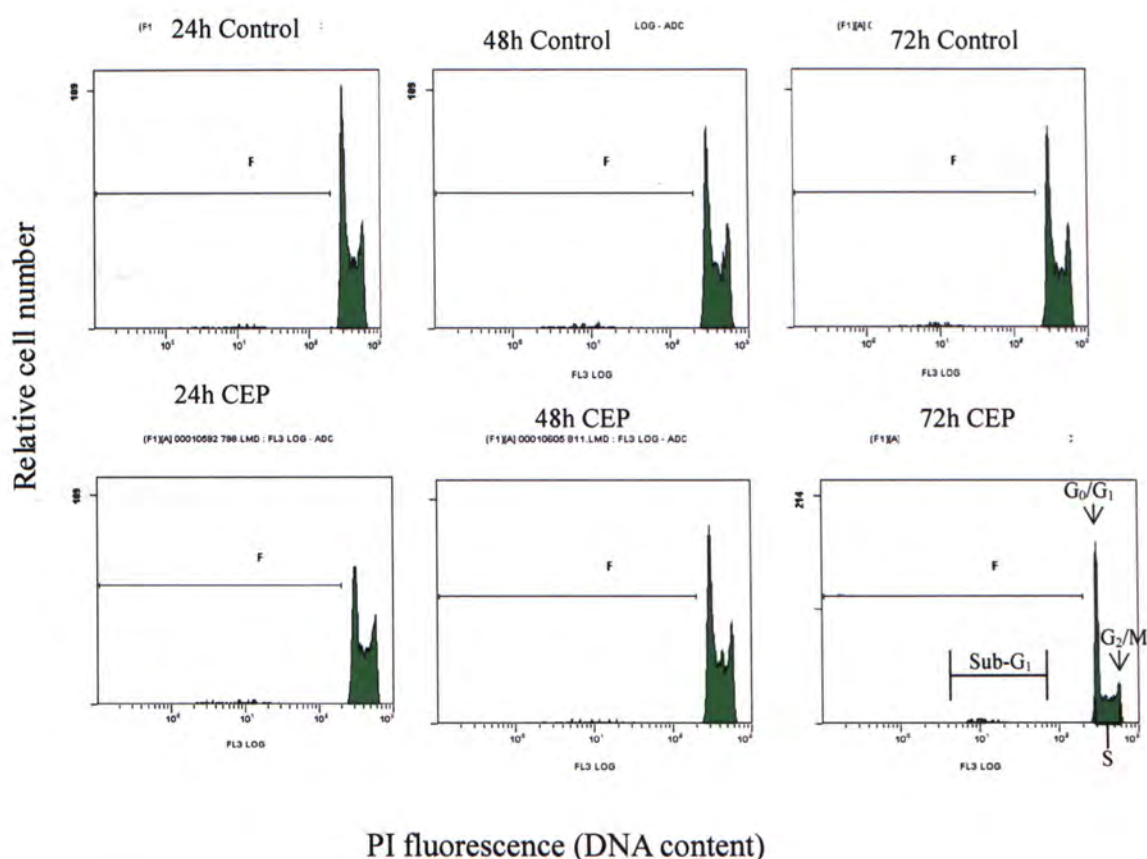


Fig. 3.11 Representative cytograms showing the effect of CEP at 300 µg/ml on the cell-cycle phases ( $G_0/G_1$ , S, and  $G_2/M$ ) and apoptosis (Sub- $G_1$  peak) of K562 cells at 24, 48 and 72 hours.

Table 3.9 Numeric expression of the relative cell number on the cell-cycle phases and apoptosis of K562 cells by CEP at 300 µg/ml.

Group	% Apoptotic cells (Sub- $G_1$ )	% Non-apoptotic cells		
		$G_0/G_1$	S	$G_2/M$
24h control	15.1±3.24	31.0±2.97	53.8±0.71	15.3±2.33
24h CEP	14.9±2.93	29.7±0.21	54.1±1.84	16.2±1.56
48h control	16.4±2.18	28.9±2.47	52.5±1.84	18.7±0.49
48h CEP	16.9±1.56	31.2±0.64	52.7±1.48	16.2±0.85
72h control	16.2±3.78	30.8±1.41	50.4±0.71	18.8±2.19
72h CEP	20.2±1.90 <sup>*</sup>	28.6±0.35	52.4±0.14	19.1±0.57

Different letters represent the significant difference between the relative number of cells in control group and treatment group by Student's t-test (<sup>\*</sup>  $p < 0.05$ , <sup>#</sup>  $p < 0.01$  and <sup>@</sup>  $p < 0.001$ ).



### 3.8.2 Effect of EDP on cell-cycle phases of HL-60 and K562 cells

EDP at 400 µg/ml induced apoptosis but not necrosis in HL-60 cells at the three time points and the apoptotic peak was the most prominent at 72 hours (Fig. 3.12 and table 3.10). Besides, an accumulation of cells at the G<sub>2</sub>/M phase which accounted for 16.3% was observed after 24 hr-incubation, significantly ( $p<0.05$ ) higher than the 11.9% found in control group (Table 3.10). Halting the cells at particular phase of the cell cycle might give time for the cell to repair the damaged DNA whereas apoptosis might eliminate the damaged cells that could not be repaired (Lu *et al.*, 2006). It was thereby hypothesized that apart from apoptosis, EDP might arrest cells at the G<sub>2</sub>/M phase after 24 hour-incubation to lower the proliferation rate of HL-60 by delaying the entry of the cells into mitosis. When 400 µg/ml of EDP was incubated with K562 cells, significant apoptotic peak was also observed and no necrosis was obtained at three time points (Fig. 3.13 and table 3.11). However, the ratio of the apoptosis between the control and treatment group was slightly decreased (5.88 for 24 hours, 4.53 for 48 hours and 4.45 for 72 hours) (Table 3.11). As the ratio is directly affected by the precision of control, further analysis is required for this survival shift.

Clearly, the growth inhibition exhibited by EDP on the HL-60 cells was mainly due to apoptosis and partly due to G<sub>2</sub>/M arrest, whereas the growth of K562 cells was inhibited by EDP mainly via apoptosis. Higher % apoptosis was found in HL-60-treated cells than K562-treated ones, suggesting that HL-60 cells was more sensitive to EDP treatment than K562 cells, consistent with the cytotoxic analyses previously (3.5.2 and 3.6.2).

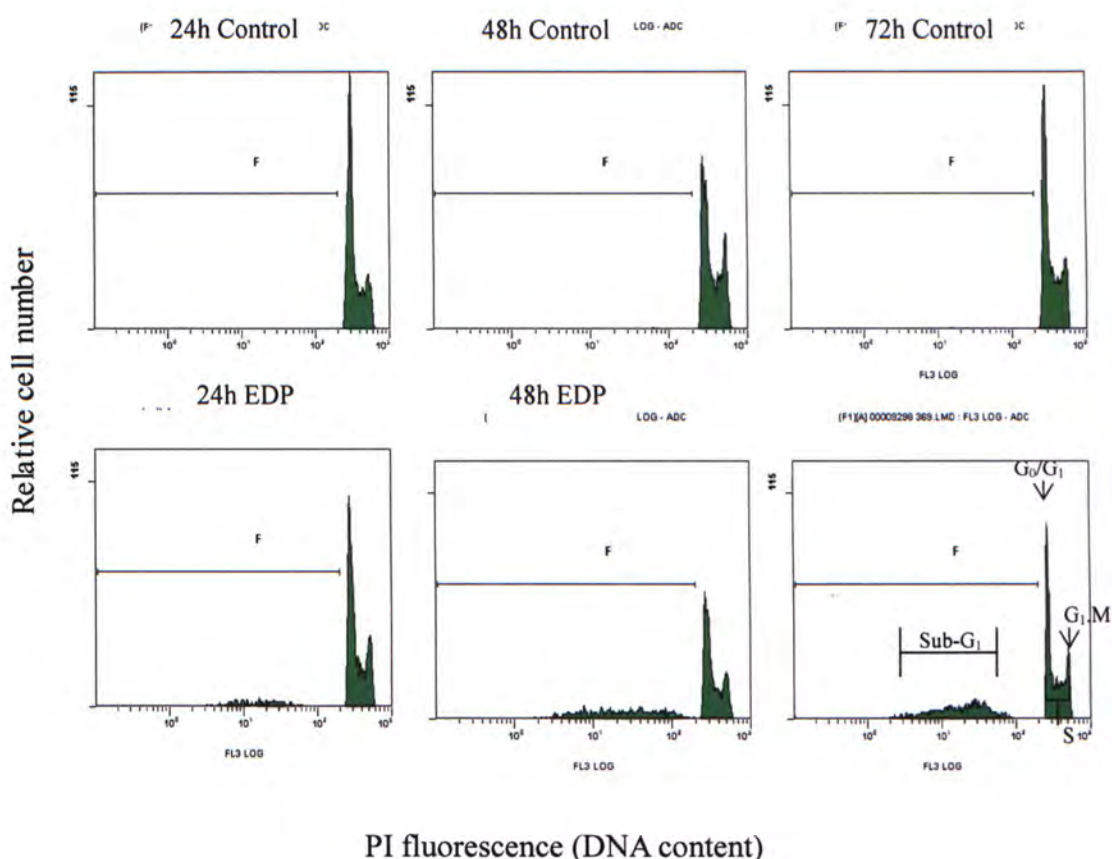


Fig. 3.12 Representative cytograms showing the effect of EDP at 400 µg/ml on the cell-cycle phases ( $G_0/G_1$ , S, and  $G_2/M$ ) and apoptosis (Sub- $G_1$  peak) of HL-60 cells at 24, 48 and 72 hours.

Table 3.10 Numeric expression of the relative cell number on the cell-cycle phases and apoptosis of HL-60 cells by EDP at 400 µg/ml.

Group	% Apoptotic cells (Sub- $G_1$ )	% Non-apoptotic cells		
		$G_0/G_1$	S	$G_2/M$
24h control	5.30±1.85	42.3±9.22	45.8±11.7	11.9±2.64
24h EDP	41.8±4.03 <sup>#</sup>	41.1±3.16	42.7±3.35	16.3±2.89 <sup>*</sup>
48h control	6.64±1.56	38.9±3.27	47.2±2.23	14.0±2.41
48h EDP	44.3±8.77 <sup>#</sup>	38.9±3.96	47.9±0.81	13.3±0.72
72h control	6.60±0.65	40.6±0.95	46.8±0.50	12.6±1.70
72h EDP	48.8±4.10 <sup>#</sup>	38.0±2.25	48.3±0.55	13.7±0.57

Different letters represent the significant difference between the relative number of cells in control group and treatment group by Student's t-test (<sup>\*</sup>  $p < 0.05$ , <sup>#</sup>  $p < 0.01$  and <sup>@</sup>  $p < 0.001$ ).



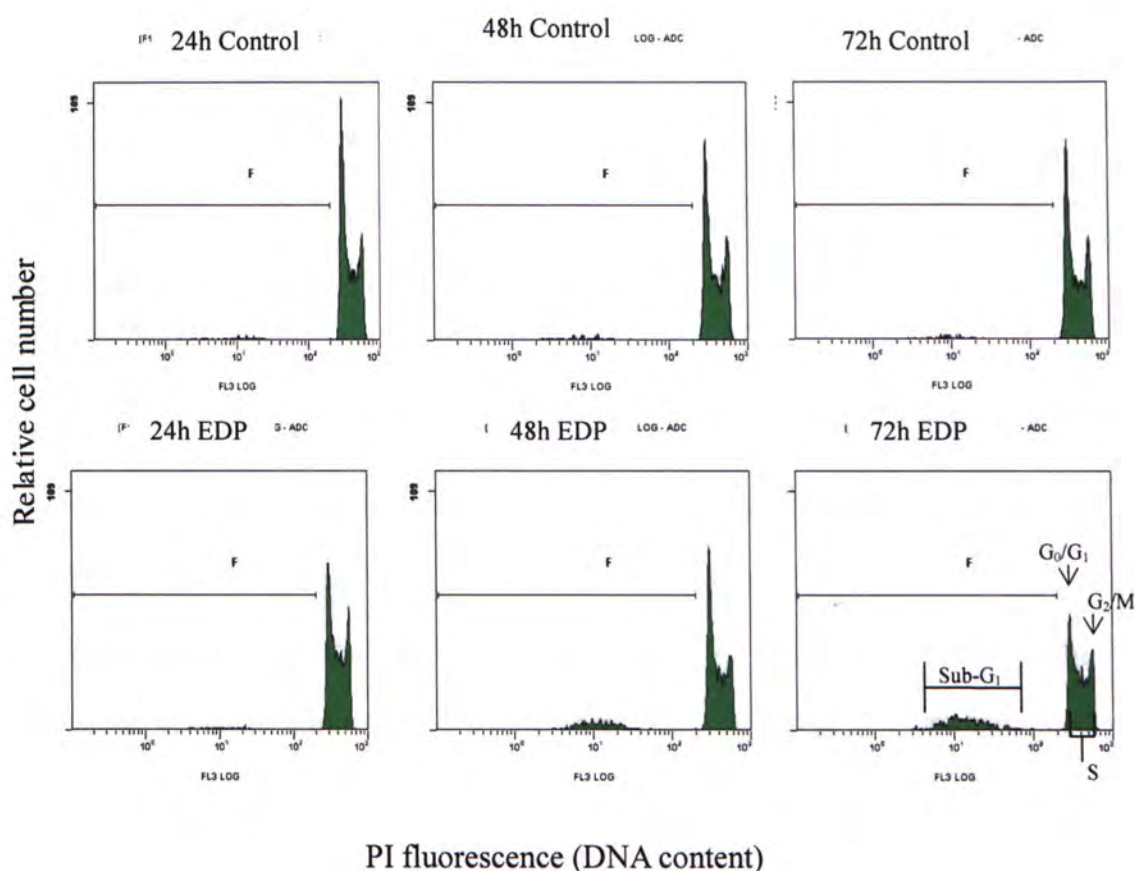


Fig. 3.13 Representative cytograms showing the effect of EDP at 400 µg/ml on the cell-cycle phases ( $G_0/G_1$ , S, and  $G_2/M$ ) and apoptosis (Sub- $G_1$  peak) of K562 cells at 24, 48 and 72 hours.

Table 3.11 Numeric expression of the relative cell number on the cell-cycle phases and apoptosis of K562 cells by EDP at 400 µg/ml.

Group	% Apoptotic cells (Sub- $G_1$ )	% Non-apoptotic cells		
		$G_0/G_1$	S	$G_2/M$
24h control	6.78±1.50	26.5±1.50	52.7±1.58	20.8±2.25
24h EDP	39.9±4.47 <sup>#</sup>	28.0±2.31	51.8±2.11	20.2±2.35
48h control	6.34±1.22	27.8±1.25	59.9±4.54	12.4±5.52
48h EDP	28.7±6.59 <sup>#</sup>	26.6±0.87	58.3±2.36	15.1±2.04
72h control	5.59±1.37	18.3±4.46	64.4±2.78	17.2±1.67
72h EDP	24.9±1.62 <sup>@</sup>	26.2±3.10	58.5±2.13 <sup>*</sup>	15.3±1.91

Different letters represent the significant difference between the relative number of cells in control group and treatment group by Student's t-test (<sup>\*</sup>  $p < 0.05$ , <sup>#</sup>  $p < 0.01$  and <sup>@</sup>  $p < 0.001$ ).



### 3.8.3 Effect of HWE1 on cell-cycle phases of HL-60 and K562 cells

When HL-60 cells were incubated with HWE1 at 400 µg/ml, a significant ( $p<0.05$ ) apoptotic peak was observed at the 48 hours and 72 hours when compared with the control (4.4% and 12.6%, respectively). The apoptotic peak at 72-hour incubation was increased to approximately 6-fold of the control (Table 3.12). Besides, it could be clearly seen that the cells were significantly accumulated at the S phase in the treatment groups, while the number of cells in the  $G_0/G_1$  phase was concomitantly smaller. From 48 to 72 hours, the percentage of the  $G_2/M$  phase cells was also decreased, reflecting that fewer number of cells progressed into the  $G_2/M$  phase in the treatment group (Fig 3.14 and table 3.12), speculating that those arrested cells might shift to apoptosis.

When 300 µg/ml of HWE1 was incubated with K562 cells, a significant ( $p<0.05$ ) accumulation of the S-phase cells was observed at 24 hours, followed by the occurrence of a significant ( $p<0.05$ ) apoptotic peak of 27.2% and 33.3% at 48 hours and 72 hours, respectively (Fig 3.15 and table 3.13). It was hypothesized that the accumulated S-phase cells might shift to apoptosis due to prolonged arrest, or apoptosis was also triggered during a longer treatment time (48 hours).

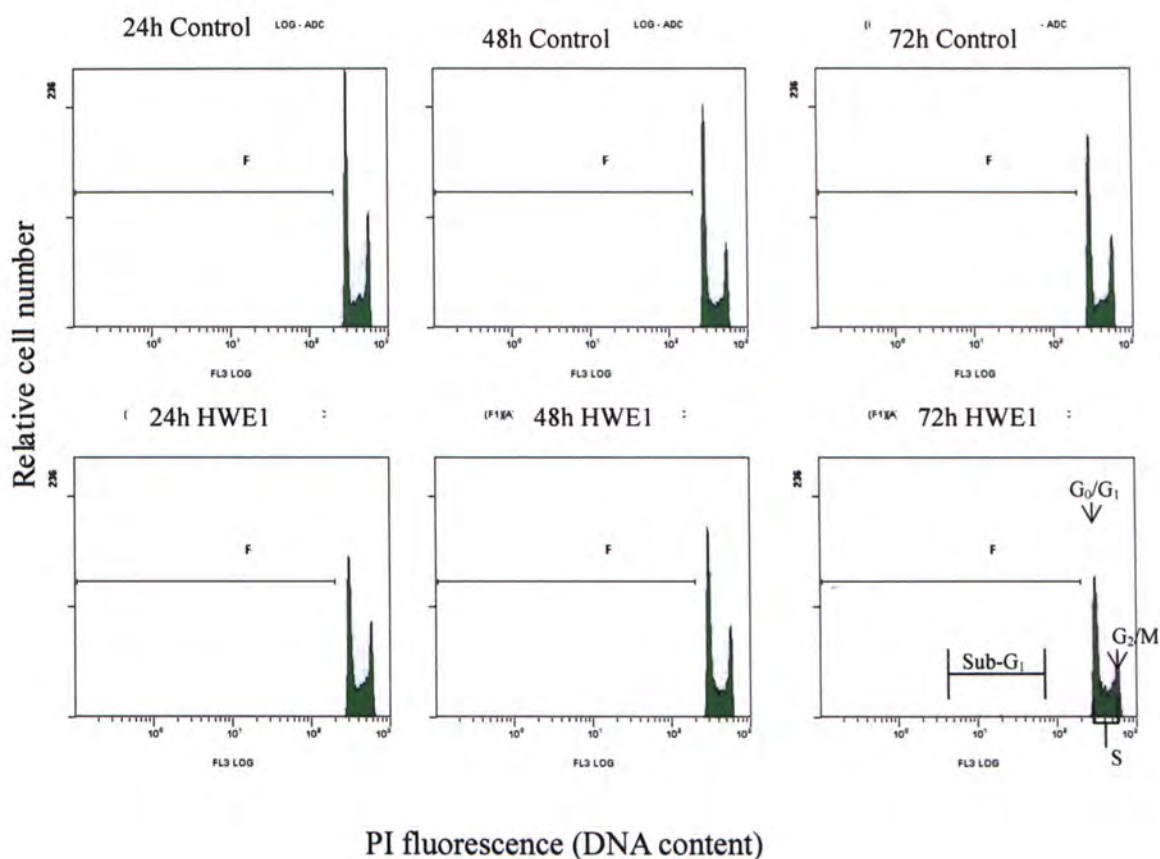


Fig. 3.14 Representative cytograms showing the effect of HWE1 at 400 µg/ml on the cell-cycle phases ( $G_0/G_1$ , S, and  $G_2/M$ ) and apoptosis (Sub- $G_1$  peak) of HL-60 cells at 24, 48 and 72 hours.

Table 3.12 Numeric expression of the relative cell number on the cell-cycle phases and apoptosis of HL-60 cells by HWE1 at 400 µg/ml.

Group	% Apoptotic cells (Sub- $G_1$ )	% Non-apoptotic cells		
		$G_0/G_1$	S	$G_2/M$
24h control	$2.3 \pm 0.7$	$43.5 \pm 0.4$	$43.6 \pm 0.6$	$16.7 \pm 0.5$
24h HWE1	$3.9 \pm 0.2$	$33.7 \pm 0.5$ <sup>#</sup>	$49.3 \pm 1.1$ <sup>#</sup>	$17.1 \pm 0.6$
48h control	$2.4 \pm 0.1$	$45.2 \pm 0.6$	$40.0 \pm 0.5$	$14.9 \pm 0.1$
48h HWE1	$4.4 \pm 0.2$ <sup>#</sup>	$39.3 \pm 0.6$ <sup>*</sup>	$43.0 \pm 1.6$	$17.7 \pm 0.9$
72h control	$2.9 \pm 0.3$	$42.8 \pm 1.3$	$40.4 \pm 1.0$	$16.9 \pm 0.4$
72h HWE1	$12.6 \pm 2.0$ <sup>*</sup>	$39.6 \pm 0.4$	$45.6 \pm 0.7$ <sup>*</sup>	$14.9 \pm 1.0$

Different letters represent the significant difference between the relative number of cells in control group and treatment group by Student's t-test (<sup>\*</sup>  $p < 0.05$ , <sup>#</sup>  $p < 0.01$  and <sup>@</sup>  $p < 0.001$ ).

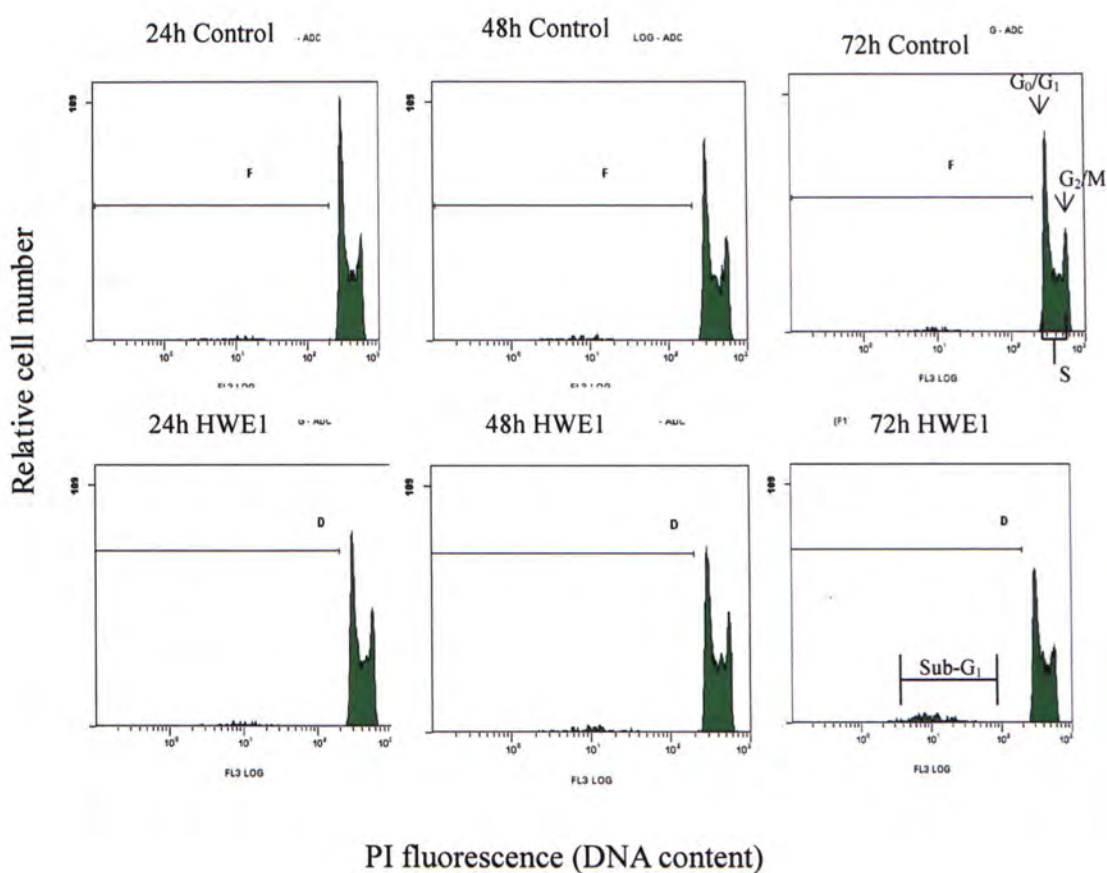


Fig. 3.15 Representative cytograms showing the effect of HWE1 at 300 µg/ml on the cell-cycle phases ( $G_0/G_1$ , S, and  $G_2/M$ ) and apoptosis (Sub- $G_1$  peak) of K562 cells at 24, 48 and 72 hours.

Table 3.13 Numeric expression of the relative cell number on the cell-cycle phases and apoptosis of K562 cells by HWE1 at 300 µg/ml.

Group	% Apoptotic cells (Sub- $G_1$ )	% Non-apoptotic cells		
		$G_0/G_1$	S	$G_2/M$
24h control	15.1±3.24	31.0±2.97	53.8±0.71	15.3±2.33
24h HWE1	14.1±1.27	24.5±3.54	59.5±2.47*	16.1±1.06
48h control	16.4±2.18	28.9±2.47	52.5±1.84	18.7±0.49
48h HWE1	27.2±0.02*	29.9±1.27	54.7±0.14	15.4±1.13
72h control	16.2±3.78	30.8±1.41	50.4±0.71	18.8±2.19
72h HWE1	33.1±6.34*	24.8±7.00	50.2±3.35	15.2±0.13

Different letters represent the significant difference between the relative number of cells in control group and treatment group by Student's t-test (\*  $p < 0.05$ , #  $p < 0.01$  and @  $p < 0.001$ ).



### 3.8.4 Effect of HWE2 on cell-cycle phases of HL-60 and K562 cells

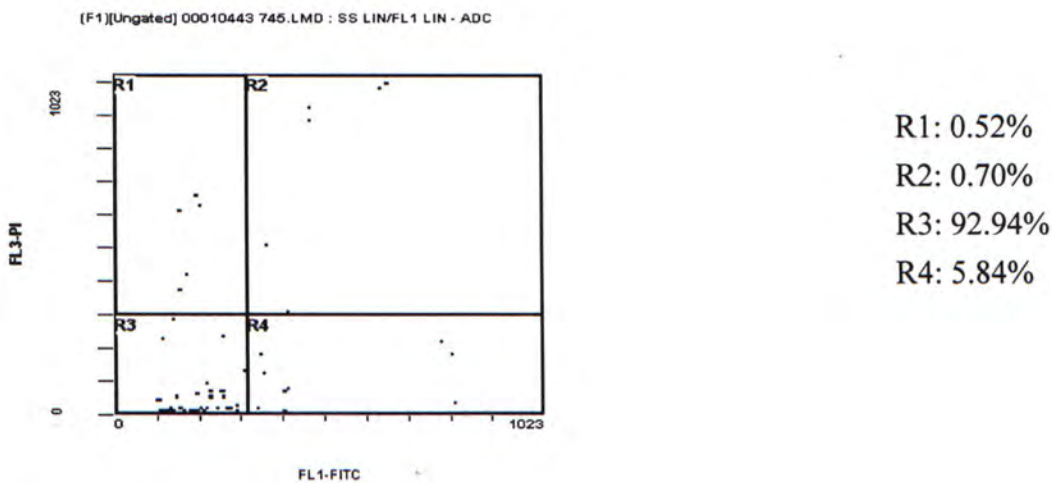
HWE2 (200 µg/ml)- treated HL60 cells were accumulated at S phase at 24 hours and 48 hours, however, it was decreased to 37.1% with a concomitant increase in the percentage of cell at G<sub>0</sub>/G<sub>1</sub> phase (Table 3.14). The apoptotic peak was increased significantly ( $p<0.05$ ) from 8.18% in the control to 14.5% in the treatment group at 48 hours. At 72 hours, it was significantly ( $p<0.001$ ) increased from 5.96% in the control to 68.1% in the treatment group (Fig 3.17 and table 3.14). No necrosis was observed at three time points (Fig 3.17). Similar result was also obtained by annexin-V/PI staining assay, showing 4.4-fold of early apoptosis and 3.5-fold of late apoptosis when compared with control (Fig. 3.16). One of the hypotheses was that HWE2 might cause S arrest at 24 and 48 hours and G<sub>1</sub> arrest was initiated only at 72 hours. Another one was HWE2 might only cause S arrest and those cells arrested at S phase was shifted to apoptosis at 72 hours so that most cells were found in the peak of G<sub>0</sub>/G<sub>1</sub> phase (Table 3.14). As a result, a high percentage of cells had undergone apoptosis that eliminated the HL-60 cells effectively.

In contrast, HWE2 at 200 µg/ml could not increase the % of K562 cells in the apoptotic peak at all three tested time points. However, increment of the % of cells in S phase was found, which was negatively correlated with the decrease of the % of G<sub>0</sub>/G<sub>1</sub> phase cells ( $R^2 = -0.9877$ ). The % of cells in the G<sub>2</sub> phase was lowered significantly from 16.5% in the control to 12.1% in the treatment group at 48 hours, consistent with the elevated % of cells in the S phase. However, at 72 hours, no significant reduction of G<sub>2</sub> phase cells was observed, implying that some cells in the S phase had shifted to G<sub>2</sub> phase (Fig 3.18 and table 3.15). Longer incubation time should be carried out to determine whether the S-phase cells had escaped from the

arrest or G<sub>2</sub>/M arrest was also begun to initiate.

It could be seen that apoptosis was only induced in the apoptosis-proficient HL-60 cells but not in the apoptosis-resistant K562 cells by HWE2. Elevation of cells in the S phase was observed in both cell lines, but further analysis should be carried out.

(a)



(b)

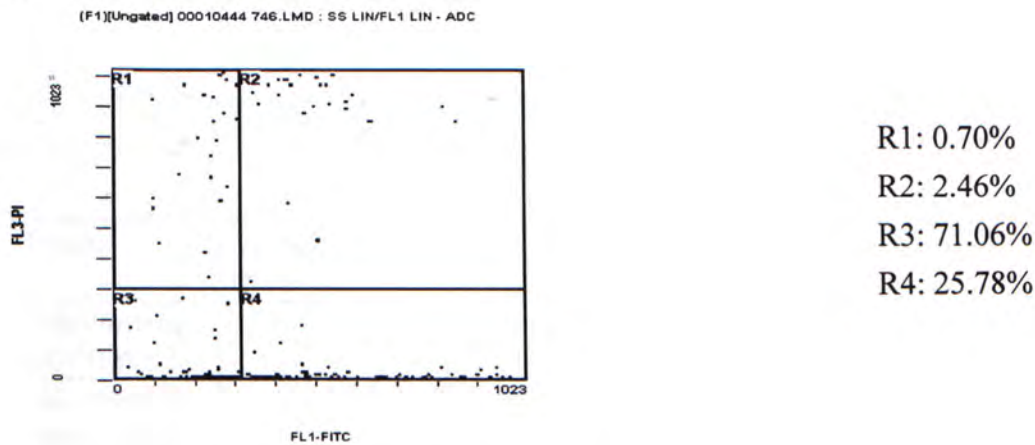


Fig. 3.16 Bivariate PI/annexin V analysis of the (a) untreated and (b) PTR HWE2-treated (200 µg/ml) HL-60 cells

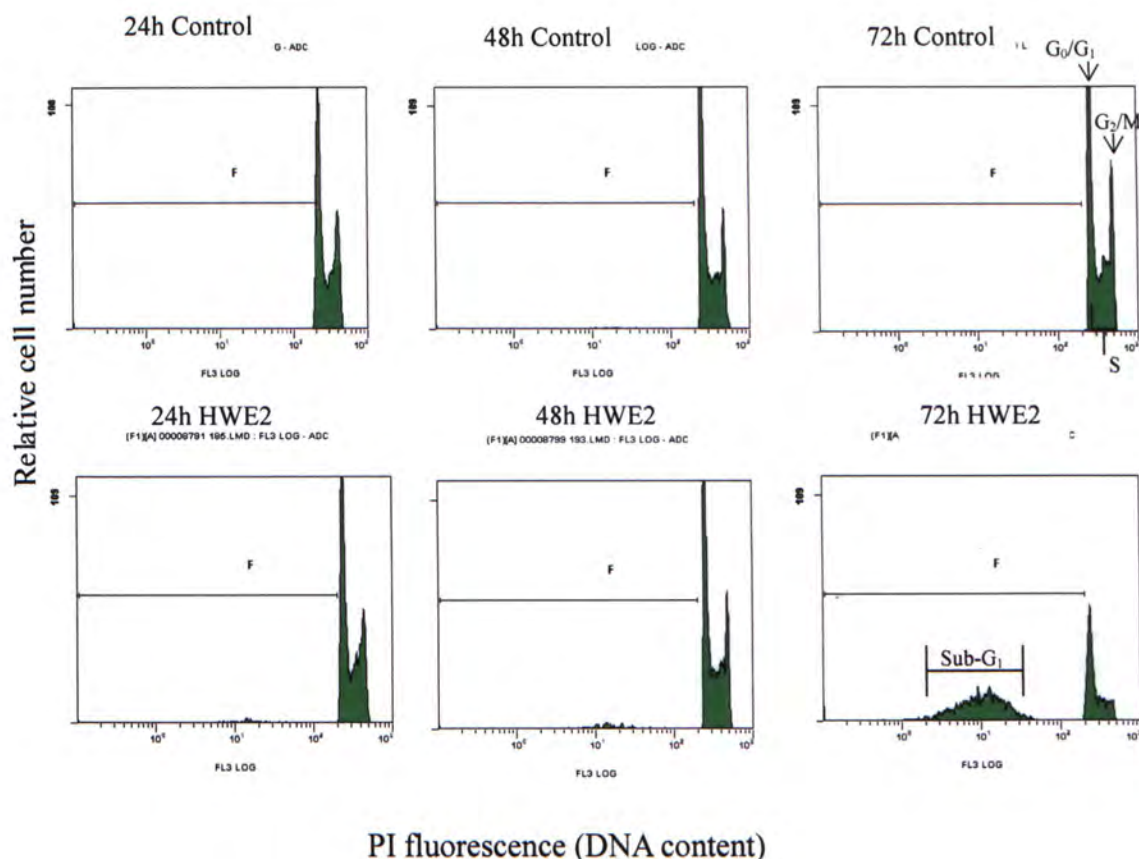


Fig. 3.17 Representative cytograms showing the effect of HWE2 at 200 µg/ml on the cell-cycle phases ( $G_0/G_1$ , S, and  $G_2/M$ ) and apoptosis (Sub- $G_1$  peak) of HL-60 cells at 24, 48 and 72 hours.

Table 3.14 Numeric expression of the relative cell number on the cell-cycle phases and apoptosis of HL-60 cells by HWE2 at 200 µg/ml.

Group	% Apoptotic cells (Sub- $G_1$ )	% Non-apoptotic cells		
		$G_0/G_1$	S	$G_0/G_1$
24h control	10.9±2.72	40.9±1.56	41.1±2.55	18.0±0.54
24h HWE2	15.7±5.30	43.0±3.37	44.8±1.45	12.2±2.63
48h control	8.18±1.85	42.6±2.00	44.7±0.61	12.7±1.41
48h HWE2	14.5±0.81 *	40.3±2.10	49.2±1.48 *	12.2±0.99
72h control	5.96±2.82	38.0±1.31	48.1±0.35	13.9±1.66
72h HWE2	68.1±4.20 @	53.6±2.11 @	37.1±3.40 #	9.4±3.17

Different letters represent the significant difference between the relative number of cells in control group and treatment group by Student's t-test (\*  $p < 0.05$ , #  $p < 0.01$  and @  $p < 0.001$ ).



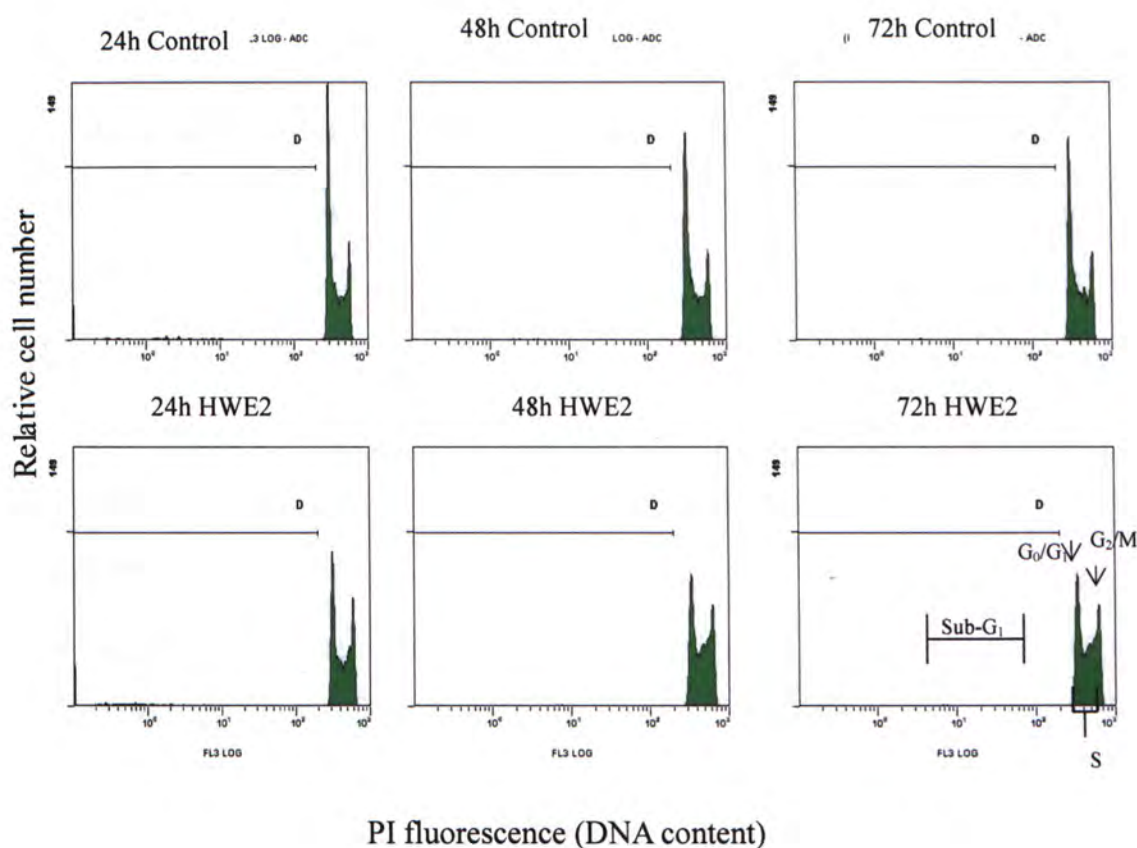


Fig. 3.18 Representative cytograms showing the effect of HWE2 at 200 µg/ml on the cell-cycle phases ( $G_0/G_1$ , S, and  $G_2/M$ ) and apoptosis (Sub- $G_1$  peak) of K562 cells at 24, 48 and 72 hours.

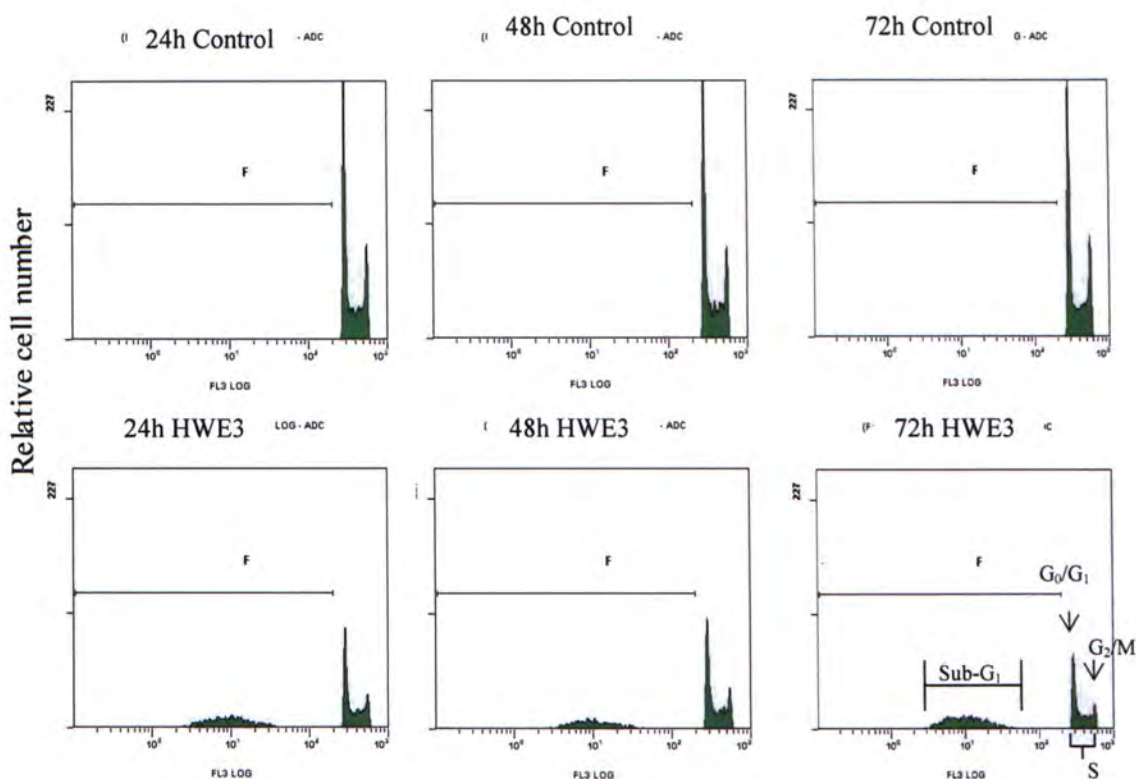
Table 3.15 Numeric expression of the relative cell number on the cell-cycle phases and apoptosis of K562 cells by HWE2 at 200 µg/ml.

Group	Apoptotic cells (Sub- $G_1$ )	Non-apoptotic cells		
		$G_0/G_1$	S	$G_2/M$
24h control	10.2±0.40	28.5±5.27	53.1±2.15	18.4±1.69
24h HWE2	10.7±0.49	24.9±4.21	55.4±3.62	19.6±1.47
48h control	8.94±0.52	30.1±3.85	53.4±2.45	16.5±1.99
48h HWE2	9.95±1.78	28.3±4.23	59.5±0.87*	12.1±1.60*
72h control	8.00±0.88	30.3±2.88	56.1±1.66	13.6±3.62
72h HWE2	8.29±2.51	21.7±3.40*	65.2±2.58 <sup>#</sup>	13.1±4.87

Different letters represent the significant difference between the relative number of cells in control group and treatment group by Student's t-test (\*  $p < 0.05$ , <sup>#</sup>  $p < 0.01$  and @  $p < 0.001$ ).

### 3.8.5 Effect of HWE3 on cell-cycle phases of HL-60 and K562 cells

When HWE3 at 200 µg/ml was incubated with HL-60 cells, significant ( $p<0.05$ ) increases of apoptotic peak and S-phase peak were observed at all three time points, having 60.0% and 51% cells in the Sub-G<sub>1</sub> peak and S peak at 72 hours, respectively (Table 3.16). On the other hand, similar ratio from control to treatment group was observed in the cell cycle of non-apoptotic HL-60 throughout the three time points (0.8 for G<sub>0</sub>/G<sub>1</sub> phase, 1.2 for S phase and 0.8 for G<sub>2</sub>/M phase) (Fig 3.19 and table 3.16). Thus, the effect of HWE3 on the cell cycle of HL-60 cells could not be enhanced by longer treatment time. HWE3 at 100 µg/ml caused no significant changes in the cell cycle of K562 cells though an increase of the % of the cells in S phase was observed (Table 3.17). Apoptotic peak was significantly ( $p<0.05$ ) increased (Fig. 3.20) but the ratio of the apoptotic cells in treatment group to control group was slightly decreased from 24 hours to 72 hours (2.1 for 24 hours, 1.4 for 48 hours, 1.3 for 72 hours), implying the rate to trigger apoptosis might be decreasing. As same as EDP-treated HL-60 cells, it might be due to the deviations between the control groups and therefore further investigation is still required for this phenomenon (Fig 3.20 and table 3.16).



PI fluorescence (DNA content)

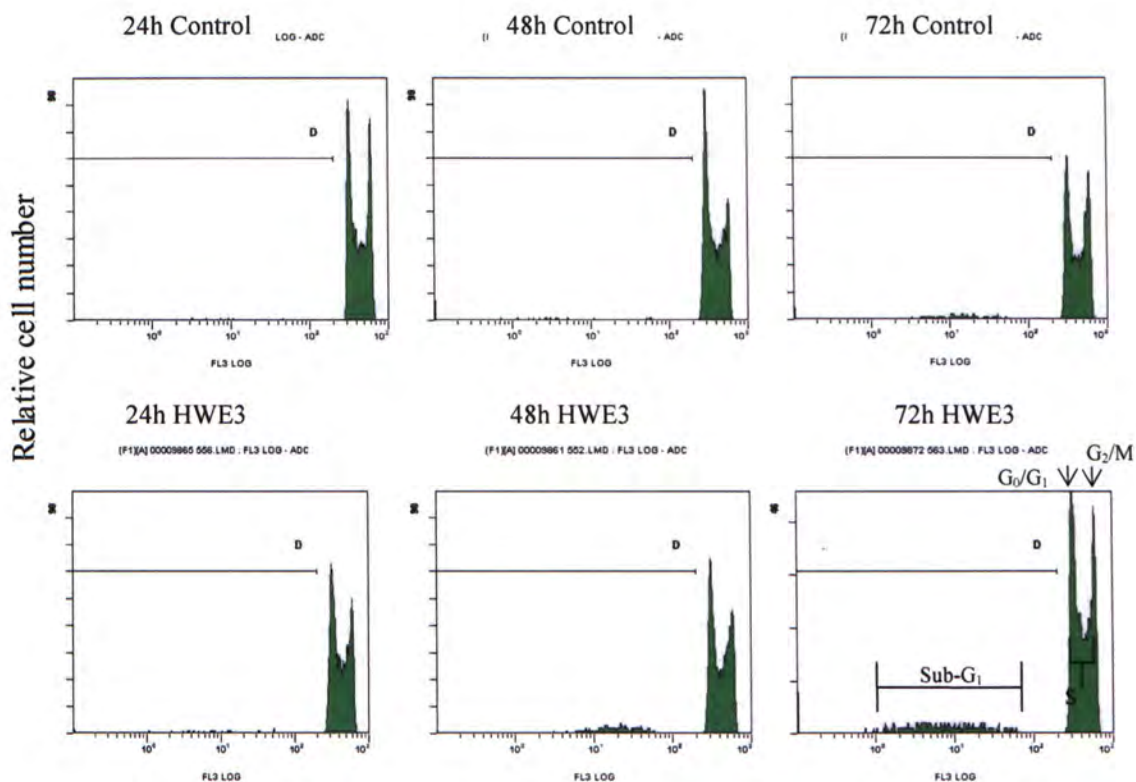
Fig. 3.19 Representative cytograms showing the effect of HWE3 at 200 µg/ml on the cell-cycle phases ( $G_0/G_1$ , S, and  $G_2/M$ ) and apoptosis (Sub- $G_1$  peak) of HL-60 cells at 24, 48 and 72 hours.

Table 3.16 Numeric expression of the relative cell number on the cell-cycle phases and apoptosis of HL-60 cells by HWE3 at 200 µg/ml.

Group	% Apoptotic cells (Sub- $G_1$ )	% Non-apoptotic cells		
		$G_0/G_1$	S	$G_2/M$
24h control	1.8±0.5	43.2±1.0	43.1±0.8	13.8±0.2
24h HWE3	47.6±3.7 *	38.4±0.4 *	50.5±2.1 *	11.2±0.7
48h control	2.2±0.9	42.3±0.7	44.0±0.2	13.8±0.9
48h HWE3	47.4±7.3 *	37.9±1.9	50.8±3.0	11.4±1.2
72h control	2.0±0.04	42.4±0.4	43.6±0.3	14.1±0.6
72h HWE3	60.0±1.3 *	37.1±2.0	51.0±2.4 *	11.9±0.4 *

Different letters represent the significant difference between the relative number of cells in control group and treatment group by Student's t-test (\*  $p < 0.05$ , #  $p < 0.01$  and @  $p < 0.001$ ).





PI fluorescence (DNA content)

Fig. 3.20 Representative cytograms showing the effect of HWE3 at 100 µg/ml on the cell-cycle phases (G<sub>0</sub>/G<sub>1</sub>, S, and G<sub>2</sub>/M) and apoptosis (Sub-G<sub>1</sub> peak) of K562 cells at 24, 48 and 72 hours.

Table 3.17 Numeric expression of the relative cell number on the cell-cycle phases and apoptosis of K562 cells by HWE3 at 100 µg/ml.

Group	% Apoptotic cells (Sub-G <sub>1</sub> )	% Non-apoptotic cells		
		G <sub>0</sub> /G <sub>1</sub>	S	G <sub>2</sub> /M
24h control	11.8±0.74	25.4±2.86	53.9±3.09	20.7±0.58
24h HWE3	24.7±1.68 @	25.5±2.60	53.2±3.44	21.4±3.75
48h control	17.7±0.21	25.5±1.47	53.7±1.63	20.9±0.61
48h HWE3	24.8±3.24 *	23.0±1.59	55.2±1.68	22.0±4.40
72h control	17.5±1.61	27.2±1.79	50±1.50	17.0±2.72
72h HWE3	22.7±0.91 *	27.0±3.34	55.7±0.2	17.4±3.25

Different letters represent the significant difference between the relative number of cells in control group and treatment group by Student's t-test (\*  $p < 0.05$ , #  $p < 0.01$  and @  $p < 0.001$ ).

The PTR extracts triggered apoptosis and/or caused cell-cycle arrest in HL-60 and K562 cells as revealed by the above results from the flow cytometry. Different responses to the PTR extracts might be due to different cell types and their sensitivity and the resistance to the extracts. Apoptosis was readily observed in HL-60 cells incubated with the PTR extracts, however, K562 cells were shown to be resistant to apoptosis when incubating with 200  $\mu\text{g/ml}$  of HWE2 and delayed apoptosis occurred in response to 300  $\mu\text{g/ml}$  of HWE1 and CEP. It is believed to be related to the characteristics of these two cell lines as it has been reported that different cancer cell lines would give different responses to the antitumor agents (Jiang *et al.*, 2004). Besides, the concentration of the PTR extracts employed in the flow cytometric analysis was the  $\text{IC}_{50}$  value estimated from the BrdU incorporation assay, thus there were inevitably slight deviations between the results from the two assays that the % apoptosis from flow cytometry might not be 50%. Since apoptosis-proficient HL-60 cells was more sensitive to PTR treatment, HL-60 cell line was chosen to further study on the expression level of cellular proteins. Among three PTR HWEs, HWE2 seemed to be the most promising one that induce S arrest and apoptosis in HL-60 cells. The cellular proteins involved in its S arrest and apoptosis were also further investigated by western blot.



### **3.9 The effect of PTR extracts on expression of cellular proteins involved in cell-cycle control and apoptotic pathway in HL-60 cells**

The cellular proteins attributed in the pathways of cell-cycle arrest and apoptosis in HL-60 cells treated with PTR extracts were investigated by western blot in order to gain insights on their mechanisms. The expression levels of proteins were semi-quantified by densitometer.

#### **3.9.1 Expression of Bcl-2 and Bax proteins in HL-60 cells treated with PTR extracts**

Bcl-2 family proteins are key regulators in apoptosis, particularly the antiapoptotic Bcl-2 and proapoptotic Bax proteins (Oltvai *et al.*, 1993). Bcl-2 locates in the outer mitochondrial membrane to inhibit the release of cytochrome *c*, while Bax is activated to antagonize the effect of antiapoptotic proteins and directly disrupts the mitochondrial membrane (Cory and Adams, 2002). Bax/Bcl-2 ratio determines the susceptibility of cells to apoptosis and the therapeutic response to the chemotherapy (Raisova *et al.*, 2001). Their expressions which were affected by PTR extracts were investigated to see whether they are responsible for the respective apoptotic induction.

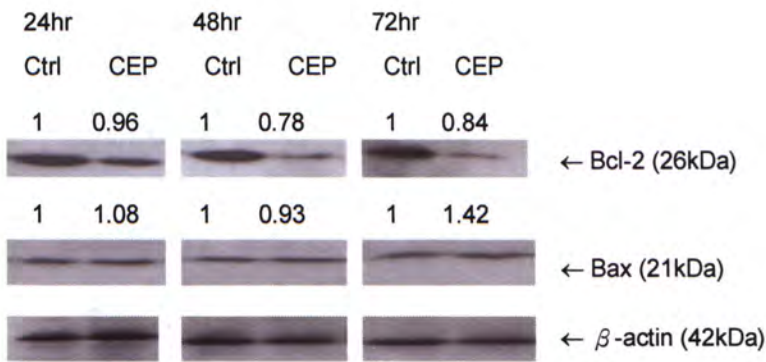
The expression of Bcl-2 protein in HL-60 cells was lowered in a time-dependent manner after CEP (Fig 3.21a) and HWE3 (Fig 3.25a) treatment, whereas that of Bax protein was increased greatly after 72-hour incubation in CEP and HWE3 treatments. Also, the increase in the apoptosis was negatively correlated with the increase in the Bax/Bcl-2 ratio and which was the highest increase at 72 hours (Fig



3.21b and 3.25b), consistent with the highest percentage of apoptosis observed in flow cytometry (Fig 3.10 and table 3.8; Fig 3.19 and table 3.16). EDP also unregulated the expression of Bax protein in a time-dependent manner and Bcl-2 protein expression was reduced evidently (Fig 3.22a). The trend of Bax/Bcl-2 ratio obtained in EDP-treated HL-60 cells at the three time points (Fig 3.22b) was consistent with that of apoptosis found from flow cytometry (Fig 3.12 and table 3.10). These PTR extracts were similar to Grifolan isolated from the fruiting bodies of *Albatrellus confluens* that inhibited the human nasopharyngeal carcinoma CNE1 *in vitro* by apoptosis involving downregulation of Bcl-2 and upregulation of Bax with a concomitant increase of Bax/Bcl-2 ratio (Ye *et al.*, 2005).

The expression of Bcl-2 protein was not modulated by HWE1 but the Bax was unregulated at 48 and 72 hours (Fig 3.23a), so the Bax/Bcl-2 ratio of the HWE1-treated HL-60 cells was increased in a time-dependent fashion that shifted the cells into apoptotic death (Fig 3.23b). In HWE2-treated cells, the expression level of the Bax protein was markedly increased at three time points while that of Bcl-2 protein was reduced in a time-dependent manner (Fig 3.24a). It seemed that the expression level of Bcl-2 protein might be a determining factor for triggering of apoptosis as the percentage of apoptosis (68.1%) was sharply increased when the Bcl-2 protein expression was the lowest at 72 hours. However, the Bax/Bcl-2 ratio was not reduced time-dependently as expected from the flow cytometric analysis (Fig 3.24b). This might due some deviations occurred in western blot and hence more repeats should be done to make a better quantification.

(a)



(b)

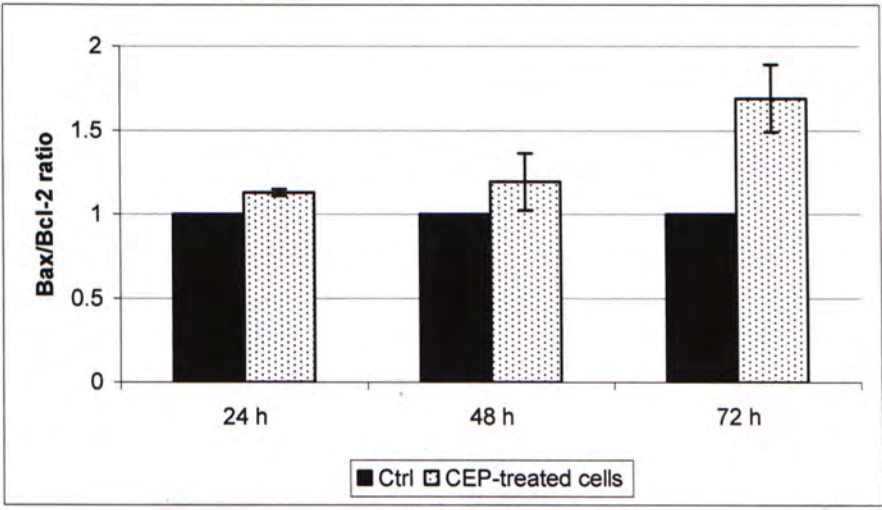
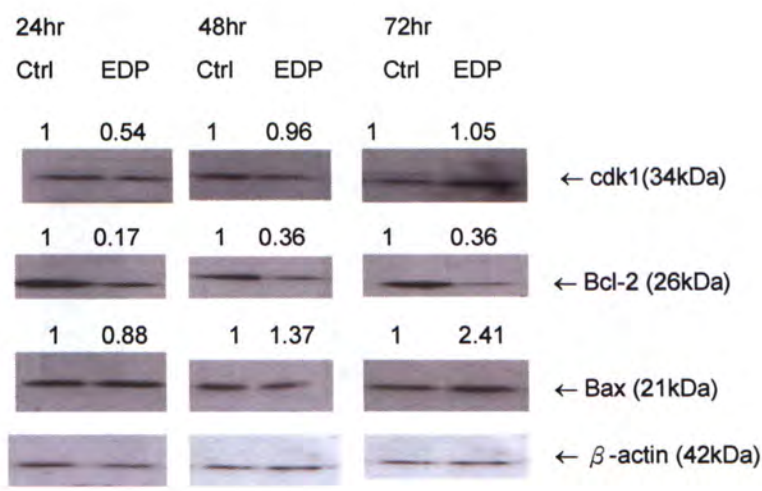


Fig. 3.21 (a) The Bcl-2 and Bax expressions in HL-60 cells incubated with CEP at 300  $\mu$ g/ml for 24, 48 and 72 h with the relative density of the band measured by densitometer.  $\beta$ -actin was used as the loading control. (b) The corresponding ratio of the relative density of Bax/Bcl-2 in CEP-treated HL-60 cells.

(a)



(b)

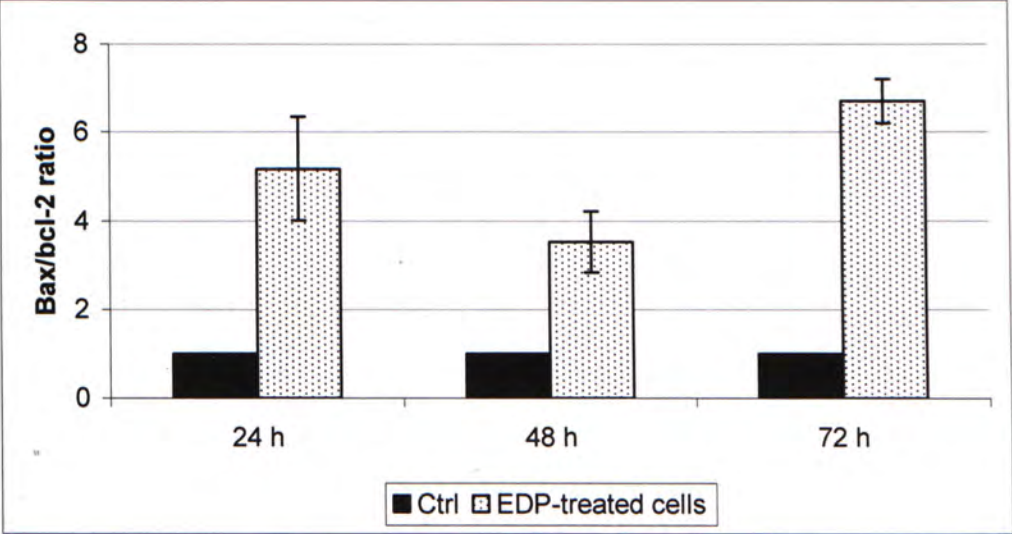


Fig. 3.22 (a) The Cdk1, Bcl-2 and Bax expressions in HL-60 cells incubated with EDP at 400  $\mu$ g/ml for 24, 48 and 72 h with the relative density of the band measured by densitometer.  $\beta$ -actin was used as the loading control. (b) The corresponding ratio of the relative density of Bax/Bcl-2 in EDP-treated HL-60 cells.



(c)

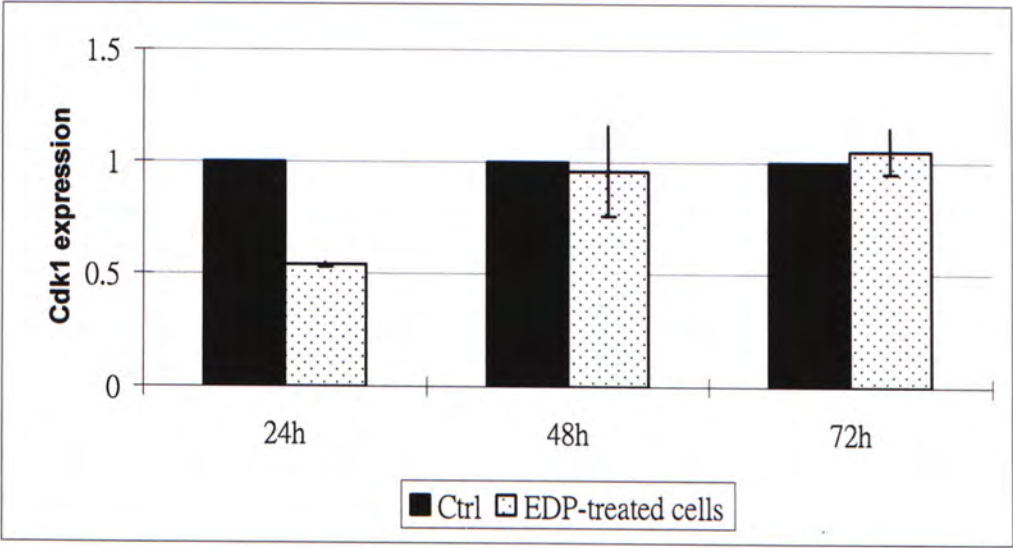
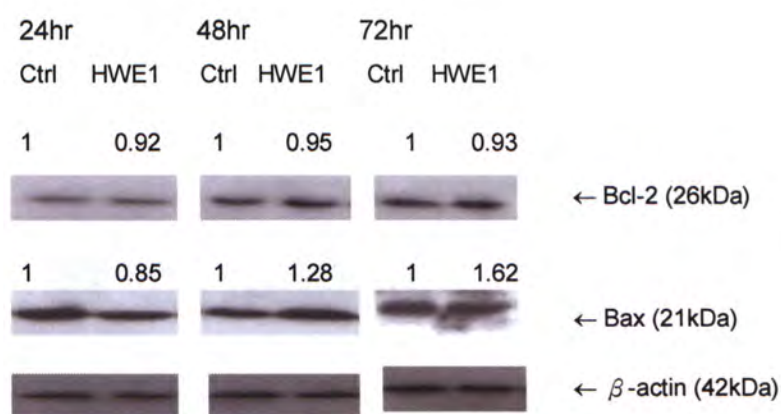


Fig 3.22 (c) The relative expression of Cdk1 in EDP-treated HL-60 cells.

(a)



(b)

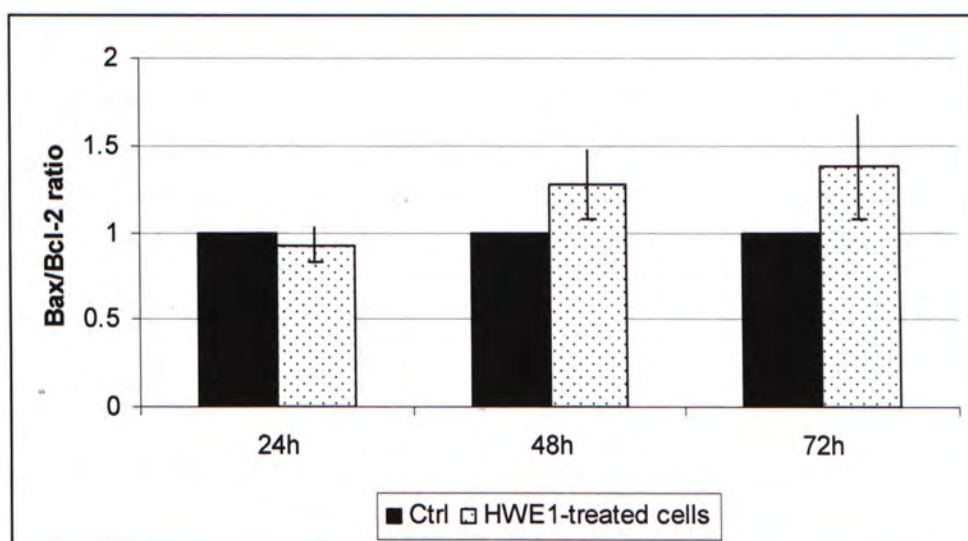
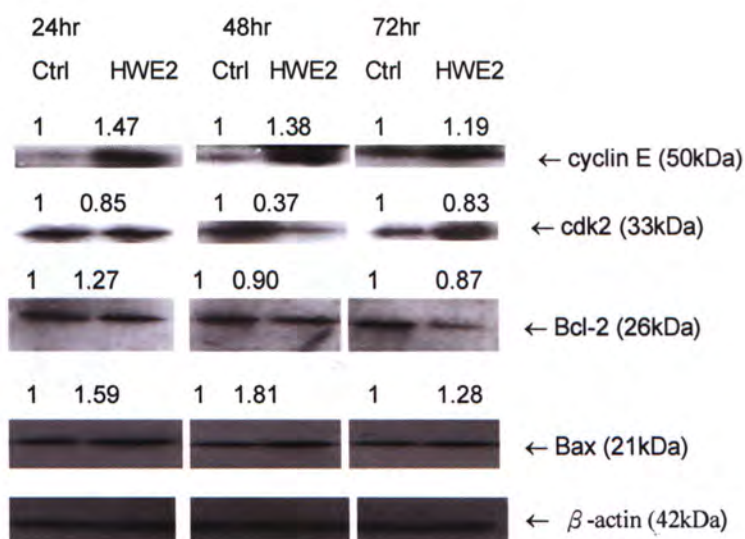


Fig. 3.23(a) The Bcl-2 and Bax expressions in HL-60 cells incubated with HWE1 at 400  $\mu\text{g/ml}$  for 24, 48 and 72 h with the relative density of the band measured by densitometer.  $\beta$ -actin was used as the loading control. (b) The corresponding ratio of the relative density of Bax/Bcl-2 in HWE1-treated HL-60 cells.

(a)



(b)

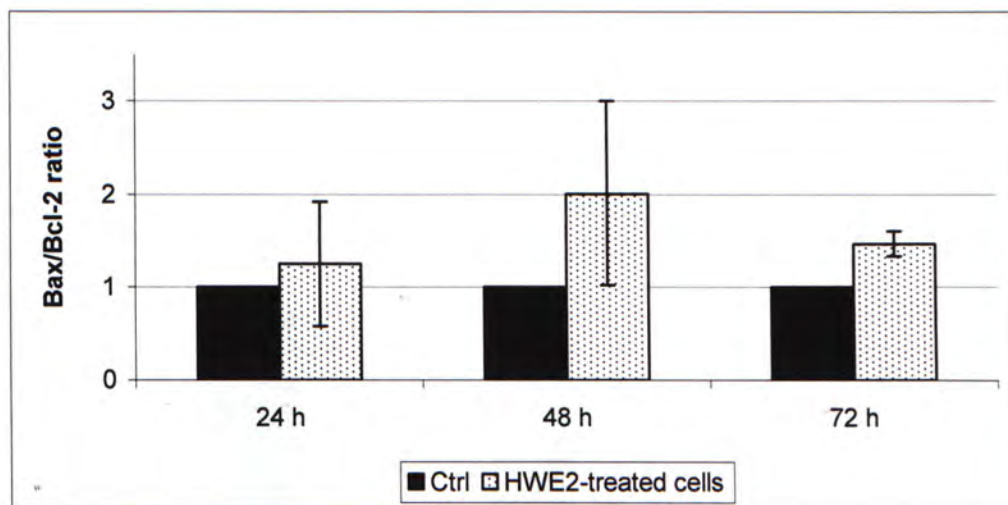
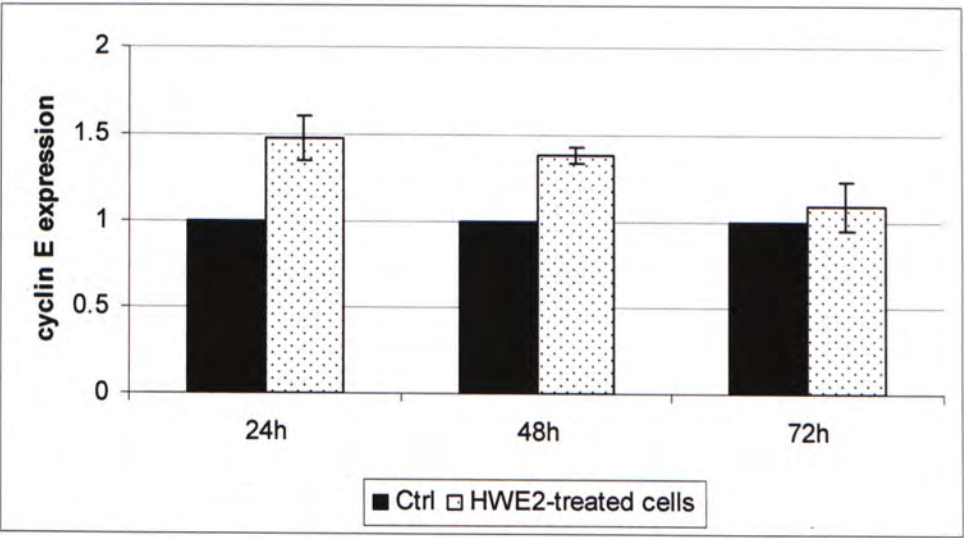


Fig. 3.24(a) The cyclin E, Cdk2, Bcl-2 and Bax expressions in HL-60 cells incubated with HWE2 at 200  $\mu$ g/ml for 24, 48 and 72 h with the relative density of the band measured by densitometer.  $\beta$ -actin was used as the loading control. (b) The corresponding ratio of the relative density of Bax/Bcl-2 in HWE2-treated HL-60 cells.



(c)



(d)

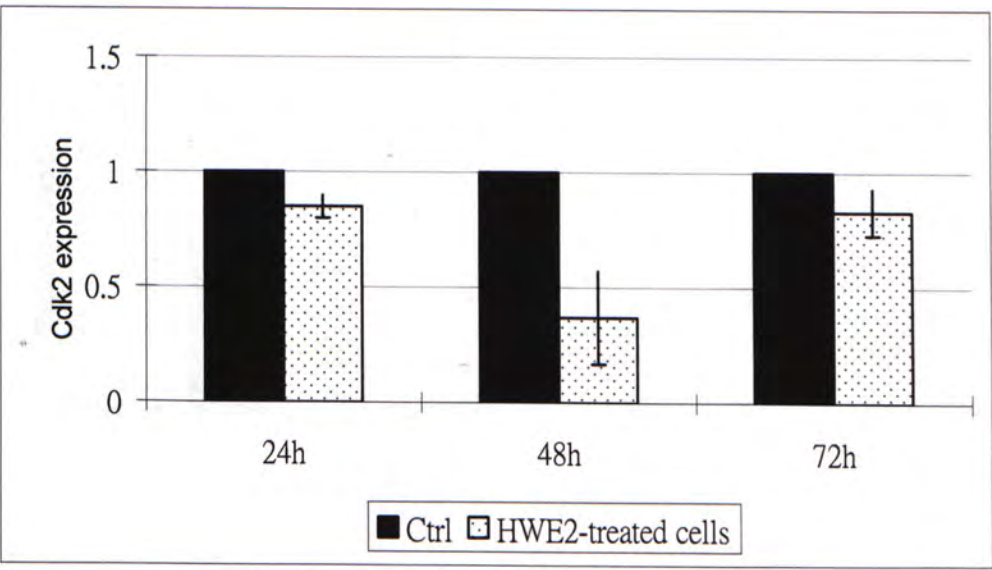
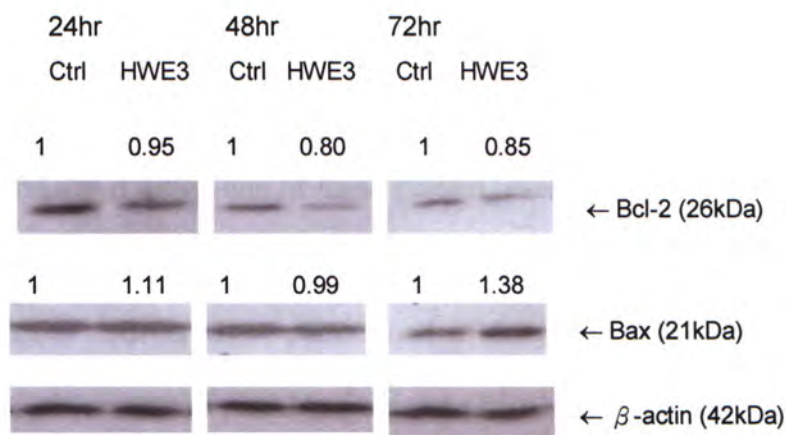


Fig. 3.24 The relative expression of (c) cyclin E and (d) Cdk2 in HWE2-treated HL-60 cells.

(a)



(b)

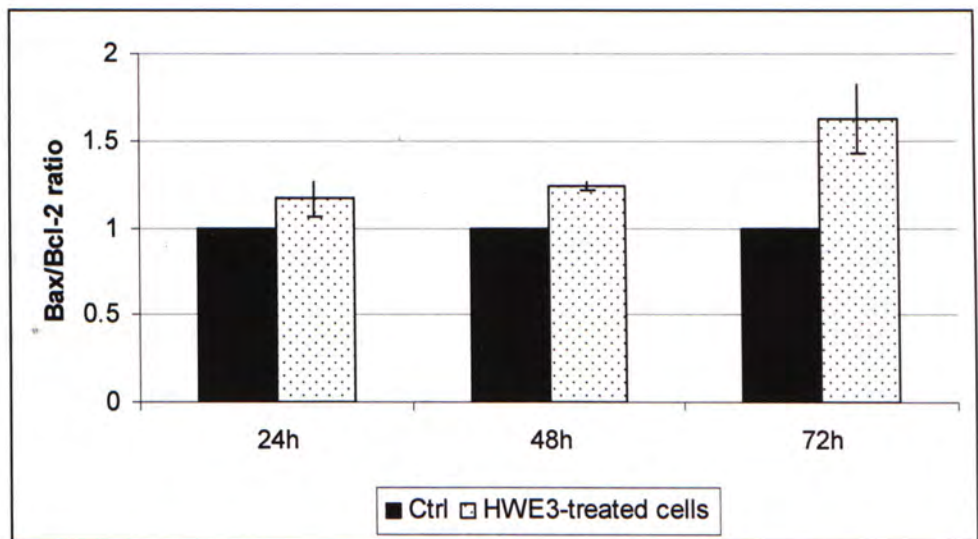


Fig. 3.25(a) The Bcl-2 and Bax expressions in HL-60 cells incubated with HWE3 at 200  $\mu$ g/ml for 24, 48 and 72 h with the relative density of the band measured by densitometer.  $\beta$ -actin was used as the loading control. (b) The corresponding ratio of the relative density of Bax/Bcl-2 in HWE3-treated HL-60 cells.

### 3.9.2 Expression of cyclins and Cdks in HL-60 cells by PTR extracts

Cyclin B/Cdk1 complex is important in the G<sub>2</sub>/M transition and it is only activated when mitosis is ready to begin (Schwartz & Shah, 2005). The cell could not progress normally if either one of these protein levels was lowered. The expression of Cdk1 was downregulated by EDP at 24 hours only (Fig 3.22c), consistent with the accumulation of cells in G<sub>2</sub>/M peak found in flow cytometry (Fig 3.12 and table 3.10). The G<sub>2</sub>/M arrest had possibly occurred which was due to the limited supply of cdk1, similar to the squamocin-induced G<sub>2</sub>/M arrest in K562 cells that decreased the protein level of Cdk1 and the subsequent formation of cyclin B1/Cdk1 complex even the cyclin B1 expression was not changed (Lu *et al.*, 2006). Besides, the inhibition of *Ganoderma lucidum* extract on PC3 prostate cancer cells was via G<sub>2</sub>/M arrest by lowering the expression of Cdk1 and cyclin B (Jiang *et al.*, 2004). Further investigation should be performed to understand the whole mechanism, for instance, the action of EDP might be similar to other natural Cdk inhibitors, such as p21, that inhibit the Cdk activation directly or target its upstream pathway that regulates its activity (Schwartz and Shah, 2005).

The expression of cyclin E was enhanced by HWE2 (Fig 3.24c), similar to the PSP isolated from *Coriolus versicolor* induced S arrest in HL-60 cells via an upregulation of cyclin E reported previously (Hui *et al.*, 2005). Moreover, the possibility that G<sub>1</sub> arrest occurred at 72 hours could be ruled out as cyclin E was upregulated at three time points. Cyclin D and cyclin E expressions should be reduced when G<sub>1</sub> arrest so that pRb protein could not be phosphorylated and cells were arrest at the G<sub>1</sub> phase. For instance, *Hypsizigus marmoreus* induced G<sub>1</sub> arrest in



HepG2 cells by lowering the expression of cyclin D1 and E (Chang *et al.*, 2004); the carboxymethylated  $\beta$ -glucan isolated from PTR sclerotium inhibited the proliferation of MCF-7 cell via G<sub>1</sub> arrest by down-regulating cyclin D1 and cyclin E expressions (Zhang *et al.*, 2006a).

Besides, Cdk2 expression level was lowered by HWE2 (Fig 3.24d). Inactivation of Cdk2 could block the loading of CDC45 onto DNA. DNA polymerase would not be recruited and so no DNA replication was initiated (Kastan and Bartek, 2004). Therefore, cells would be halted at the S phase. Cdk2 could form complex with cyclin E and cyclin A which are responsible for G<sub>1</sub>/S transition and S phase progression, respectively. Based on the result of flow cytometry and cyclin E expression, Cdk2 might be inactivated after the cell has already passed through the G<sub>1</sub>/S boundary. The function of CDC 45 was then affected and the S phase progression might be hindered due to the inhibited activity of cyclin A/Cdk2 complex. Further investigations are required to find out time that Cdk2 is inactivated to support this hypothesis.

In summary, the inactivation of Cdk2 and upregulated cyclin E might be associated with the S arrest in the HL-60 cells caused by HWE2. After considering the cytogram of HWE2-treated HL-60 cells, the highest percentage of cells observed in G<sub>1</sub> phase might be due to the cells in S and G<sub>2</sub>/M phases might shift to apoptosis after long incubation period. There was relatively smaller amount of cells in these phases, leading to an increase in the numeric expression of cells found in G<sub>1</sub> phase.

### 3.9.3 The plausible antiproliferative mechanism(s) involved in PTR extracts on HL-60 cells

It has been realized that tumor growth was an equilibrium between cell proliferation and cell death. Therefore, delaying the proliferation rate and promoting apoptosis in cancer cells would be an effective strategy in cancer treatment. PTR extracts had been revealed that they could modulate the protein expressions contributed in the pathways of cell cycle arrest and apoptosis.

Although HL-60 cells lost the p53 tumor suppressor protein, PTR extracts still induced apoptosis via the upregulation of its downstream product, Bax protein. It was thereby revealed that the upregulation of the Bax level by PTR extracts to promote apoptosis in the HL-60 cells was through a p53-independent pathway. It is well known that Bcl-2 and Bax are involved in the intrinsic mitochondrial-dependent pathway. Bax protein neutralizes the anti-apoptotic effect of Bcl-2 protein and increases the mitochondrial membrane permeability, leading to the release of cytochrome *c*. It would further bind to Apaf-1 and caspase 9 to form apoptosome. The caspase 9 would cleave and activate the effector caspase 3, a series of apoptotic changes was then triggered (Cory and Adam, 2002; Okada and Mak, 2004). Although the pathway mediated by the PTR extracts in HL-60 cells was not fully understood from the present results, it was suggested that the apoptosis induced by the PTR extracts was associated with the augment of Bax/Bcl-2 ratio and might be partially controlled by the mitochondrial-dependent pathway.

The fact that the PTR extracts could induce S or G<sub>2</sub>/M arrest, instead of G<sub>1</sub> arrest, in HL-60 cells might be due to the lack of functional p53 protein in HL-60



cells. G<sub>1</sub> arrest is solely regulated by the tumor suppressor proteins p53 and pRb (Murray, 2004). It has been reported that cells with p53 are usually arrested at the G<sub>1</sub> phase whereas those that lack p53 would preferentially be arrested at the S and G<sub>2</sub>/M phases (Eastman, 2004). For instance, an alkaline-soluble  $\beta$ -glucan extracted from the mycelium of *Poria cocos* was reported to have antiproliferative activity MCF-7 cells which has an intact p53 protein. It was also found that this  $\beta$ -glucan caused cell-cycle arrest at G<sub>1</sub> phase and apoptotic induction, revealed by western blot showing that cyclin D1 and E expressions were reduced whereas Bax/Bcl-2 ratio was elevated (Zhang *et al.*, 2006b). PSP (25  $\mu$ g/ml) isolated from *Coriolus versicolor* mycelia could arrest the HL-60 cells at the S and G<sub>2</sub>/M phases with elevation of cyclin E expression (Hui *et al.*, 2005). Recently, many mushroom polysaccharides showed *in vitro* antiproliferative effect by cell cycle arrest and apoptosis. *Ganoderma lucidum* extract, containing polysaccharides and triterpenes, inhibited the growth of PC3 prostate cancer cells by G<sub>2</sub>/M arrest to halt its cell cycle (Jiang *et al.*, 2004). Protein-bound polysaccharides (PL) isolated from *Phellinus linteus* inhibited the growth of SW480 human colon cancer cells significantly via G<sub>2</sub>/M arrest and apoptosis, which were associated with the decrease of the Bcl-2 level and an increase in the cytochrome *c* level which promoted the occurrence of apoptosis and a decrease of cyclin B1 expression so as to delay the G<sub>2</sub> to M phase progression (Li *et al.*, 2004).

Besides, the carboxymethylated  $\beta$ -glucan isolated from PTR sclerotium was shown to exhibit antiproliferative activity towards MCF-7 cells via G<sub>1</sub> arrest and apoptotic induction by depletion of cyclin D1 and cyclin E expressions and lowering Bcl-2 expression to increase the Bax/Bcl-2 ratio, respectively (Zhang *et al.*, 2006a). This suggested that the polysaccharides isolated from various developmental stage of PTR could exert *in vitro* antiproliferative activity against HL-60 and MCF-7 cells by



cell cycle arrest and/or apoptotic induction. It is likely that their mode of action was associated with the characteristics of cell line tested.

#### 4.1 Conclusions

Aqueous extracts from the different morphological forms of PTR varied greatly not only in their chemical composition but also their potency and mechanism of antiproliferative activities. CEP and EDP were high in carbohydrate content (83.4% and 87.2%, respectively) and low in protein content (15.9% and 3.24%, respectively). In contrast, three HWEs had comparatively higher protein content (>30.4%) but lower carbohydrate content. Mannose was dominant in CEP while glucose was the major monosaccharides in the EDP and HWEs. Besides, the amount of mannose and galactose were substantial in the HWEs. HWEs had a higher molecular weight (above  $156 \times 10^4$ ) than CEP and EDP (MW of  $4.4 \times 10^4$  and  $50.9 \times 10^4$ , respectively).

The present study was the first one to demonstrate that CEP, which was suggested to be a mannan according to the previous results (Wong, 2004), reduced the viability and rate of proliferation of HL-60 cells significantly ( $p < 0.05$ ) via apoptosis involving downregulation of Bcl-2 and upregulation of Bax with a concomitant increase of Bax/Bcl-2 ratio. Moreover, EDP, probably a glucan as previously described (Wong, 2004), caused a G<sub>2</sub>/M arrest and induced apoptosis in the HL-60 cells, which might be correlated with the reduced Cdk1 and Bcl-2 expressions, as well as augmented expression of Bax and the Bax/Bcl-2 ratio. This was different from our previous study of a (1→3)-β-glucan obtained from *Poria cocos* mycelium which was found to inhibit the proliferation of MCF-7 cancer cells by G<sub>1</sub> arrest and apoptotic induction via downregulating anti-apoptotic protein Bcl-2

(Zheng *et al.*, 2006). Also, the water-soluble carboxymethylated (1→3)- $\beta$ -glucans obtained from sclerotia of PTR had been shown to inhibit the proliferation of MCF-7 cell via G<sub>1</sub> arrest by downregulating cyclin D1 and cyclin E expressions and apoptotic induction by lowering Bcl-2 expression and increasing the Bax/Bcl-2 ratio (Zhang *et al.*, 2006a). The above different observations might be due to the difference in the cell lines used as MCF-7 cell was p53-positive while HL-60 cell was p53-defective. Previous findings have revealed that cells that are lack of p53 protein preferentially arrested at S and G<sub>2</sub>/M phases but cells with functional p53 would usually have G<sub>1</sub> arrest (Eastman, 2004). Also, other factors such as molecular weight, conformation and linkage between the glucose residues would affect the antiproliferative activity. Besides, it has been previously reported that the water-soluble sclerotial polysaccharides (SCP) from PTR had a MW of  $43.5 \times 10^4$  and was suggested to be glucan which showed less effective growth inhibition on HL-60 cells than other PTR extracts (Zhang *et al.*, 2006a).

Furthermore, HWEs isolated from PTR fruiting body consisted of mainly glucose, mannose and galactose, and strong UV absorbance was observed in HPLC, speculating they are likely to be a heteropolysaccharide-protein complex. The HWE2 fraction seemed to be the most potent ones among the three HWEs having the highest carbohydrate content and lowest protein amount as well as a higher molecular weight, all of which might facilitate its cytotoxicity towards cancer cells. Its antiproliferation against HL-60 cells via apoptosis and S arrest might be associated with the downregulated Bcl-2 and Cdk2 levels and the upregulated cyclin E, consistent with a previous study on PSP, which is a polysaccharide-protein complex from *Coriolus versicolor*, that also caused the S phase arrest and apoptosis in HL-60 cells by an increase of the Bax/Bcl-2 ratio and elevation of cyclin E level



(Hui *et al.*, 2005; Yang *et al.*, 2005).

In summary, the mannose-rich CEP with the smallest molecular weight induced apoptosis in HL-60 cells *in vitro* whereas the glucose-rich EDP with moderate molecular weight inhibited the HL-60 cells *in vitro* by G<sub>2</sub>/M arrest and apoptosis. HWE2, having the highest molecular weight, was the most potent extract among the three PTR HWEs. HWE2 had considerable amount of protein which might be heteropolysaccharide-protein complex that exerted its *in vitro* antiproliferative activity towards HL-60 cells via S arrest and apoptosis.

## 4.2 Future works

HWE2 had a stronger antiproliferative activity than HWE1 and HWE3, suggesting it might have potential bioactive components that had substantial growth inhibitory effect. Therefore, further analysis on the detailed structure of PTR extracts including their glycosidic linkages, degree of branching, molecular conformation in solution, the amount of bound protein and its moiety are required in order to explain their different mode of actions towards the antiproliferation of cancer cells. Also, the PTR extracts were quite heterogeneous and hence fractionation and deproteinization could be done and attempt to find out the bioactive components they contained and the association with their antiproliferative potency. It is anticipated that the understanding of such structure-activity relationship in mushroom polysaccharides can provide more insights on their applications in cancer treatment.

Moreover, the detailed mechanistic pathway of the PTR-induced cytotoxicity

is not yet fully understood. The cellular molecules involving in the signal transduction pathways regulating the cell-cycle control and the two apoptotic pathways (extrinsic and the intrinsic ones) should be further analyzed in details.

Besides, as the PTR extracts could generally inhibit the growth of HL-60 and K562 cells *in vitro*, they might be effective in treating these two types of cancer, In future, *in vivo* animal studies should be carried out to check whether the PTR extracts could also exert their antiproliferative activities.

## Reference:

- Adachi, Y., Ohno, N., Ohsawa, M., Oikawa, S. and Yadomae, T., 1990, Change of biological activities of (1 → 3)- $\beta$ -D-glucan from *Grifola frondosa* upon molecular weight reduction by heat treatment. *Chemical & Pharmaceutical Bulletin*, 38, 477-481
- Akindahunsi A.A. and Oyetayo F.L., 2006, Nutrient and antinutrient distribution of edible mushroom, *Pleurotus tuber-regium* (fries) singer, *LWT - Food Science and Technology*, 39, 548-553
- A.O.A.C., 1996, In *Official Methods of Analysis*. Association of Official Analytical Chemists. Washington, D.C., USA.
- Baguley B.C., A Brief History of Cancer Chemotherapy, in *Anticancer drug development*, 2002, Baguley B.C. and Kerr. D.J., Academic Press, San Diego, California and London, pp1-9
- Beelman R.B., Royse D.J. and Chikthimmah N., 2003, Bioactive components in button mushroom *Agaricus bisporus* (J. Lge) imbach (Agaricomycetideae) of nutritional, medicinal, and biological importance (review), *International Journal of Medicinal Mushrooms*, 5, 321-337.



- Blakeney A.B., Harris P.J., Henry R.J. and Stone, B.A., 1983, A simple and rapid preparation of alditol acetates for monosaccharide analysis. *Carbohydrate Research*, 113: 291-299
- Bohn J.A. and BeMiller J.N., 1995, (1→3)- $\beta$ -D-Glucans as biological response modifiers: a review of structure-functional activity relationships, *Carbohydrate Polymers*, 28, 3-14
- Boivin J.F., 1990, Second cancers and other late side effects of cancer treatment. A review, *Cancer*, 65(3 Suppl), 770-775
- Brant D., McIntire T. and Gascoigne L., 1997, Understanding why stiff triple-stranded polysaccharides form cyclic structures. *Book of Abstracts, 213<sup>th</sup> ACS National Meeting, San Francisco, April 13-17, COMP-072*
- Browder, I.W., Williams, D.L., Sherwood, E.R., McNamee, R.B., Jones, E.L. and Di Luzio, N. R., 1987, Synergistic effect of non-specific immunostimulation and antibiotics in experimental peritonitis. *Surgery*, 102, 206-214
- Camelini C.M., Maraschin M., Matos de Mendonca M., Zucco C., Ferreira A.G. and Tavares L.A., 2005, Structural characterization of  $\beta$ -glucans of *Agaricus brasiliensis* in different stages of fruiting body maturity and their use in nutraceutical products, *Biotechnology Letters*, 27, 1295-1299.

- Cao D.X., Qiao B., Ge Z.Q. and Yuan Y.J., 2004, Comparison of burst of reactive oxygen species and activation of caspase-3 in apoptosis of K562 and HL-60 cells induced by docetaxel, *Cancer Letters*, 214, 103-113.
- Carlile M.J., Watkinson S.C. and Gooday G.W., 2000, Spores, dormancy and dispersal ,in *The Fungi*, Academic Press, San Diego, pp. 245-250
- Chang S.T. and Miles P.G., Overview of the biology of fungi, in: *Mushrooms: cultivation, nutritional value, medicinal effect, and environmental impact*, 2004, Boca Raton, Fla.: CRC Press, pp 53-92
- Chang J.S., Son J.K., Li G., Oh E.J., Kim J.Y., Park S.H., Bae J.T., Kim H.J., Lee I.S., Kim O.M., Kozukeu N., Han J.S., Hirose M. and Lee K.R., 2004, Inhibition of cell cycle progression on HepG2 cells by hypsiziprenol A<sub>9</sub>, isolated from *Hypsizigus marmoreus*, *Cancer Letters*, 212, 7-14.
- Cheung P.C.K. and Lee M.Y., 1998, Comparative chemical analysis of fibre material prepared by enzymatic and chemical methods from two mushroom (*Pleurotus sajor-caju* and *Pleurotus tuber-regium*), *Journal of Agricultural Food Chemistry*, 46, 4854-4857.
- Chihara, G., 1992, Immunopharmacology of Lentinan, a polysaccharide isolated from *Lentinus edodes*: Its application as a host defense potentiator. *International Journal of Oriental Medicine*, 17, 57-77.

- Chihara G., Hamuro Y., Maeda Y. Y.A. and Fukuoka F., 1970, Antitumor polysaccharide derived chemically from natural glucan (pachyman). *Nature*, 225, 943.
- Chihara G., Maeda Y.Y., Hamuro J., Sasaki T. and Fukuoka F., 1969, Inhibition of mouse sarcoma 180 by polysaccharides from *Lentinus edodes* (Berk.) Sing. *Nature*, 222, 687-688.
- Chow L.W.C., Lo G.S.Y., Loo W.T.Y., Hu X. and Sham J.S.T., 2003, Polysaccharide peptide mediates apoptosis by up-regulating p21 gene and down-regulating cyclin D1 gene, *The American Journal of Chinese Medicine*, 31, 1, 1-9
- Cory S. and Adams J.M., 2002, The bcl2 family: regulators of the cellular life-or-death switch, *Nature*, 2, 647-656
- Cui J. and Chisti Y., 2003, Polysaccharopeptides of *Coriolus versicolor*: physiological activity, uses, and production, *Biotechnology Advances*, 21, 109-122.
- Daba A.S. and Ezeronye O.U., 2003, Anti-cancer effect of polysaccharides isolated from higher basidiomycetes mushrooms, *African Journal of Biotechnology*, 2, 672-678.
- Deng C., Yang X., Gu X., Wang Y., Zhou J. and Xu H., 2000, A  $\beta$ -D-glucan from the sclerotia of *Pleurotus tuber-regium* (Fr.) Sing, *Carbohydrate Research*, 328, 629-633



- Dong Y., Kwan C.Y., Chen Z.N., Yang M.M.P., 1996, Antitumor effects of a refined polysaccharide peptide fraction isolated from *Coriolus versicolor*: *in vitro* and *in vivo* studies, *Research communications in molecular pathology and pharmacology*, 92, 140
- Dong Y., Yang M. M.P. and Kwan C.Y., 1997, *In vitro* inhibition of proliferation of HL-60 cells by tetrandrine and *Coriolus versicolor* peptide derived from Chinese medicinal herbs, *Life Sciences*, 60, 135-140
- Du G.J., Lin H.H., Xu Q.T. and Wang M.W., 2006, Bcl-2 switches the type of demise from apoptosis to necrosis via cyclooxygenase-2 upregulation in HeLa cell induced by hydrogen peroxide. *Cancer Letters*, 232, 179-188
- Dubois M., Gilles K.A., Hamilton J.K., Reber P.A. and Smith F., 1956, Colorimetric method for determination of sugars and related substances, *Analytical Chemistry*, 28, 350
- Eastman A., 2004, Cell cycle checkpoints and their impact on anticancer therapeutic strategies, *Journal of Cellular Biochemistry*, 91, 223-231
- Engeland M.V., Nieland L.J.W., Ramaekers F.C.S., Schutte B. and Reutelingsperger C.P.M., 1998, Annexin V-affinity assay: a review on an apoptosis detection system based on phosphatidylserine exposure, *Cytometry*, 31, 1-9
- Fasidi I.O. and Kadiri M., 1995, Toxicological screening of seven Nigerian mushrooms, *Food Chemistry*, 52, 419-422.

Fesik S.W., 2005, Promoting apoptosis as a strategy for cancer drug discovery. *Nature*, 5, 876-885

Fujimiya Y., Suzuki Y., Oshiman K. and et al, 1998, Selective tumoricidal effect of soluble proteoglycan extracted from the basidiomycete, *Agaricus blazei* Murill, mediated via natural killer cell activation and apoptosis. *Cancer immunology, immunotherapy: CII*, 46, 147-159.

Gibbs, W.W., 2003, Untangling the root of cancer. *Scientific American*, 289, 48-57

Gu Y.H. and Belury M.A., 2005, Selective induction of apoptosis in murine skin carcinoma cells (CH72) by an ethanol extract of *Lentinula edodes*, *Cancer Letters*, 220, 21-28.

Hoffman E.J., Medicinal Uses of Fungi, in *Cancer and the Search for Selective Biochemical Inhibitors*, 1999, Boca Raton, Fla: CRC Press, pp 173-184

Hobbs C.R., 2005, The chemistry, nutritional value, immunopharmacology, and safety of the traditional food of medicinal split-gill fungus *Schizophyllum commune* Fr.:Fr. (Schizophyllaceae). A literature review. *International Journal of Medicinal Mushrooms*, 7, 127-139

Howard A. and Pelc S., 1953, Synthesis of deoxyribonucleic acid in normal and irradiated cells and its relation to chromosome breakage. *Heredity*, 6 (Suppl.), 261-273.

- Hsieh T.C., Kunicki J., Darzynkiewicz Z. and Wu J.M., 2002, Effects of extracts of *Coriolus versicolor* (I'm-Yunity) on cell-cycle progression and expression of interleukins-1 beta,-6, and -8 in promyelocytic HL-60 leukemic cells and mitogenically stimulated and nonstimulated human lymphocytes. *Journal of Alternative & Complementary Medicine*, 8, 591-602.
- Huang Q., Zhang L., Cheung P.C.K. and Tan X., 2006, Evaluation of sulfated  $\alpha$ -glucans from *Poria cocos* mycelia as potential antitumor agent, *Carbohydrate Polymers*, 64, 337-344
- Hui K.P., Sit W.H., Wan J.M.F., 2005, Induction of S phase cell arrest and caspase activation by polysaccharide peptide isolated from *Coriolus versicolor* enhanced the cell cycle dependent activity and apoptotic cell death of doxorubicin and etoposide, but not cytarabine in HL-60 cells. *Oncology Report*. 14, 145-155.
- Igney F.H. and Krammer P.H., 2002, Death and anti-death: tumor resistance to apoptosis, *Nature Reviews*, 2, 227-288.
- Ikekawa T., Nakanishi M., Uehara N., Chihara G. and Fukuoka F., 1968, Antitumor action of some basidiomycetes, especially *Phellinus linteus*. *Japanese Journal of Cancer Research : Gann*, 59, 155-157.
- Ikekawa T., Uehara N., Maeda Y., Nakanishi M. and Fukuoka F., 1969, Antitumor activity of aqueous extracts of edible mushrooms. *Cancer Research*, 29, 734-735.



- Jiang J., Slivova V., Valachovicova T., Harvey K. and Sliva D., 2004, *Ganoderma lucidum* inhibits proliferation and induces apoptosis in human prostate cancer cells PC-3. *International Journal Oncology*, 24, 1093-1099.
- Jin Y., Zhang L., Zhang M., Chen L., Cheung P.C.K., Ooi V.E.C. and Lin Y., 2003, Antitumor activities of heteropolysaccharides of *Poria cocos* mycelia from different strains and culture media, *Carbohydrate Research*, 338, 1517-1521
- Jones T.M. and Albersheim P., 1972, A gas chromatographic method for the determination of aldose and uronic acid constituents of plant cell wall polysaccharides, *Plant Physiology*, 49, 926-936.
- Kadiri, M. and Fasidi, T.O., 1990, Studies on enzyme activities of *Pleurotus tuber-regium* (Fries) Singer and *Tricholoma lobayensis* Heim at various fruiting body stages. *Die Nahrung*, 34, 695-699
- Kastan M.B. and Bartek J., 2004, Cell-cycle checkpoints and cancer, *Nature*, 432, 316-323
- Kiho, T., Yoshida, I., Nagai, K. and Ukai, S., 1989, (1→3)- $\alpha$ -D-glucan from an alkaline extract of *Agrocybe cylindracea*, and antitumor activity of its O-(carboxymethyl)ated derivatives, *Carbohydrate Research*, 189, 273-279

- Lau C.B.S., Ho C.Y., Kim C.F Leung K.N., Fung K.P., Tse T.F., Chan H.H.L. and Chow M.S.S., 2004, Cytotoxic activities of *Coriolus versicolor* (Yunzhi) extract on human leukemia and lymphoma cells by induction of apoptosis, *Life Sciences*, 75, 797-808.
- Lavi I., Friesem D., Geresh S., Hadar Y. and Schwartz B., 2006, An aqueous polysaccharide extract from the edible mushroom *Pleurotus ostreatus* induces anti-proliferative and pro-apoptotic effects on HT-29 colon cancer cells, *Cancer Letters*, in press
- Lee C.L., Yang X., Wan J.M.F., 2006, The culture duration affects the immunomodulatory and anticancer effect of polysaccharopeptide derived from *Coriolus versicolor*, *Enzyme and Microbial Technology*, 38, 14-21.
- Li G., Kim D.H., Kim T.D., Park B.J., Park H.D., Park J.I., Na M.K., Kim H.C., Hong N.D., Lim K., Hwang B.D. and Yoon W.H., 2004, Protein-bound polysaccharide from *Phellinus Linteus* induces G2/M phase arrest and apoptosis in SW 480 human colon cancer cells, *Cancer Letters*, 216, 175-181
- Lin Y., Zhang L., Chen L., Jin Y., Zeng F., Jin J., Wan B. and Cheung P.C., 2004, Molecular mass and antitumor activities of sulfated derivatives of alpha-glucan from *Poria cocos* mycelia, *International Journal of Biological Macromolecules*, 34, 289-294.

- Lowry, O. H. Rosebrough, N. J. Lewis Farr, A. and Randall, R. J. (1951). Protein measurement with the folin phenol reagent. *Journal of Biological Chemistry*, 193, 265-275.
- Lu M.C., Yang S.H., Hwang S.L., Lu Y.J., Lin Y.H., Wang S.R., Wu Y.C. and Lin S.R., 2006, Induction of G2/M phase arrest by squamocin in chronic myeloid leukemia (K562) cells, *Life Sciences*, 78, 2378-2383
- Malumbres M. and Barbacid M., 2001, To cycle or not to cycle: a critical decision in cancer., *Nature Reviews. Cancer*, 3, 222-231
- Marchessault, R. H., Deslandes, Y., Ogawa, K. and Sundararajan, P. R. (1977). X-ray diffraction data for  $\beta$ -(1 $\rightarrow$ 3)-D-glucan. *Canadian Journal of Chemistry*, 55, 300-303.
- Martins L. M., Mesner P.W., Kottke T. J., Basi G. S., Sinha S., Tung J. S., Svingen P.A., Madden B.J., Takahashi A., McCormick D.J., Earnshaw W.C., Kaufmann S.H., 1997, Comparison of caspase activation and subcellular localization in HL-60 and K562 cells undergoing etoposide-induced apoptosis, *Blood*, 90, 4283-4296.
- Miles P.G. and Chang S.T., Mushroom biology. In: *Concise Basics and Current Developments*, 1997, World Scientific, Singapore, New Jersey, London, Hong Kong, pp194.



- Mischnick, 1995, Structural analysis of polysaccharides and polysaccharide derivatives. *Macromolecule Symposia*, 3-13, pp.99.
- Mizuno, T. 1989. Development and utilization of bioactive substances from mushroom fungi – introduction. *Nippon Nogeikagaku Kaishi*. 63, 861-862.
- Mizuno T, 1996, A development of antitumor polysaccharides from mushroom fungi. *Food and Food Ingredient Journal (Japan)*. 167, 69-85.
- Mizuno T., 1999, The extraction and development of anti-tumor-active polysaccharides from medicinal mushrooms in Japan (review). *International Journal of Medicinal Mushrooms*, 1, 9-29.
- Mizuno T., Saito H., Nishitoba T. and Kawagashi H, 1995, Antitumor-active substances from mushrooms. *Food Review International*, 11, 23-61
- Mosmann, T., 1983, Rapid colorimetric assay for cellular growth and survival: application to proliferation and cytotoxicity assay. *Journal of Immunological Methods*. 63, 55-63.
- Murray A.W., 2004, Recycling the Cell Cycle: Cyclins Revisited. *Cell*, 116, 221-234.
- Ng, T. B., 1998, A review of research on the protein-bound polysaccharide (polysaccharopeptide, PSP) from the mushroom *Coriolus versicolor* (basidiomycetes: Polyporaceae), *General Pharmacology: The Vascular System*, 30, 1-4

- Ohno N., 2005, Structural diversity and physiological functions of  $\beta$ -glucans, *International Journal of Medicinal Mushrooms*, 7, 167-173.
- Ohno N., Furukawa M., Miura N.N., Adachi Y., Motoi M. and Yadomae T., 2001, Antitumor  $\beta$ -glucan from the cultures fruit body of *Agaricus blazei*, *Biological & Pharmaceutical Bulletin*, 24, 820-828.
- Ohno, N., Miura, N.N., Chiba, N., Adachi, Y. and Yadomae, T., 1995, Comparison of the immunopharmacological activities of triple and single-helical schizophyllan in mice *Biological & pharmaceutical bulletin*, 18, 1242-1247
- Okada H., Mak T.W., 2004, Pathways of apoptotic and non-apoptotic death in tumour cells, *Nature Reviews. Cancer*, 4, 592-603
- Oltvai Z.N., Milliman C.L., Korsmeyer S.J., 1993, Bcl-2 heterodimerizes in vivo with a conserved homolog, Bax, that accelerates programmed cell death, *Cell*, 74, 609-619
- Ooi V.E.C., Medicinal important fungi, in *Science and cultivation of edible fungi : proceedings of the 15th International Congress on the Science and Cultivation of Edible Fungi, Maastricht/Netherlands/15-19 May 2000*, Van Griensven L.J.L.D., Rotterdam ; Brookfield, Vt. : A.A. Balkema, pp. 41-51
- Ooi V.E.C. and Liu F., 1999, A review of pharmacological activities of mushroom polysaccharides, *International Journal of Medicinal Mushrooms*, 1, 195-206

- Ooi V.E.C. and Liu F., 2000, Immunomodulation and anti-cancer activity of polysaccharide-protein complexes, *Current Medicinal Chemistry*, 7, 715-729.
- Oso, B.A., 1977, *Pleurotus tuber-regium* from Nigeria. *Mycologia*, 69, 271-279.
- Pazur, J. H., Neutral Polysaccharides. in *Carbohydrate Analysis-A practical approach*, 2<sup>nd</sup> ed, 1994, Chaplin, M. F. and Kennedy, J. F. eds. Oxford University Press Inc, New York. pp. 73-122.
- Peng Y., Zhang L., Zeng F. and Kennedy J.F., 2005, Structure and antitumor activities of the water-soluble polysaccharides from *Ganoderma tsugae* mycelium, *Carbohydrate Polymers*, 59, 385-392.
- Peng Y., Zhang L., Zeng F. and Xu Y., 2003, Structure and antitumor activity of extracellular polysaccharides from mycelium. *Carbohydrate Polymers*, 54, 297-303.
- Pommier Y., Yu Q. and Kohn K.W., Novel Targets in the Cell Cycle and Cell Cycle Checkpoints, in *Anticancer drug development*, 2002, Baguley B.C. and Kerr. D.J., Academic Press, San Diego, California and London, pp: 13-25
- Raisova M., Hossini A.M., Eberle J., Riebeling C., Wieder T., Sturm I., Daniel P.T., Orfanos C.E. and Geilen C.C., 2001, The Bax/Bcl-2 ratio determines the susceptibility of human melanoma cells to CD95/Fas-mediated apoptosis. *The Journal of investigative dermatology*, 117, 333-340



- Reshetnikov S.V., Wasser S.P. and Tan K.K., 2001, Higher Basidiomycota as a source of antitumor and immunostimulating polysaccharides. *International Journal of Medicinal Mushrooms*, 3, 361–394.
- Riggi, S. J. and Di Luzio, N. R., 1962, Hepatic function during reticuloendothelia hyperfunction and hyperplasia. *Nature*, 193: 1292-1294
- Ritke M.K., Rusnak J.M., Lazo J.S., Allan W.P., Dive C., Heer S. and Yalowich J.C., 1994, Differential induction of etoposide-mediated apoptosis in human leukemia HL-60 and K562 cells, *Molecular Pharmacology*, 605-611.
- Roche Applied Science, 2003, Instructional manual of cell proliferation ELISA, BrdU (chemiluminescence), pp1-21.
- Schwartz G.K. and Shah M.A., 2005, Targeting the cell cycle: a new approach to cancer therapy, *Journal of Clinical Oncology*, 23, 9408-9421.
- Sherr C.J., 1995, D-type cyclins. *Trends Biochemical Science*, 20, 187-190.
- Sherr C.J., 2000, The pezcoller lecture: cancer cell cycle revisited, *Cancer Research*, 60, 3689-3695.
- Solary E., Droin N. and Sordet O., Cell Death Pathways as Targets for Anticancer Drugs, in *Anticancer drug development*, 2002, Baguley B.C. and Kerr. B.C., Academic Press, San Diego, California and London, pp: 55-70

- Sone Y., Okuda R., Wada N., Kishida E. and Misaki, A., 1985, Structure and antitumor activities of the polysaccharides isolated from fruiting body and the growing culture of mycelium of *Ganoderma lucidum*. *Agricultural Biological Chemistry*, 49, 2641-2653.
- Smith J.E., Sullivan R., and Rowan N., 2003, The role of polysaccharides derived from medicinal mushrooms in cancer treatment programs: current perspectives (review), *International Journal of Medicinal Mushrooms*, 5, 217-234.
- Stamets, P. and Chilton, J. S., 1983. An overview of techniques for mushroom cultivation. In *The mushroom cultivator — A practical guide to growing mushrooms at home*. Agarikon Press. Olympia. Washington.
- Surenjav U., Zhang L., Xu X., Zhang X. and Zeng F., 2006, Effects of molecular structure on antitumor activities of (1→3)-β-D-glucans from different *Lentinus Edodes*. *Carbohydrate Polymers*. 63, 97-104.
- Svingen P. A., Madden B. J., Takahashi A., McCormick D. J., Earnshaw W. C. and Kaufmann S. H., 1997, Comparison of Caspase Activation and Subcellular Localization in HL-60 and K562 Cells Undergoing Etoposide-Induced Apoptosis, *Blood*, 90, 4283-4296
- Theander O., Aman O., Westerlund, E., Andersson R. and Petersson D., 1995, Total dietary fiber determined as neutral sugar residues, uronic acid residues, and Klason lignin (The Uppsala method): collaborative study. *Journal of Association of Official Analytical Chemists*, 78: 1033-1044.

- Tsuchida H., Mizuno M., Taniguchi Y., Ito H., Kawade M. and Akasaka K., 2001, Glucomannan separated from *Agaricus Blazei* mushroom culture and antitumor agent containing as active ingredient. *Japanese Patent 11-080206*, 26.
- Tsukagoshi S., Hashimoto Y., Fujii G., Kobayashi H., Nomoto K. and Orita K., 1984, Krestin (PSK). *Cancer Treatment Reviews*, 11, 131-155
- Ude C.M., Ezenwugo A.E.N. and Agu R.C., 2003, Composition and food value of sclerotium (Osu) and edible mushroom (*Pleurotus tuber-regium*). *Journal of Food Science and Technology*, 38, 612–614.
- Vermes I., Haanen C. and Reutellingsperger C, 2000, Flow cytometry of apoptotic cell death. *Journal of Immunological Methods*. 243, 167-190.
- Vermes I., Haanen C., Steffens-Nakken H. and Reutellingsperger C., 1995, A novel assay for apoptosis Flow cytometric detection of phosphatidylserine expression on early apoptotic cells using fluorescein labeled Annexin V. *Journal of Immunological Methods*. 184, 39-51.
- Vinogradov E., Petersen B.O., Duus J.O. and Wasser S., 2004, The structure of the glucuronoxylomannan produced by culinary-medicinal yellow brain mushroom (*Tremella mesenterica* Ritz.:Fr., Heterobasidiomycetes) grown as one cell biomass in submerged culture. *Carbohydrate Research*, 339, 1483-1489.



- Wang G., Zhang J., Mizuno T., Zhuang C., Ito H., Mayuzumi H., Okamoto H. and Li J., 1993, Antitumor active polysaccharides from the Chinese mushroom Songshan Lingzhi, the fruiting body of *Ganoderma tsugae*. *Bioscience Biotechnology Biochemistry*, 57, 894-900.
- Wang H.X., Liu W.K., Ng T.B., Ooi V.E.C. and Chang S.T., 1995, Immunomodulatory and antitumor activities of a polysaccharide-peptide complex from a mycelial culture of *Tricholoma* sp., a local edible mushroom. *Life Science*, 57, 269-281.
- Wang Y., Zhang L., Li Y., Hou X., Zeng F., 2004, Correlation of structure to antitumor activities of five derivatives of a  $\beta$ -glucan from *Poria cocos* sclerotium, *Carbohydrate Research*, 339, 2567-2574.
- Wasser S.P., 2002, Medicinal mushrooms as a source of antitumor and immunomodulating polysaccharides. *Applied Microbiology and Biotechnology*. 60, 258-274
- Wasser S.P. and Weis A.L., 1999, Medicinal properties of substances occurring in higher Basidiomycetes mushrooms: current perspectives (review). *International Journal of Medicinal Mushrooms*. 1, 31-62
- Williams, D.L., Pretus, H. A., McNamee, R.B., Jones, E. L., Ensley, H. E. and Browder, I. W., 1992, Development of a water-soluble, sulfated (1 $\rightarrow$ 3)-D-glucans biological response modifier derived from *Saccharomyces cerevisiae*. *Carbohydrate Research*, 235, 247-257

- Williams, D.L., Sherwood, E.R., McNamee, R.B., Jones, E. L., Browder, I. W. and Di Luzio, N. R., 1985, Therapeutic efficacy of glucan in a murine model of hepatic metastatic disease. *Hepatology*, 5, 198-206
- Wong, K.K., 2004, Effect of carbon source (carbohydrate) on the chemical structure of water-soluble mushroom polysaccharides produced by submerged fermentation. M.Phil. Thesis, The Chinese University of Hong Kong
- Wu J.Z., Cheung P.C.K., Wong K.H. and Huang N.L., 2003, Studies on the submerged fermentation of *Pleurotus tuber-regium* (Fr.) Singer: 1. Physical and chemical factors affecting the rate of mycelial growth and bioconversion efficiency, *Food Chemistry*, 81, 389–393.
- Wu J.Z., Cheung P.C.K., Wong K.H. and Huang N.L., 2004, Studies on the submerged fermentation of *Pleurotus tuber-regium* (Fr.) Singer: 2. Effect of carbon-to-nitrogen ratio of the culture medium on the content and composition of the mycelial dietary fibre, *Food Chemistry*, 85, 101-105.
- Yang X., Sit W. Chan D. K. and Wan J. M., 2005, The cell death process of the anticancer agent polysaccharide-peptide (PSP) in human promyelocytic leukemia HL-60 cells, *Oncology Reports*, 13, 1201-1210
- Yassin M., Mahajna J.A. and Wasser S.P., 2003, Submerged culture mycelium extracts of higher basidiomycetes mushrooms selectively inhibit proliferation and induce differentiation of K562 human chronic myelogenous leukemia cells, *International Journal of Medicinal Mushrooms*, 5, 261-276.

- Ye M., Liu J., Lu Z., Zhao Y., Liu S., Li L., Tan M., Weng X., Li W. and Cao Y., 2005, Grifolin, a potential antitumor natural product from the mushroom *Albatrellus confluens*, inhibits tumor cell growth by inducing apoptosis in vitro, *FEBS Letters*, 3437-3443
- Ying J., Mao X., Ma Q., Zong Y. and Wen H., (translated by Yuehan X), 1987, Icons of medicinal fungi from China, *Science Press, Beijing*, pp 307
- Zhang L., Li X., Xu X. and Zeng F., 2005, Correlation between antitumor activity, molecular weight, and conformation of lentinan, *Carbohydrate Research*, 340, 1515-1521.
- Zhang L., Zhang M., Dong J., Guo J., Song Y. and Cheung, P. C. K., 2001, Chemical structure and chain conformation of the water-insoluble glucan isolated from *Pleurotus tuber-regium*, *Biopolymers*, 59, 457-464.
- Zhang M., Cheung P. C. K., Chiu L. C. M., Wong E. Y. L. and Ooi V. E. C., 2006a, Cell-cycle arrest and apoptosis induction in human breast carcinoma MCF-7 cells by carboxymethylated  $\beta$ -glucan from the mushroom sclerotia of *Pleurotus tuber-regium*. *Carbohydrate Polymers. In Press*
- Zhang, M., Cheung, P. C. K. Ooi, V. E. C. and Zhang, L., 2004a, Evaluation of sulfated fungal  $\beta$ -glucans from the sclerotium of *Pleurotus tuber-regium* as a potential water-soluble anti-viral agent. *Carbohydrate Research* 339, 2297-2301.



- Zhang, M., Cheung P. C. K., Zhang, L., Chiu C.M. and Ooi V. E. C., 2004b, Carboxymethylated  $\beta$ -glucans from mushroom sclerotium of *Pleurotus tuber-regium* as novel water-soluble anti-tumor agent. *Carbohydrate Polymers*. 57, 319-325.
- Zhang M., Chiu L.C., Cheung P.C. and Ooi V.E., 2006b, Growth-inhibitory effects of a beta-glucan from the mycelium of *Poria cocos* on human breast carcinoma MCF-7 cells: cell-cycle arrest and apoptosis induction. *Oncology Reports*, 15, 637-643.
- Zhang, M., Zhang, L., Cheung P. C. K. and Ooi V. E. C., 2004c, Molecular weight and anti-tumor activity of the water-soluble polysaccharides isolated by hot water and ultrasonic treatment from the sclerotia and mycelia of *Pleurotus tuber-regium* . *Carbohydrate Polymers*. 56, 123-128.
- Zhang, M., Zhang, L., Wang, Y. and Cheung, P. C. K., 2003, Chain conformation of sulfated derivatives of  $\beta$ -glucan from sclerotia of *Pleurotus tuber-regium*, *Carbohydrate Research*, 338, 2863-2870
- Zoberi, M.H., 1973, Some edible mushrooms from Nigeria. *Nigerian Field*, 38, 81-90.

## Related Publications

Wong S. M. and Cheung, P. C. K. (2005). *In vitro* study of antiproliferation of cancer cells by non-starch polysaccharides isolated from different developmental stages of *Pleurotus tuber-regium*. Abstract of *Institute of Food Technologists (IFT) annual meeting*, New Orleans, Louisiana, USA.

Lai, C. K. M. Wong, S. M. Cheung, P. C. K. and Ooi, V. E. C. (2005). *In vitro* study of antiproliferation of cancer cells by polysaccharides isolated from the mycelium and sclerotium of *Pleurotus tuber-regium*. Abstract of Fifth International Conference on Mushroom Biology and Mushroom Products, Shanghai, China.

Wong S. M., Wong K. K., Chiu L. C. M., Cheung P. C. K. (2006). Non-starch polysaccharides from different developmental stages of *Pleurotus tuber-regium* inhibited HL-60 cell growth by cell cycle arrest and/or apoptotic induction. *Carbohydrate Polymers*





CUHK Libraries



004359257